

Increasing Haptic Fidelity and Ergonomics in Teleoperated Surgery

THÈSE N° 5412 (2012)

PRÉSENTÉE LE 6 JUILLET 2012

À LA FACULTÉ DES SCIENCES ET TECHNIQUES DE L'INGÉNIEUR
LABORATOIRE DE SYSTÈMES ROBOTIQUES 1
PROGRAMME DOCTORAL EN SYSTÈMES DE PRODUCTION ET ROBOTIQUE

ÉCOLE POLYTECHNIQUE FÉDÉRALE DE LAUSANNE

POUR L'OBTENTION DU GRADE DE DOCTEUR ÈS SCIENCES

PAR

Laura SANTOS CARRERAS

acceptée sur proposition du jury:

Prof. P. Xirouchakis, président du jury
Prof. H. Bleuler, Prof. R. Gassert, directeurs de thèse
Prof. O. Blanke, rapporteur
Prof. V. Hayward, rapporteur
Prof. A. Okamura, rapporteur



ÉCOLE POLYTECHNIQUE
FÉDÉRALE DE LAUSANNE

Suisse
2012

*To my parents and my sister
Arturo, Margarita y Beatriz.*

Acknowledgements

I would like to start by thanking my thesis supervisors. First, I would like to thank Prof. Hannes Bleuler for welcoming me at the Laboratoire de Systèmes Robotiques (LSRO) at EPFL. The trust and freedom that he provided all along the thesis highly increased my confidence and initiative. I am also deeply grateful to Prof. Roger Gassert for his great help and guidance and for letting me be involved in projects parallel to the thesis that were of great interest for me.

My gratitude also goes to the jury members who evaluated this work and contributed to the last version of this document: Prof. Paul Xirouchakis for his efficient moderation of the private exam; Prof. Vincent Hayward for his suggestions to improve the quality of the thesis and for coming to EPFL in such a busy period; Prof. Allison Okamura for her helpful feedback and for attending despite the difficult time schedule due to the geographic distance; and Prof. Olaf Blanke for his comments from a neuroscientist point view, which enriched the conclusions and the possible applications of this work.

I would also like to acknowledge the help of all the people I collaborated with in EPFL, ETHZ and within the context of the European Project. Thanks to all the students who performed a master or semester project with me, for their motivation, creativity and efforts. I wish them all the best for the rest of their career. Special thanks to Kaspar Leuenberger, whose robust prototype developed as a master project, could be then applied to perform part of this research. I am as well grateful to all the staff of the mechanical workshops. Special thanks to Alfred Thomas and Marc Salle for the friendly atmosphere, their helpful manufacturing advice and the running coaching.

I want to specially thank all my colleagues at LSRO1 for making the workplace convivial, creative, stimulating and productive. The lab could not function without many people creating this environment and I am indebted to all of them. Thanks Beira for all your advise in mechanical design and your pragmatism, Giulio and Evren for the experiment discussions, Ricardo Pérez for the writing tips, Ali and Lionel for being always willing to help, David Hippert for your funny laugh, Silvia (Chipi) for being fantastic, Philippe Rétornaz and Daniel Burnier for your recommendations in electronic design, Dominique for being both a colleague and a salsa partner. I have been extremely fortunate to share the office with great colleagues that were joyful, helpful and could deal with my messy desk without complaining too much: Solaiman, Masayuki, Ding, Jeremy and Simone. It was an unforgettable experience to work

with you all.

Thanks also to my good friends at Lausanne: to Alexandra for being a so nice neighbor and for her style tips; to Elena for being such great rowing coach; to Ceren, Evren and Alexey because you made me feel like at home.

My enormous gratitude to all my friends in Spain for keeping in touch and make me feel less far, for all the unforgettable joyful moments we share together every time I come back and during their visits.

I would like to thank my family for their love, for their continuous support over the last four years despite the distance, for their understanding and for patiently waiting for my visits. I especially dedicate this thesis to my parents and my sister.

“Dedico esta tesis a mi familia, en especial a mis padres y a mi hermana, por todo su cariño, por su constante apoyo a pesar de la distancia, por su comprensión y por esperar pacientemente mi vuelta a casa.”

And last but not least I would like to thank Mathieu for his love, great help, patience and encouragement. He is the main reason why I came here but in no way regretted, not even for a millisecond.

This work was funded by the European Commission in the framework of the ARAKNES FP7 European Project EU/IST-2008-224565.

Abstract

Over the past few decades, surgical procedures have made enormous progress, shifting from traditional open procedures to less and less invasive approaches, with the promise of smaller incisions, less complications, better cosmetic results and shorter recovery times. With these developments came a reduced dexterity and more complex control through the fulcrum effect and modified eye-hand coordination. These complications were greatly mitigated by the recent introduction of surgical robots, allowing the surgeon to sit in a comfortable posture, and restoring natural visuomotor coordination. To date, the issue of the lack of [haptic feedback](#), which initially allowed the surgeon to intervene without vision, identify pathological tissue, feel arteries, etc., has not been resolved, despite the fact that it is crucial in certain interventions. Besides, the added value of [haptic feedback](#) is subject to controversy. Surgeons experienced in robotic surgery have adapted to the lack of [haptic feedback](#) and learned how to rely only on vision and proprioceptive cues as compensation. Nevertheless, previous studies have shown that substituting haptic information through various sensory channels can increase surgeons' performance. As a complete restoration of the sense of touch is extremely challenging in minimally invasive surgery, the advantages of [haptic feedback](#) have to be demonstrated and quantified to justify the additional cost and complexity. This is the aim of the present work.

We hypothesized that tactile feedback as well as force is crucial in surgery and we investigated the haptic information involved in several representative surgical tasks. Dedicated hardware and a virtual reality environment to simulate suturing and palpation tasks were developed to address these questions. Ergonomic design guidelines were established based on an in-depth literature review and surgeons' comments gathered in a survey. These guidelines were then used to design and benchmark an ergonomic haptic handle featuring active grasping feedback and additional safety features.

The results of the first two studies suggest that the benefits of haptic information highly depend on the surgical task in question. During a suturing task, force feedback significantly increased users' accuracy whereas torque feedback did not result in any significant improvement. In a palpation task, a higher recognition rate was achieved with tactile feedback than with visual sensory substitution. The performance of the haptic device integrating the ergonomic handle was assessed and compared with the standard omega.7 haptic device. Results showed that the index of performance of the original device was not degraded with the additional hardware. The index of performance was slightly increased for a manipulation task involving orientations. The ergonomic assessment of the handle showed a slight decrease of the tension

in the adductor pollicis and flexor digitorum muscles, and therefore a potential decrease of fatigue.

Although just a subset of surgical tasks could be investigated, the results indicate that [haptic feedback](#) and sensory substitution would greatly benefit teleoperated robotic surgery. Providing the surgeon with tactile information can potentially restore the feeling of “contact with the patient” and other surgeries that are highly reliant on the sense of touch could become possible again. This thesis presents a novel multidisciplinary approach to systematically analyzing surgical tasks in order to improve safety in two dimensions. Firstly, in the area of patient safety by providing the surgeon with haptic information to increase performance and reduce the risk of errors and secondly, in the area of surgeon safety by providing a more ergonomic master console. We expect this work to be a first step in establishing a general design method for more ergonomic surgeon consoles and trust that it will inspire research to investigate the sensory mechanisms underlying highly dexterous tasks such as those performed in surgery.

Keywords– surgical robotics, haptics, force feedback, tactile feedback, sensory substitution, ergonomics, haptic device evaluation

Version Abrégée

Ces dernières décennies, les protocoles chirurgicaux ont fait d'énormes progrès, passant des procédures traditionnelles de chirurgie ouverte à des approches de moins en moins invasives, permettant des incisions plus petites, moins de complications, de meilleurs résultats cosmétiques et un rétablissement plus rapide. Ces développements se sont malheureusement accompagnés d'une dextérité diminuée et d'un contrôle plus complexe en raison de l'effet de levier et de la modification de la coordination entre les yeux et les mains. Ces difficultés ont été grandement réduites par l'introduction des robots chirurgicaux, qui permettent au chirurgien d'être assis dans une posture confortable et rétablissent la coordination visio-motrice naturelle. À ce jour, la sensation de toucher, qui permet au chirurgien d'intervenir sans voir, d'identifier des tissus pathologiques, de localiser des artères, etc., n'est pas transmise, bien que ce soit un élément crucial pour certaines interventions. De plus, l'intérêt même de rendre cette information est sujet à controverses. Les chirurgiens expérimentés en chirurgie robotique se sont adaptés à l'absence de toucher et ont appris à opérer en n'ayant accès qu'à des informations visuelles et proprioceptives. Néanmoins, des études précédentes ont montré que les performances des chirurgiens peuvent être améliorées en transmettant des informations tactiles par d'autres canaux sensoriels. Comme une restitution complète du sens du toucher en chirurgie mini-invasive est un grand défi technique, les avantages du retour haptique doivent être démontrés et quantifiés pour justifier le coût et la complexité additionnels. C'est l'objet du travail présenté ici.

Nous sommes partis de l'hypothèse que l'information tactile ainsi que sur les forces exercées est cruciale en chirurgie et nous avons étudié les signaux sensoriels impliqués dans plusieurs tâches chirurgicales. L'appareillage dédié et un environnement de réalité virtuelle ont été développés pour chaque de ces études. Des recommandations pour une conception ergonomique ont été établies en se basant sur une analyse approfondie de la littérature et des commentaires de chirurgiens collectés par sondage. Ces recommandations ont ensuite été utilisées pour la conception et l'évaluation d'une poignée haptique ergonomique permettant un retour actif de la sensation de prise en main ainsi que des éléments de sécurité additionnels.

Les résultats des deux premières études suggèrent que les bénéfices de l'information tactile dépendent beaucoup de la tâche en question. Lors d'une suture, le retour de force a permis d'améliorer significativement la précision alors que l'information sur le couple ne semblait pas avoir d'influence. Lors d'une palpation, l'information tactile a permis d'atteindre une vitesse d'indentification plus élevée qu'en substituant cette information par un canal visuel.

Les performances du dispositif intégrant la poignée ergonomique ont été évaluées et comparées avec le dispositif standard omega.7. Les résultats montrent que l'indice de performance du dispositif original n'est pas dégradé par l'ajout de matériel. De plus, cet indice était même légèrement meilleur pour une tâche d'assemblage simple dans laquelle la pièce devait être correctement orientée avant son insertion. L'évaluation ergonomique de la poignée a montré une légère diminution de la tension musculaire dans les muscles adductor pollicis et flexor digitorum, et donc une possible diminution de la fatigue musculaire.

Bien que seul un sous-ensemble des tâches chirurgicales ait pu être étudié, les résultats indiquent que le retour de la sensation tactile et la substitution sensorielle seraient grandement bénéfiques pour la chirurgie robotique télé-opérée. Rendre au chirurgien accès à l'information tactile peut potentiellement rétablir la sensation de "contact avec le patient", et d'autres types de chirurgies qui dépendent du sens du toucher pourraient redevenir possibles. Cette thèse présente une approche multidisciplinaire novatrice pour analyser systématiquement des tâches chirurgicales afin d'améliorer la sécurité à deux niveaux. Premièrement, pour la sécurité du patient, en donnant au chirurgien accès à des informations sensorielles améliorant son efficacité et réduisant le risque d'erreurs, et deuxièmement, pour la sécurité du chirurgien en proposant un poste de travail plus ergonomique. Nous nous attendons à ce que ce travail soit une première étape dans l'établissement de procédures générales pour la conception de postes de travail ergonomiques pour les chirurgiens, et nous espérons qu'il inspirera des recherches futures pour étudier les mécanismes sensoriels impliqués dans des tâches de haute dextérité comme celles effectuées en chirurgie.

Mot clés– chirurgie robotique, retour tactile, retour de force, substitution sensorielle, ergonomie, évaluation des dispositifs haptiques

Contents

Acknowledgements	v
Abstract (English, French)	vii
1 Introduction	1
1.1 Motivation	1
1.2 Objectives and Approach	6
2 State of the Art	9
2.1 Surgical Robotic Systems	9
2.2 Haptic Devices	17
2.3 Tactile Feedback and Sensory Substitution	19
I General and Task-Specific Requirements for Haptic Devices	23
3 Guidelines for the Specification of Haptic Interfaces	25
3.1 Requirements Imposed by the Human User	26
3.1.1 Human Perception (Input) Limits	26
3.1.2 Human Motor (Output) Limits	27
3.1.3 Transparency	28
3.1.4 Safety	28
3.2 Task-Specific Requirements	29
3.3 Quantifying the Level of Telepresence	31
3.3.1 Psychophysical Assessment	32
3.3.2 VR-based Testbeds	35
4 Influence of Force & Torque Feedback in a Suturing task	37
4.1 Methods and Protocol	38
4.1.1 Hardware	38
4.1.2 VR-based Testbed	40
4.1.3 Suture Performance Assessment	45
4.1.4 Experimental Protocol	47
4.2 Results	48

4.3	Post-experiment Questionnaire	52
4.3.1	Questions	53
4.3.2	Results	53
4.4	Discussion and Conclusions	53
5	Tactile Feedback during Surgery	57
5.1	Tactile Pulse Display	58
5.1.1	Implementation	58
5.1.2	Technical Performance	60
5.1.3	Psychophysical Evaluation	63
5.1.4	Discussion and Conclusions	67
5.2	Tactile <i>vs.</i> Visual Feedback in a Palpation Task	67
5.2.1	Experimental Setup	68
5.2.2	Experiment 1: Exploration Task	70
5.2.3	Experiment 2: Absolute Identification Paradigm	76
5.2.4	Post-experiment Questionnaire	80
5.2.5	Discussion	82
5.3	Summary and Conclusions	83
II	Towards an Ergonomic Surgeon's Console	85
6	Survey on Surgical Instrument Handles	87
6.1	Statistical Methods and Questionnaire Content	88
6.2	Results	90
6.3	Discussion	96
6.4	Conclusions	99
6.5	Survey Form	99
7	Ergonomic guidelines	101
7.1	Seat and Table Clearances	102
7.2	Display Arrangement	102
7.3	Reach and Work Envelopes	104
7.4	Handle Specifications	107
7.4.1	Wrist Posture and Mobility	107
7.4.2	Grasping Strength	108
7.5	Summary and Conclusions	109
8	Design and Evaluation of an Ergonomic Handle	111
8.1	State of the Art	112
8.2	Design Requirements	112
8.3	Prototype	114
8.3.1	Spherical Mechanism	114
8.3.2	Grasping Force Feedback	117

8.3.3	Safety Features	118
8.4	Technical Evaluation	119
8.4.1	Workspace	119
8.4.2	Grasping Feedback	120
8.4.3	Brake Performance	123
8.4.4	Discussion and Conclusions	125
8.5	Psychophysical Evaluation	125
8.5.1	Methods	126
8.5.2	Results	130
8.5.3	Discussion and Conclusions	131
8.6	Ergonomic Evaluation	132
8.6.1	Methods	133
8.6.2	Results	135
8.6.3	Discussion and Conclusions	136
8.7	Post-experiment Questionnaire	137
8.7.1	Questionnaire	137
8.7.2	Results	137
8.8	Chapter Summary and Conclusions	138
9	Conclusions	141
9.1	Contributions and Originality	143
9.1.1	Task-specific and Physiologically Motivated Developments	143
9.1.2	Approach Combining Technology, Psychophysics and Ergonomics	144
9.1.3	Survey and Ergonomic Guidelines	144
9.2	Outlook and Further Research Directions	144
9.2.1	Haptics Research	144
9.2.2	Ergonomics in Robotic Surgery	145
	Bibliography	160
	Glossary and Acronyms	164
	List of Figures	167
	List of Tables	169
	Curriculum Vitae	171

Chapter 1

Introduction

1.1 Motivation

The Evolution of Surgery and its Impact on Ergonomics and Motor Performance

Over the past twenty years the field of surgery has drastically changed in an attempt to offer patients less invasive solutions. With this idea of minimizing invasiveness, laparoscopy - the first type of [Minimally Invasive Surgery \(MIS\)](#) - was developed and is now established as the gold standard. Novel MIS techniques such as [Single Incision Laparoscopic Surgery \(SILS\)](#) and [Natural Orifice Translumenal Endoscopic Surgery \(NOTES\)](#) are gaining recognition and clinical cases are growing rapidly ([Chamberlain and Sakpal, 2009](#)). Reducing the size of the incision decreases the risks of infection and trauma, resulting in a faster recovery, shorter hospitalization and better cosmetic outcome for patients.

Surgical instrumentation has evolved significantly from open to laparoscopic and robotic surgery. A consequence of this evolution has been a tremendous change in the surgeon's working conditions. During traditional open surgery, the surgeon performs a large incision in the patient's abdomen to access the abdominal cavity. The internal tissues and organs can then be directly seen, touched and manipulated by the surgeon. The surgeon is generally standing near the operating table while performing open surgery and is able to see and reach the patient's organs by gently bending over the patient, as shown in [Fig. 1.1](#).

[MIS](#) procedures are applied for the same purposes as open surgery, with the advantage of being less invasive. Endoscopic tools (long and narrow instruments) inserted into the body through small openings on its surface are usually used to accomplish the [MIS](#) procedure. These incisions induce the inversion of hand and tip movements, called the "fulcrum effect". As shown in [Fig. 1.2](#) (left), surgeons must move their hands in the opposite direction to where the tip of the instrument is intended to go. An image of the internal organs and tissue is generally displayed on a screen allowing the surgeon to make diagnosis, visually identify internal organs and perform surgery on them. However, this indirect observation of the surgical field modifies



Figure 1.1: Open surgery: surgeon's work-conditions (image from MD Web). Surgeons can perform direct manipulation and natural eye-hand coordination.

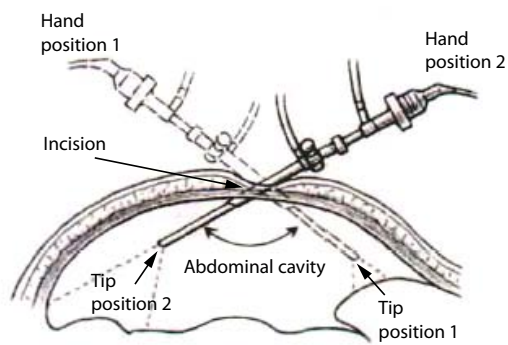


Figure 1.2: (left) The fulcrum effect: inversion of the instrument's movements due to an incision on the abdominal cavity (Klaiber et al., 1993) and (right) examples of laparoscopic instruments manipulations (Image from Ever Green Surgical)

the eye-hand coordination as compared to traditional open surgery and provides a 2D view of the internal organs resulting in a loss of depth perception. This 2D vision - in addition to the fulcrum effect - significantly increases the complexity of the procedure and results in awkward and uncomfortable postures for the surgeon, who is required to stand and hold long instruments while looking at the screen monitor (Fig. 1.2, right). A variant of this technique is **SILS**, which reduces the number of incisions to one, generally wider which makes the introduction of several instruments through the same surgical cut possible. The complexity of this procedure is even greater than standard laparoscopy as the dexterity is considerably reduced and the surgical instruments have to be crossed to allow triangulation, as shown in Fig. 1.3 (left).

A **NOTES** procedure is usually defined as “scarless”. With this technique, abdominal operations can be performed with an endoscope passed through a natural orifice (vagina, mouth, urethra, etc.) and then through an internal incision in the stomach, uterus, or colon,

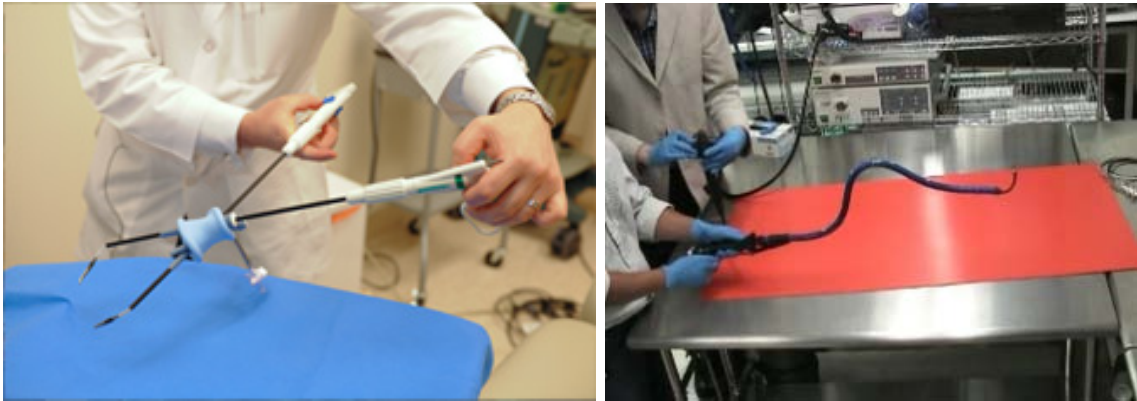


Figure 1.3: Manipulation examples of (left) SILS (image from UFirstHealth Web) and (right) NOTES instrumentation (TransPortTM Multi-lumen Operating Platform image from USGI Medical Inc.)

thus avoiding any visible, external scars. To reach the desired location inside the patient’s body a highly dexterous or flexible endoscope is needed. Up to now, snake-like endoscopes featuring several tool channels have been being used. As shown in Fig. 1.3 (right), these instruments are extremely complex and generally need two surgeons to control the orientation of the tip and the operation of inserted tools.

These techniques might provide several advantages over open surgery procedures such as faster recovery, shorter hospitalization, lower postoperative pain and better cosmetic results. However, the medical community is increasingly concerned about the ergonomic disadvantages associated with such complex systems and their surgical instruments (Berguer, 1999; Glickson, 2012). The consequences suffered by the surgeons range from mental stress to physical discomfort that can a posteriori lead to severe musculoskeletal disorders (Wauben et al., 2006; Van Veelen et al., 2003).

Some of these ergonomic drawbacks have been overcome with the introduction of telemanipulated surgical robotic systems, composed of two main elements: (1) a patient-side surgical robot (the “slave”) and (2) a console from where the surgeon remotely controls the surgical robot (the “master console”). As can be seen on Fig. 1.4, surgeons are seated, their forearms rest on pads, the manipulation is highly simplified and the 3D display restores the critical element of depth perception found in open surgical techniques. Still, recent studies suggest that sources of discomfort are also present in surgical robotic systems, especially neck and back muscle hardening caused by the non-neutral back position (Lawson et al., 2007; Lee et al., 2005). Due to the above-mentioned issues of surgical instruments’ ergonomics, the involvement of surgeons in the design process of new surgical instruments is central: it not only does it ensure the acceptance of the new device, it also promises good surgical performance while maintaining both patient and surgeon safety.

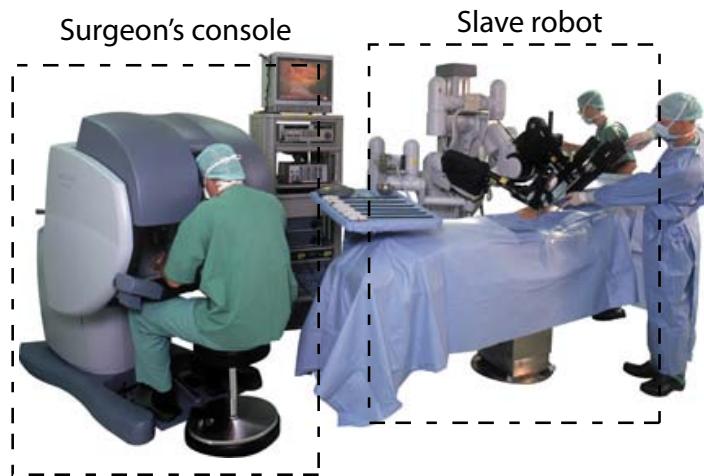


Figure 1.4: Robotic surgery: surgeon's work conditions (Da Vinci Surgical system, [Intuitive Surgical Inc. \(2010\)](#))

According to the [Institute Of Medicine \(IOM\)](#), about 1.3 million Americans are seriously injured each year by adverse events involving medical technology. Consequently, the US [Food and Drug Administration \(FDA\)](#) highlights the importance of ergonomics in this field ([Rados, 2003](#)).

Numerous studies have addressed the ergonomic factors that should be considered while designing a surgical instrument for a specific surgical technique ([Berguer, 1999](#); [Berguer et al., 1998](#)). These and other studies mainly investigated posture ([Nguyen et al., 2001](#); [Lawson et al., 2007](#); [Gofrit et al., 2008](#)), mental workload ([Carswell et al., 2005](#); [Zheng et al., 2010](#); [Berguer et al., 2001](#)) and pressure distribution ([Matern and Waller, 1999](#); [Lawther et al., 2002](#)).

The Robotic Boundary

As invasiveness is being gradually reduced, the access to the patient's abdominal cavity can only be achieved through adapted surgical instruments, such as endoscopes, laparoscopic tools or surgical robots. This means that the process keeps surgeons' hands outside, far from the patient's organs. Surgical operations in the abdominal cavity generally involve the manipulation of organs and soft tissues and thus, surgeons rely on their sense of touch while performing open surgery. In other types of surgery where the tissues are very fragile, such as neurosurgery or eye-surgery, this sense of touch is even more crucial. Currently, robotic surgery experts are trained to use visual feedback to limit their movements and avoid large forces applied on fragile tissues.

The sense of touch conveys essential information about the applied forces, tissue properties and organ disposition. The palpation of internal tissues is often performed during open surgery in order to assess the quality of tissue, to localize a problem or to determine its dimensions.

According to our surgeon collaborators, tactile exploration of the internal organs is often performed during open surgery to:

- assess the vascularization of an organ or tissue. This task is regularly performed to avoid the accidental rupture of arteries or to differentiate healthy from calcified arteries during an artery bypass;
- estimate the quality of an internal suture before concluding the operation;
- determine the extension of a tissue necrosis to be resected;
- find small tumors to be extirpated during a metastasectomy;
- distinguish the contours of internal hernias, a complication that frequently occurs after bariatric surgery; and
- evaluate the fibrosis of internal surgical adhesions (organ to organ attachment). Adhesion-related twisting and pulling of internal organs can result in complications such as infertility, chronic pelvic pain, or small bowel obstruction.

These tasks can no longer be performed through palpation during MIS procedures.

The goal of a haptic device is to bridge the mechanical gap between surgeons' hands and remote patients, allowing surgeons not only to manipulate organs and tissues but also to feel their mechanical characteristics. In an ideal context, the surgeons would feel like being present or immersed in the environment where they are teleoperating. This leads to the definition of concepts like *telepresence* or *immersion*. The term *presence* is the state of accepting the ambient sensory information as the physical surroundings. Consequently, the concept of [telepresence](#) has been defined as the experience of being there at the remote site ([Sheridan, 1992](#)), or the experience of being in the location of the slave robot ([Loomis, 1993](#)).

Adding [haptic feedback](#) in today's commercial surgical robotic systems is the focus of attention for many research groups. Many of their developments are very promising but, despite the intense press coverage and feverish anticipation, very few of them have been implemented in the hospitals. This is mainly due to the increased complexity and price that the addition of [haptic feedback](#) incurs. Therefore, it is still necessary to scientifically prove and quantify the benefits of this technology. Although it remains unclear as to how different modalities of [haptic feedback](#) can affect surgeons' performance, some studies have shown that giving the surgeon extra information about the forces applied by the slave robot can reduce errors even for expert surgeons ([Kitagawa et al., 2005a](#)). However, additional feedback signals are only desirable if the mental workload during the surgical procedure is not compromised ([Leung et al., 2007](#)).

Whereas most of the research groups concentrate in the already challenging addition of kinesthetic feedback (forces and motions), we believe that tactile feedback (roughness, temperature, softness) is necessary for some surgical or diagnostic tasks. This assumption goes further and we think that if sense of touch is finally restored, intuitiveness and [telepresence](#) will be enhanced and therefore performance of both experts and trainees can be ameliorated.

The evaluation of different [haptic feedback](#) modalities in terms of ergonomics, workload

and performance will shed some light on this issue, proving whether different modalities of [haptic feedback](#) help or disturb surgeon's attention.

1.2 Objectives and Approach

This thesis was initially motivated by the development of an ergonomic multimodal haptic interface for a teleoperated surgical robotic system to overcome the previously mentioned drawbacks. This objective also implies investigating aspects such as the ergonomics in robotic surgery applications, the types of [haptic feedback](#) that the surgeon should be receiving and the influence of each type of feedback on the surgeon's performance.

The sense of touch conveys various kinds of information including sensations of force, temperature, pressure, roughness, pain, etc. Task specific experiments needed to be performed for each kind of sensory feedback to investigate its influence on the surgeon's performance. This implied an in-depth study of the surgical task, the [haptic feedback](#) involved in that task, the development of a hardware prototype and a [Virtual Reality \(VR\)](#)-based testbed mimicking the surgical task. Following these steps made this work highly multidisciplinary and challenging, requiring expertise in many diverse fields. Studying the influence of complete [haptic feedback](#) in surgery entail time-consuming and broad research beyond the scope of a thesis. This work only investigated a subset of tactile information involved in very common surgical tasks. Nevertheless, the findings already suggest that [haptic feedback](#) and sensory substitution would greatly benefit teleoperated robotic surgery by improving dexterity and increasing patient safety.

Even though robotic surgery improves the surgeon's working conditions, some ergonomic issues remain unresolved. As this field is relatively new, there are no ergonomic standards for the design of a surgeon's console. To maintain the final user - the surgeon - in the design loop, a survey was carried out to gather surgeons' preferences on surgical instruments design and their comments on ergonomic problems associated with different surgical techniques. Ergonomic standards for industrial workstations that could be applied to a surgeon's console have been reviewed and compiled.

This thesis aims at proposing guidelines that could improve robotic surgery ergonomics and dexterity. These two happen to be among the main reasons for introducing robotic surgery in the first place (along with the advantages of [MIS](#)). Some of the guidelines developed in this work have been applied and demonstrated in the design of a dedicated haptic device that is presented in detail in [Chapter 8](#).

This work has been published in four conference proceedings, three journal papers and presented in a workshop at the IEEE International Conference on Intelligent Robots and Systems (IROS) 2011.

Thesis Outline

This thesis is structured as follows. The state of the art of surgical robotic systems, force feedback devices and tactile displays can be found in Chapter 2. In Chapter 3, the requirements of haptic devices that are imposed either by human factors or the intended application are examined. From this point the thesis is divided into two parts. Part I is dedicated to the research aiming to restore [haptic feedback](#) in robotic surgery. Chapter 4 and Chapter 5 present the details of two studies that investigate the influence that [haptic feedback](#) can have on surgeons' performance. The experimental setups, the protocols and the results are described in detail.

Part II focuses in the ergonomic issues faced in the field of robotic surgery. Chapter 6 presents the outcomes of a survey inquiring surgeons about their working conditions, physical complains and surgical instrument preferences. Guidelines for the design of ergonomic surgeons' consoles are given in Chapter 7. Chapter 8 shows the design of an ergonomic haptic handle and the results of its assessment in terms of technical performance, psychophysics and ergonomics.

Finally, the contributions of this thesis are summarized in Chapter 9 and possible future research directions are discussed in the outlook Section.

Chapter 2

State of the Art

2.1 Surgical Robotic Systems

Since 1988, when the first surgical robot was introduced in an [Operating Room \(OR\)](#) ([Kwoh et al., 1988](#)), robotic technology has been progressively employed, as a mean to overcome the difficult working conditions during [MIS](#) procedures. To date, surgeons control a robotic system that works as a surgical instrument and generally does not perform automatic tasks. Most of the surgical robotic systems share the same master-slave configuration. The slave robot end-effectors are essentially the surgical instruments; the surgeon controls their movements through the master console. Such systems are called teleoperated surgical robotic systems. Currently, the best-known and most used surgical system is the da Vinci Surgical System developed by [Intuitive Surgical Inc. \(2010\)](#). [Fig. 2.1](#) shows this system with a surgeon console (master) on the left, and a patient-side slave robot on the right. As it is the most commonly used system nowadays, it will be taken as a reference throughout this chapter to compare the features of the newly developed surgical systems.

The success of the da Vinci system is based on its ergonomic working position, the augmented dexterity of the endo-wrist instruments and its intuitive control. The system's control maps the surgeon's finger movements directly to the robot's end-effector making its control straightforward and liberating the surgeon from dealing with the fulcrum effect introduced by laparoscopic surgery. Furthermore, it provides natural visuomotor coordination and stereoscopic view. Despite all the above-mentioned advantages, some issues are not addressed, and surgeons suggest introducing additional features such as:

- surgical instruments with additional degrees of freedom to extend the access to different organs;
- a more compact slave design to easily reach the patient if something goes wrong and to simplify the [OR](#) setting;
- [haptic feedback](#) to restore the surgeon's sense of touch to improve safety and increase [telepresence](#) during surgery.

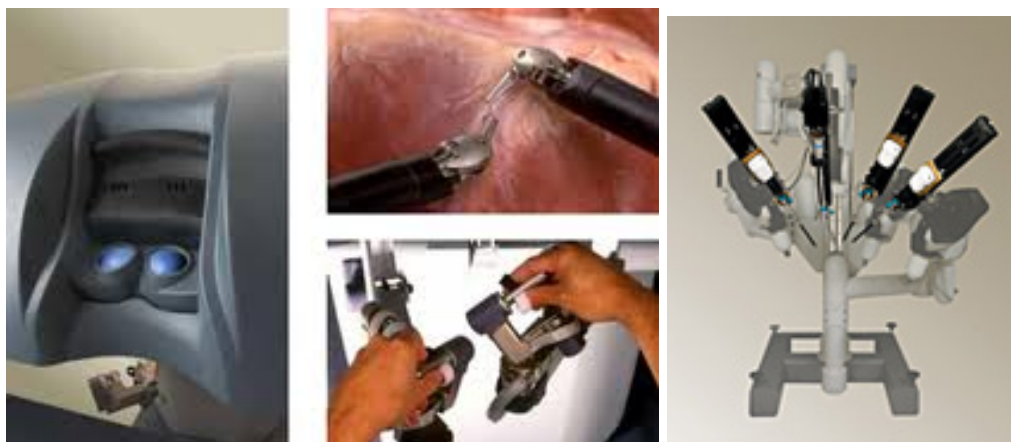


Figure 2.1: Components of the da Vinci Surgical System: from left to right, the master console; handles and instruments; and the slave robot. (Intuitive Surgical Inc., 2010)

In an attempt to fulfill these queries, new research groups and companies are emerging, offering and developing robotic systems for a wide variety of surgical interventions. In this section the most recent developments in the field of teleoperated surgical robotic systems are presented.

The Sensei Robotic Catheter of Hansen Medical is a FDA-approved and commercially available system, an illustration is given in Fig. 2.2. This system targets cardiovascular procedures with a master-slave system in which the robotic catheter is teleoperated by the surgeon through a customized omega.3 device called Instinctive Motion Controller. Their slave catheter is able to measure the force transmitted along the shaft of the catheter as a result of catheter tissue contact (Hansen Medical Inc., 2011). These measurements are displayed visually and rendered as vibrotactile cues to the surgeon through the Instinctive Motion Controller (Force Dimension, 2011).

Currently, a potential competitor to the da Vinci system is about to enter the market: Amadeus ComposerTM, developed by the Canadian public company Titan Medical Inc. (2011). Little is known about this system as the newborn company is putting huge efforts to protect its intellectual property. It is known that the robot has four arms with seven Degree(s) Of Freedom (DOF) each, including the surgical instrument. The company claims that the system will provide force feedback and more dexterity than the current da Vinci system. Its master console, shown in Fig. 2.3, is composed of two haptic devices that are very similar to Quanser's five-DOF Haptic Wand (Quanser, 2011). This haptic interface has five DOF of force feedback allowing for three translations and two rotations (roll and pitch). This is achieved by using a dual-pantograph arrangement.

In May 2008, a surgical robot called neuroArm (Fig. 2.4) made history in the field of neurosurgery by performing the first image-guided robotic neurosurgery to remove a brain tumor (Neuroarm Project, 2008). The slave robot is composed by two Magnetic Resonance Imaging (MRI)-compatible Selective Compliance Assembly Robot Arm (SCARA)-like arms



Figure 2.2: Sensei Robotic Catheter developed by [Hansen Medical Inc.](#) (2011)

and a surgeon's console that can provide force feedback in three **DOF** ([Sutherland et al., 2003](#)).

Several research platforms present highly promising new features. For instance, for abdominal and thoracic **MIS**, the Miro Surge robot developed at [German Aerospace Research Establishment \(DLR\)](#) and the Sophie-robot from [Technische Universiteit Eindhoven \(TU/e\)](#) are very compact when compared with the da Vinci system and aim to render the instrument-organ interaction forces to the surgeon ([Hagn et al., 2010](#); [van den Bedem, 2010](#)). A picture of the Miro Surge robotic system is shown in Fig. 2.5, its surgeon's console features two sigma.7 haptic devices able to provide force feedback in seven **DOF** ([Force Dimension, 2011](#)). The end-effectors of its slave robot, called Mica instruments, integrate a six-**DOF** force sensor in the instrument wrist.

The Sophie-robot surgeon's console, shown in Fig. 2.6, is also bimanual and can render four **DOF** of force feedback ([Meenink, 2011](#)). The same institute developed another interesting system called Eye-robot that targets vitreo-retinal eye surgery. As shown in Fig. 2.7, this system has an easy clipping way to interchange the surgical instruments, it is compact, lightweight, and directly attached to the patient's bed ([Hendrix, 2011](#)). The slave robot integrates a six-**DOF** force sensor (Nano 17, ATI Industrial Automation Inc., NC, USA) to measure the forces that will then be rendered to the surgeon. The Eye-robot shares the previously described Sophie-robot surgeon's console.

The University of Vanderbilt is developing a system to perform endonasal skull surgery. This type of procedure is very challenging because the workspace is extremely small and difficult to reach. This research group proposes a solution that uses tentacle-like concentric-tube continuum robots as tool shafts ([Burgner et al., 2011](#)). These tentacles consist of precurved concentric tubes made of superelastic nitinol, and have diameters comparable to surgical needles. The curve of the tubes inside the patient can be controlled by axially rotating and translating each tube at its base. Each tube has two **DOF** (a rotation and a translation), and



Figure 2.3: Amadeus Composer™ Robotic System developed by Titan Medical Inc. (2011)

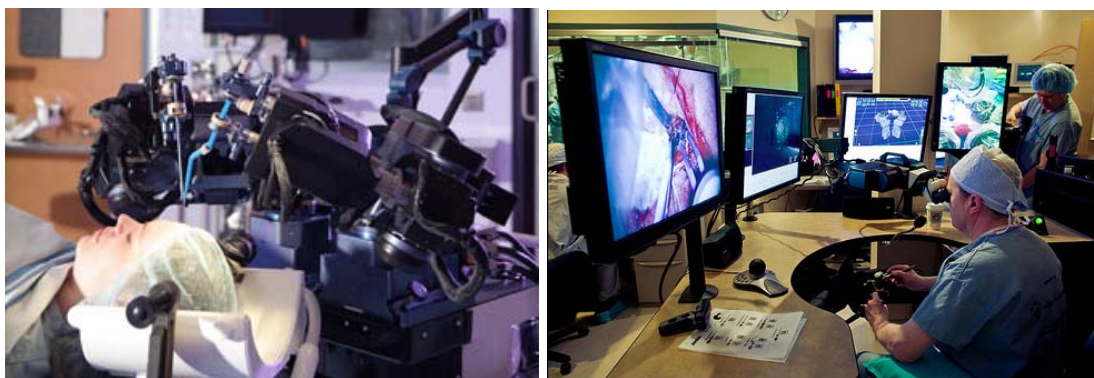


Figure 2.4: NeuroArm project from the University of Calgary (Sutherland et al., 2003)

thus features two actuators. In total, this system provides six **DOF** to position and orientate the instrument introduced through the tubes. The master console is composed of two Phantom Omni devices (Sensable Technologies, 2011). This group is currently conducting research to provide force feedback by measuring the deflection of the end-effector and calculating the forces applied on it.

The Raven Surgical Robot is a two-arm robot with seven **DOF** per arm. It is a cable-actuated surgical manipulator designed to perform both **MIS** and open surgery. This system was developed by a multidisciplinary team of engineers from the University of Washington and the University of California-Santa Cruz (Lum et al., 2009). The slave robot is teleoperated using a single bi-directional **User Datagram Protocol (UDP)** socket via a remote surgeon's console with two Phantom Omni haptic devices (Fig. 2.9). Recently, this group has developed six RAVEN II platforms as an open source platform for research purposes that will be used by different robotics laboratories in the USA.

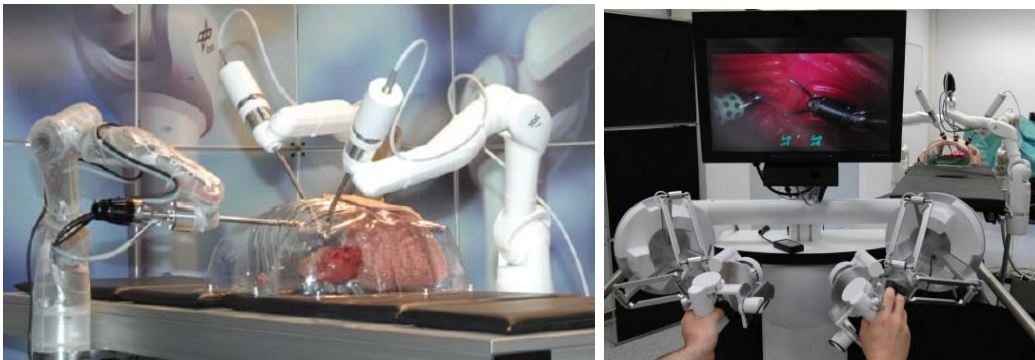


Figure 2.5: Miro Surge system from DLR (Hagn et al., 2010)

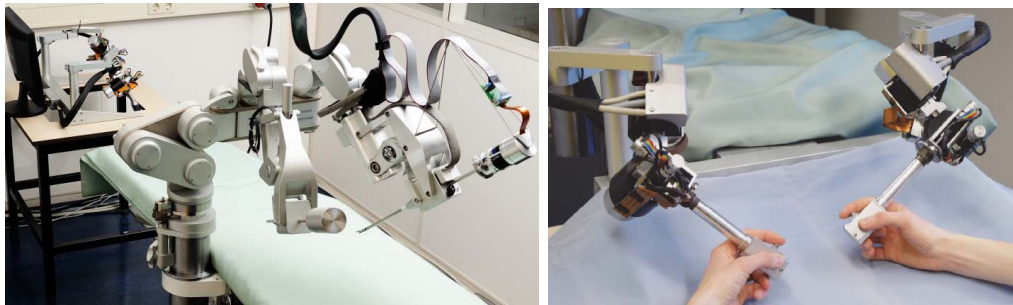


Figure 2.6: Sophie-robot from TU/e (van den Bedem, 2010; Meenink, 2011)

The group of the Prof. Shane Farritor at University of Nebraska-Lincoln has developed a NOTES system that consists in a miniature bimanual robot that is fixed to the abdominal wall of the patient by using external magnets (Lehman et al., 2009). The miniature robot is controlled by the surgeon by using a small console with two joysticks. This system has been tested in animal models. The characteristics of the surgical robotic systems presented in this chapter are summarized in Table 2.1.

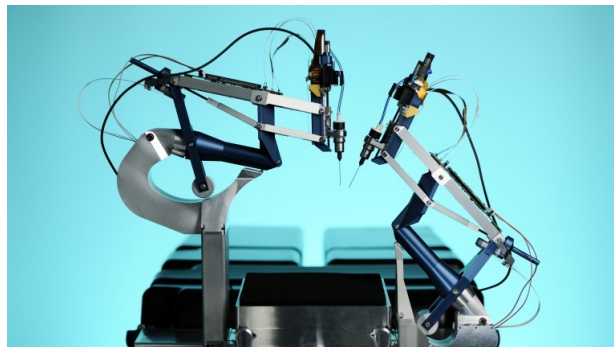


Figure 2.7: Eye-robot from TU/e, the master console is the same as for the Sophie-robot (Hendrix, 2011; Meenink, 2011)

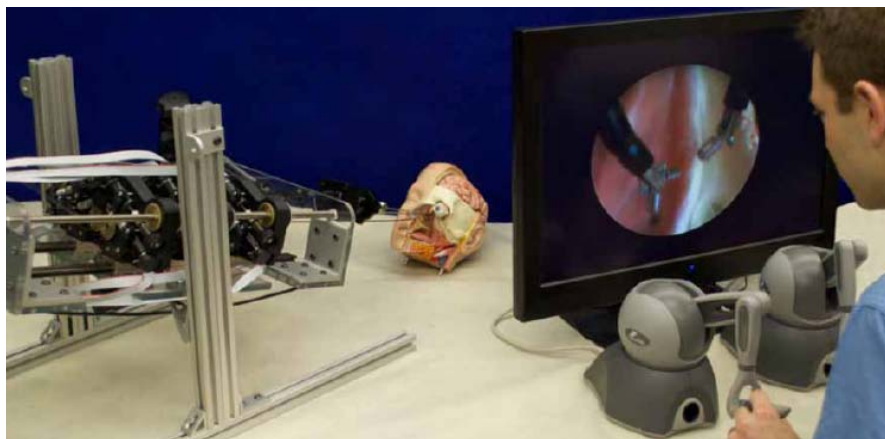


Figure 2.8: Robot for endonasal surgery developed at Vanderbilt University (Burgner et al., 2011)

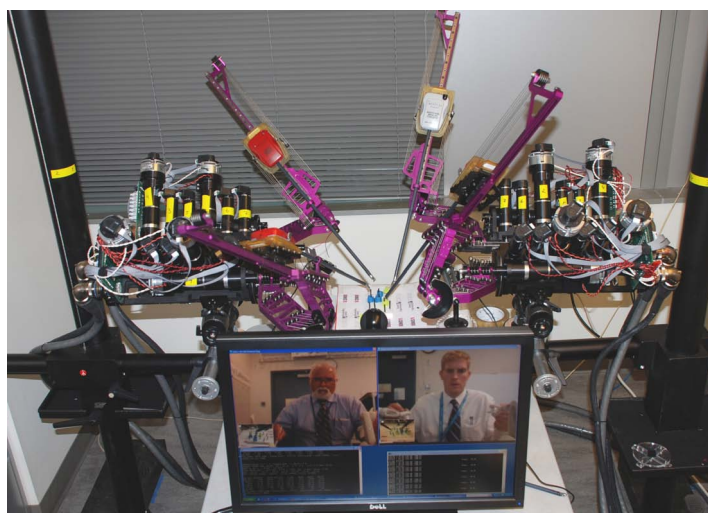


Figure 2.9: Open source surgical robot called RAVEN from the University of Washington and the University of California-Santa Cruz (Lum et al., 2009)

Table 2.1: Summary of current Teleoperated Surgical Robotic Systems

Surgical System	Master		Slave robot		Others	Intended Surgery	Ref.
	Active (A) Passive (P) DOF	Kinematics	Workspace (10^{-3}m^3)	Max. continuous F & T			
<i>da Vinci Surgical system</i> (Intuitive Surgical)	(P) 7	serial	—	—	6 plus the instrument DOF	no	Bimanual. Commercial. Many clinical cases. (Intuitive Surgical Inc., 2010)
<i>Sensei Robotic Catheter</i> (Hansen Medical)	Customized omega.3 (A) 3	parallel	2.2	12 N	6 DOF at the tip and an extra bend articulation	yes	Catheter-based cardiovascular procedures (Hansen Medical Inc., 2011)
<i>NeuroArm</i> (University of Calgary)	(A) 3, (P) 3	serial	—	—	7 plus the instrument DOF SCARA-like	3 DOF	Micro-neurosurgery and stereo-taxy (Sutherland et al., 2003)
<i>Amadeus ComposerTM</i> (Titan Medical Inc.)	Seems to be Quanser (A) 5-DOF Haptic Wand	parallel	2.4	Quanser's data: Fx 2.3 N, Fy 2.1 N, Fz 3.0 N, Tx 0.23 Nm, Ty 0.25 Nm	7 plus the instrument DOF	—	MIS Abdominal and thoracic surgery (Titan Medical Inc., 2011)
<i>RAMS</i> (NASA)	(A) 3, (P) 3	Serial Slave master same kinematics	—	—	6	6-DOF tip-force sensing	Brain, eye, ear, face, and hand microsurgery (Jet Propulsion Laboratory (JPL), NASA, 2011)

Continued on Next Page...

Surgical System	master			Slave robot		Others	Intended Surgery	Ref.
	Active (A) Passive (P) DOF	Kinematics	Workspace ($10^{-3}m^3$)	Max. continuous F & T	DOF (per arm)			
<i>Miro Surge</i> (DLR)	Sigma.7 (A) 7	Parallel plus serial wrist	3.6 (base) $235 \times 140 \times$ 200° (wrist)	20.0 N 0.4 N.m	7	6-DOF MICA instruments	Bimanual. Sigma.7 commercially available. Force sensing in the Master. Lab platform.	(Hagn et al., 2010) (Force Dimension, 2011)
<i>Eye-robot</i> (TU/e)	(A) 4	serial	$\Psi \pm 90^\circ$ $\Phi -88, +45^\circ$ $\Theta \pm 175^\circ$ $Z \pm 8$ mm	Ψ 3 N Φ 3 N Θ 0.049 N.m $Z \pm 2.4$ N	6 plus the instrument DOF	6-DOF (ATI Nanol7)	Bimanual. Lab platform.	(Hendrix, 2011) (Meenink, 2011)
<i>Sofie-robot</i> (TU/e)	(A) 4	serial	$\Psi \pm 90^\circ$ $\Phi -88, +45^\circ$ $\Theta \pm 175^\circ$ $Z \pm 8$ mm	Ψ 3 N Φ 3 N Θ 0.049 N.m $Z \pm 2.4$ N	7	—	Bimanual. Same master device as <i>Eye-robot</i> . Lab platform.	Meenink (2011)
<i>Endonasal robot</i> (Vanderbilt University)	Phantom Omni (A) 3, (P) 3	serial	1.9	0.9 N	6 plus the instrument DOF	Ongoing work ; deflection- based force sensing	Bimanual. Concentric- cube contin- uum robot. Tested on cadaver.	(Burgner et al., 2011) (Sensable Technolo- gies, 2011)
<i>RAVEN</i> (Univ. of Washington & Univ. of California- Santa Cruz)	Phantom Omni (A) 3, (P) 3	serial	1.3	0.9 N	7	Ongoing work	Bimanual. Open-source lab platform. Tested on animal model.	(Lum et al., 2009) (Sensable Technolo- gies, 2011)
<i>NOTES</i> robot (Univ.of Nebraska- Lincoln)	Joystick (P) 3 and but- tons	—	—	—	3 plus in- strument	no	Bimanual Tested on ani- mal model	(Lehman et al., 2009)



Figure 2.10: Phantom Premium 1.5/6 DOF from [Sensable Technologies \(2011\)](#), omega.3 and omega.7 haptic devices from [Force Dimension \(2011\)](#)

2.2 Haptic Devices

As it was shown in the previous section, some of the key features of a teleoperated surgical robotic system depend on the characteristics of the [Human Machine Interface \(HMI\)](#) that compose the surgeon's workstation. As this thesis mainly addresses the addition [haptic feedback](#) a review of the commercially available haptic devices is presented in this section. Some of these devices have already been mentioned in the previous section because they have been already integrated into a teleoperated surgical robotic system. Most of them have been developed for general purposes and do not target a specific field of application. For instance, the Phantom Omni device used in the Endonasal robot (Fig. 2.8) and in the RAVEN robot (Fig. 2.9) is widely used in research platforms for its low price. Phantom Omni is a serial-kinematics haptic device that can provide force feedback only in the three translational [DOF](#) but it can sense the motion of a total of six [DOF](#). The same company ([Sensable Technologies, 2011](#)), produces the Phantom Premium 1.5/6-DOF (Fig. 2.10, left), a full actuated version that provides six active [DOF](#) and achieves higher forces.

The company [Force Dimension \(2011\)](#) offers high performance haptic devices based on parallel kinematics. These devices range from the three-DOF version called omega.3 (Fig. 2.10, center), passing by the omega.7 a seven-DOF interface with only a subset of active [DOF](#) (Fig. 2.10, right), to a fully actuated device called sigma.7. This last device is used by [DLR](#) in the Miro Surge platform previously shown in Fig. 2.5.

[Mimic Technologies \(2011\)](#) is a haptic technology supplier, providing force-feedback hardware and software solutions, primarily to the medical simulation industry. They developed the dV-TrainerTM a simulator of the da Vinci Surgical System that can provide force feedback in the three translations through a cable driven mechanism (Fig. 2.11). The Maglev 200TM haptic device is the first commercial haptic interface actuated by magnetic levitation ([Mimic Technologies, 2011](#)). It can provide high position and force resolution and wide bandwidth but a very limited workspace.

The previous haptic devices are all desktop solutions but for some applications such as teleoperation of big industrial robots, assembly simulation or ergonomic studies, a larger

workspace is required. To satisfy this demand the company **Haption SA (2011)** offers the Virtuouse 6D40-40 and the IncaTM 6D systems. The Virtuouse 6D40-40 is a six-DOF device with serial kinematics that provides a workspace of 40 cm³ (Fig. 2.12, left). The IncaTM 6D is a cable-driven haptic device based on the SpidarTM of Professor Makoto Sato that can provide different workspace volumes depending on the actuator configuration (Fig. 2.12, right). In a configuration of a cube : 3 × 3 × 3 m, the workspace will be 1.5 × 1.5 × 1.50 m with a rotation of ±40 ° in all directions.

Table 2.2 summarizes the most important technical characteristics of the haptic devices mentioned in this section.



Figure 2.11: (left) dV-TrainerTM , simulator of the da Vinci Surgical system with force feedback capabilities (**Mimic Technologies, 2011**) and (right) the magnetically levitated haptic device Maglev 200TM (**Butterfly Haptics, LLC, 2010**)



Figure 2.12: High workspace haptic devices for industrial applications from the company **Haption SA (2011)**: Virtuouse 6D40-40 on the left and IncaTM 6D on the right

Table 2.2: Summary of the presented haptic devices and their technical characteristics

Haptic device	Structure	Workspace (10^{-3}m^3)	DOF	Max. continuous force & torque	Position resolution	Reference
Phantom Omni	serial	1.4	(A) 3, (P) 3	0.9 N	0.055 mm	Sensable Technologies (2011)
Premium 1.5/6DOF	serial	19.4	(A) 6	6.2 N	0.007 mm	
omega.3	parallel	2.2	(A) 3	12 N	< 0.01 mm	Force Dimension (2011)
omega.7	hybrid	2.2	(A) 3, (P) 3	12 N ± 8.0 N (grasp)	< 0.01 mm 0.09 ° 0.006 mm (grasp)	
sigma.7	hybrid	3.6 (base) $235 \times 140 \times$ 200 ° (wrist)	(A) 6	20.0 N 400 mN.m ± 8.0 N (grasp)	0.012 mm 0.013 ° 0.006 mm (grasp)	
Freedom 7	serial	12	(A) 7	2.5 N	0.002 mm	Hayward et al. (1998)
Virtuose 6D40-40	serial	More than 64	(A) 6	30 N 3 N.m	0.02 mm 0.05 °	Haption SA (2011)
Inca TM	parallel structure of cables	3375	(A) 6	15 N 1.5 N.m	0.2 mm	
Maglev 200	magnetic levitation	0.1	(A) 6	40 N	0.002 mm	Butterfly Haptics, LLC (2010)

2.3 Tactile Feedback and Sensory Substitution

One of today's biggest challenges in robotic surgery is to allow the surgeons to differentiate the various types of tissue, perceive the amount of force applied, and generally determine the contour and compliance of organs. This information cannot be rendered by providing only force feedback. The addition of tactile feedback in teleoperated surgery is even more challenging than the addition of force feedback alone. For instance, measuring distributed stiffness and texture requires an array of pressure sensors whereas force feedback may require placement of only a few sensors. Besides, local pressure is only part of the information conveyed by the sense of touch, as it is also sensitive to temperature, texture, roughness, etc.

There are two current trends to provide this information. One approach consists of stimulating alternative sensory channels (e.g. auditory or visual) to display the tactile information to the surgeon. This first approach is called sensory substitution. The second trend is the

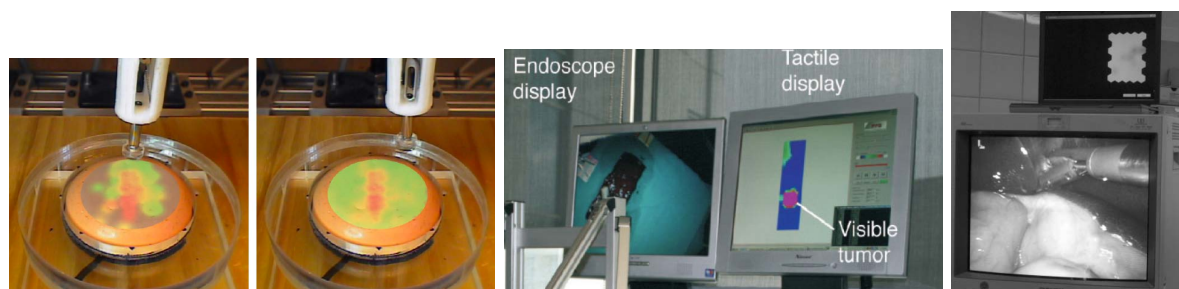


Figure 2.13: Examples of sensory substitution giving tactile information visually during robotic and laparoscopic procedures: (left) Sensory substitution overlying the tissue (Yamamoto et al., 2009), (center) and (left) 2D color-map representing distributed stiffness developed by Trejos et al. (2009) and Schostek et al. (2006) respectively

development of tactile displays rendering directly the tactile stimuli on the surgeon's fingertip.

Sensory Substitution

Sensory substitution is a cost-effective option and is usually easier to implement. This approach is sometimes based on tactile illusions produced by the complex mechanism of sensory integration. This type of illusions has been already used to compensate the lack of certain perceptual information. For instance, it has been found that the visual simulation of a spring and its characteristic stiffness evokes the haptic sensation of a real spring without using a haptic device (Lécuyer, 2009). Generally, when we talk about sensory substitution the tactile information is conveyed as visual or auditory information but it can also be transmitted by a different tactile sensation, generally easier or cheaper to reproduce than the original one. As an example, Konyo et al. (2008) developed a way of rendering friction force using a vibrotactile display without rendering any tangential force. After performing user experiments they saw that the friction perceived with the tactile display was only about one-seventh smaller than the real friction force.

The research group of Professor Allison Okamura has already performed numerous studies that show the potential benefits that this approach could bring to robotic surgery. In the study described in (Kitagawa et al., 2005b), this research group conducted an experiment in which three surgeons performed hand and robot-assisted surgical knot ties. There were four different feedback conditions: (1) directly using the hands, (2) with the surgical robot, (3) surgical robot plus visual sensory substitution and (4) surgical robot plus auditory sensory substitution. They found that visual and auditory cues indicating the force applied improve the consistency of robotically applied forces and results were more similar to the hand knot ties. The same group developed a visual feedback that could be projected over the palpated tissue indicating the local stiffness with different colors (Yamamoto et al., 2009). As shown in Fig. 2.13 (left), with this information, hard objects hidden in the soft tissue could be easily located. The main goal of this system was to localize calcified arteries.

Trejos et al. (2009) integrated a tactile sensor on a robot to perform telepalpation. The

tactile information was shown visually in a 2D-map representing local pressure distribution (Fig. 2.13, center). Users telepalpated a real liver with hidden hard lumps by using both direct manipulation of the tactile sensor and the robotic system. Results showed that by using the robotic system the force applied was reduced by 35% and the detection accuracy increased by 50%.

Schostek et al. (2006) developed a cost-effective tactile sensor that could be integrated into the jaws of a 10 mm laparoscopic grasper (Fig. 2.13, right). The tactile data was transferred via Bluetooth and presented visually to the surgeon. This institute carried out in-vitro and in-vivo experiments to test the usability of the device. The task to fulfill was to localize and identify different hard objects hidden beneath the tissue. In this case, the performance using the instrumented grasper and a normal one was not significantly.

Tactile Displays for Surgical Applications

Ottermo et al. (2008) realized one of the first endoscopic instruments integrating a tactile sensor and a tactile display. The local pressure distribution was rendered to the surgeon by an array of pins located in the handle of the endoscopic instrument (Fig. 2.14, left). These pins were actuated by miniaturized DC-motors. A recent development from Professor Allison Okamura's group targets the detection of hard lumps embedded in soft tissue. This device is able to render lumps under the fingertip with various stiffnesses and sizes by varying the width and the pressure of an air-jet applied into the surgeon's fingertip (Gwilliam et al., 2012).

King et al. (2009) developed a pneumatic array of balloons that rendered the local forces applied by the da Vinci robot grippers on the tissue, using five pressure levels on surgeons' fingertips (Fig. 2.14, right). An experiment was performed in which the subjects were asked to grasp an object with and without tactile feedback. The results indicated that less force was applied when tactile feedback was present. Therefore, the risk of damaging the tissues decreases.

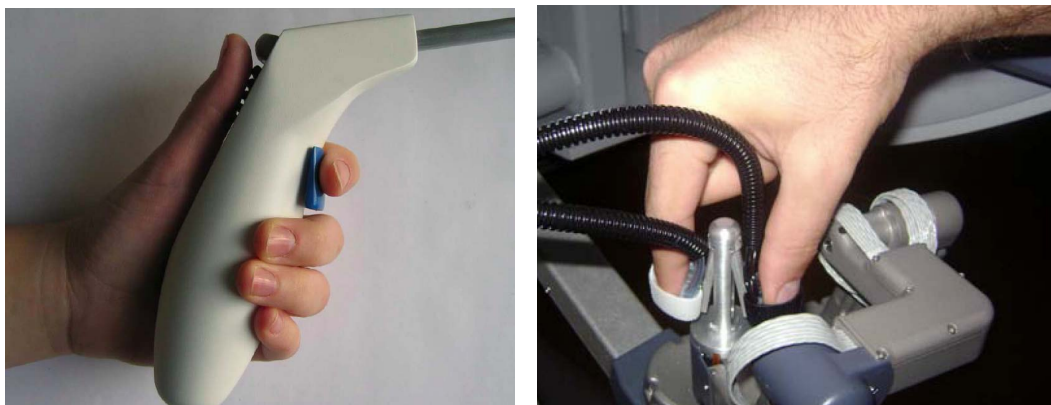


Figure 2.14: (left) Laparoscopic tool handle integrating a tactile display and (right) the da Vinci surgeon's console integrating a pneumatic tactile display (Ottermo et al., 2008; King et al., 2009)



Figure 2.15: The Verrotouch system is composed of two parts: (left) the impact sensors assembled on the slave and (right) the vibrators assembled on the da Vinci surgeon's console [McMahan et al. \(2011a\)](#)

The group led by Professor Katherine J. Kuchenbecker invented a system that measures the impact of the da Vinci robotic instruments on their environment and transmitted them to the surgeon's hands as vibrations (Fig. 2.15). This feedback can be useful while manipulating hard surfaces such as teeth or bones or to render the collisions between the robot end-effectors. In a later study ([McMahan et al., 2011b](#)), this group measured the performance of 11 surgeons during three manipulation tasks (peg transfer, needle pass, and suturing). Each task was performed under four different feedback conditions: with only visual feedback, adding audio cues, adding vibrations and adding both vibrations and audio cues. Surgeons preferred working with the tool impact feedback in form of audio and/or vibrations because it allowed them to be aware of tool actions. However, this additional feedback did not increase the surgeon's performance.

The local temperature of the tissues and organs also give important information about the tissue oxygenation. For instance, tissues in the first stage of necrosis are usually colder than other tissues. Many research groups have investigated the role of temperature or thermal flow sensation in the tactile discrimination of materials and tissues and have developed temperature displays to simulate different materials ([Yamamoto et al., 2004](#); [Guiatni et al., 2008](#); [Ino et al., 1993](#)). Besides, it is known that skin temperature can significantly influence how humans perceive other tactile sensations such as pressure, vibrations, etc. ([Gescheider et al., 1997](#)). Thermal feedback is often underestimated because the humans' response to thermal stimuli it is known to be very slow. However, it has been recently shown that preliminary adjusting the skin can considerably speed up the response time ([Akiyama et al., 2012](#)).

The aforementioned developments show that robotic surgery can potentially benefit from force feedback and from tactile, auditory or visual cues providing tactile information. However, from a technical point of view, we are still far from providing a fully realistic sense of touch. Even though many interesting haptic devices and tactile displays have been developed, the main issues continue to be how to sense the tactile information (temperature, texture, forces) in a compact manner and how to combine this information and render it, in an intuitive way, to the surgeon.

Part I

General and Task-Specific Requirements for Haptic Devices

Chapter 3

Guidelines for the Specification of Haptic Interfaces

Nowadays, visual and audio signals can be easily measured, transferred and reproduced with very high fidelity. But, why is this is still not possible with the sense of touch?

This is due to an intrinsic difference between these sensory channels: sight and hearing senses are passive while the sense of touch is partly active. This means that one can sense visual or audio information about one's physical surrounding without modifying it. By contrast the sense of touch always needs an exchange of energy, produced by the existence of a mechanical contact between the person's body and the outside world (Hayward and Astley, 1996). This exchange of energy explains the bidirectional nature of the sense of touch and it is why the design of haptic devices is extremely challenging.

To develop any interface with the aim of measuring, transferring and displaying to a human user any kind of information (visual, auditory or tactile), it is necessary to understand the sensing capabilities of humans for that specific sensory channel. For instance, due to technological limitations we are not yet capable of reproducing a visual stimulus continuous in space and time, as it actually happens to be in reality. Nevertheless, since the human eyes sensitivity is limited to visual changes up to 30 frames per second, technology has learnt how to exploit this limitation to provide a visual information that is perceived by the user as an accurate reflection of reality. Similarly, the perception (input) limits of the sense of touch in terms of position, motion, forces and tactile stimuli will determine the necessary performance of the device. Besides, as it was previously pointed out, the sense of touch is bidirectional and thus the human motor performance (output) will also determine part of the technical specifications of the haptic device.

This chapter represents a short guideline to collect technical requirements for the design of haptic interfaces based on the human sensorimotor performance and on the application in which the device is intended to be used.

3.1 Requirements Imposed by the Human User

The goal of this section is to describe the human input and output capabilities and the consequent technical constraints.

3.1.1 Human Perception (Input) Limits

Position Perception

The smallest difference that can be perceived by humans is generally called **Just Noticeable Difference (JND)**. In the study of [Tan et al. \(1994\)](#), the reported JND of the joint angles were 2.5° for the finger, 2° for the wrist and elbow and 0.8° for the shoulder. Absolute detection thresholds range from 0.6° to 1.1° for the elbow and shoulder ([Van Beers et al., 1998](#)). However, several studies have shown that the force and position information are generally combined to provide the perception of motion of a limb. In fact, for some tasks, such as the exploration of different shapes, the force perception seems dominant compared to the position perception ([Robles-De-La-Torre and Hayward, 2001](#)).

Technical repercussion: the sensing resolution of the human will determine the necessary output precision of the haptic interface. Therefore, as the finger length for the fifth percentile of women (smaller finger length) is around 60 mm ([Pheasant and Haslegrave, 2006](#)), the positioning error should not exceed 2 mm.

Force Discrimination

The finger force JND between the thumb and the index is in average 7% of the applied force in the range of 2.5 N to 10 N ([Pang et al., 1991](#)). Regarding the torque resolution, [Jandura and Srinivasan \(1994\)](#) determined a mean torque JND of 12.7% for 60 mN.m reference torque.

Technical repercussion: the input force resolution of the user determines the output force precision of the haptic device. Therefore, to have smooth force transitions, the minimum increments of force must be below 0.15 N. This value is determined by the finger force JND at low frequencies.

Proprioceptive and Kinesthetic Bandwidth

The bandwidth of human proprioception of position and forces applied on the joints is between 20 and 30 Hz ([Brooks, 1990](#); [Leist et al., 1987](#)). However, the human tactile sense has a much higher bandwidth and can detect vibrations up to 1 kHz ([Tan et al., 1999](#)).

Technical repercussion: the haptic device should avoid producing unwanted vibrations under 1 kHz because they would be felt by the user and consequently decrease realism. Producing forces or motions at higher frequencies would not increase realism.

3.1.2 Human Motor (Output) Limits

Motion Production

Little information exists on the maximum velocity produced by human joints or maximum velocities achieved during representative manipulation tasks. [Hasser \(1995\)](#) measured the maximum metacarpophalangeal joint speed across different subjects and the obtained averaged was about 17 rad/s. [Gassert et al. \(2006\)](#) proposed 30 cm/s as a guideline for devices that were moved with the whole arm.

Technical repercussion: maximum velocity can be useful as an upper bound for no-load velocities of a haptic device. Acceptable no-load velocities are especially important for systems that are not backdrivable or that must compensate for friction and inertia.

The human's output bandwidth of movements ranges from 2 to 12 Hz: the values reported are between 2 and 4 Hz for voluntary movements ([Neilson, 1972](#)), ranging from 4 to 8 Hz during skilled actions like hand writing, typing or playing musical instruments ([Kunesch et al., 1989](#); [Jones, 2000](#)), 10 Hz for reflexive movements and between 8 and 12 Hz for finger tremor ([Safwat et al., 2009](#)).

Technical repercussion: as it will be discussed later (Section 3.2, about the impedance range) the haptic interaction should be evaluated in this range of frequencies (1 to 10 Hz). A study of the behavior of the system above these frequencies would be important for a standard robotic device. However, for a haptic interface, high frequencies matter only when it comes to rendering textures with a kinesthetic interface.

Force Production

Human strength depends on a lot of parameters (muscle under study, gesture, gender and age of the subject, etc.) and therefore there is a high variety of information available in the literature. The maximum grasping forces generally range from 80 to 100 N for men and from 60 to 80 N for women ([Swanson et al., 1970](#); [Mathiowetz et al., 1985](#)). The tests performed by [Tan et al. \(1994\)](#) reported the following maximum values: 50 N exerted by the finger, 65 N exerted by the wrist and 100 N exerted by the elbow and the shoulder. Force control resolution is a measure of the precision with which the subject can produce a target force. It has been found that humans can control larger forces with a smaller percentage error than smaller forces: 2% of error for forces between 10 to 50 N ([Tan et al., 1999](#)) and 16% of error for a force of 0.25 N ([Srinivasan and Chen, 1993](#)).

Technical repercussion: in order to preserve the human performance, the maximum force exerted by the device should meet or exceed the maximum force that the user can produce. However, as it will be shown later, maximum forces sometimes have to be decreased to guarantee the ergonomics of the task.

Regarding the human force output, the literature generally reports a bandwidth ranging from 2 to 7 Hz ([Jones and Hunter, 1990](#); [Jones, 2000](#); [Brooks, 1990](#)).

Technical repercussion: the bandwidth of the device when it is backdriven by the operator should at least match the force control bandwidth of the human and thus it should be above 7 Hz.

3.1.3 Transparency

If the user has the feeling of [telepresence](#), the manipulation of the remote or virtual environment will be more intuitive as the physical separation between master and slave is not perceivable. In order to enhance telepresence, the user should not feel the physical properties of the teleoperation system itself. In other words, the inertia, stiffness, friction, time delays and other artifacts should be “invisible” or “transparent” to the user. This idea leads to the concept of [transparency](#), which is used to quantify the fidelity with which the haptic properties of the distal objects are rendered to the user ([Lawrence et al., 1996](#)).

Technical repercussions:

- Low backlash: the transmission system has to be carefully designed. Generally, [direct drive](#), [friction drive](#) and [capstan or cable drive](#) solutions are chosen instead of gears because they are backlash free.
- Minimum inertia: ideally, to achieve a robust causal relationship between the input force and the perceived motion, the inertia of the haptic device should be less than the inertia of the finger tissue deformed by the device ([Hayward et al., 1994](#)). Furthermore, in order to provide a good degree of realism while rendering shocks and rapid changes of velocity, the device should provide high and uniform acceleration ([Hayward and Astley, 1996](#)). This should be taken into account when selecting the actuators but also means that the inertia of the device should be minimized.
- Structural response: the lowest natural frequency should be higher than the needed frequency response. A study performed by [Campion and Hayward \(2005\)](#) found that the ability of a kinesthetic device to render a texture is not only affected by the resolution or the sampling rate but also, and mainly, by the structural response of the device.
- High stiffness: as for any robotic system, high structural stiffness is desired because a stiff transmission including links and joints provides a reliable calculation of the end-effector position and better structural response under dynamic loading. The structural stiffness of a haptic device can be measured by blocking all the joints and measuring the deflection of the end-effector while applying a known external load.

3.1.4 Safety

In contrast to industrial robots that operate in a “safe mode” when an operator is in its surroundings (e.g. working at lower speed), the haptic interfaces physically interact with a human subject using their full dynamic capabilities. To prevent accidents that could cause

harm to the user (and to the patient in the context of surgical robotics), redundant safety measures must be implemented: mechanical stops to limit the movements, software limitation of motor command values, activation of brakes when high speeds or instabilities are detected, redundant sensors, etc. Generally, a continuous force produced by the interface should not be larger than those required by the targeted task. Only in some cases, the forces exerted by the slave robot to perform the task must be scaled to a comfortable range for the operator (e.g. forces should be scaled up for nano-object telemanipulation and scaled down for the teleoperation of mining machines).

Another dimension of safety that should be considered is ergonomics. As for any HMI design, a haptic device should fulfill special ergonomic requirements to optimize human well-being and the overall system performance. An ergonomic design should prevent the user from adopting any posture or movement that could induce fatigue, pain or physical trauma disorder. This topic will be discussed in detail in Chapter 7.

3.2 Task-Specific Requirements

Degrees of Freedom and Workspace

The number of DOF and the workspace of a haptic device are task-specific. For instance, for the sake of realism, any haptic device for a simulator should imitate the real task mobility conditions (e.g. a laparoscopic simulator must emulate the fulcrum effect and the workspace constraints of the trocar (Baumman, 1997)). Similarly, in teleoperation, the workspace and the number of DOF are generally imposed by the task that the slave robot will perform. In this aspect, redundancy is usually avoided because each additional DOF increases significantly the cost and the complexity of the system.

Manipulability

The term *manipulability* was introduced in the robotic field by Yoshikawa (1985). This concept characterizes the ability of a serial kinematic chain - robotic manipulator or natural limb - to move quickly its end-effector in any direction of its workspace in response to given joint velocities. In a point of the workspace with zero manipulability, the robot end-effector cannot be moved in any direction. By contrast, a non-zero manipulability expresses the possibility for the robot end-effector to be moved in some directions of its workspace, the maximum manipulability being reached if the end-effector can be moved in any direction with high velocity.

This performance metric is widely used to characterize robotic manipulators. The *manipulability* (μ) is defined as

$$\mu = \sqrt{\det(\mathbf{J}\mathbf{J}^T)} \quad , \quad (3.1)$$

where \mathbf{J} is the Jacobian, which is a matrix that represents the relationship between joint space velocities and task space velocities $v = \mathbf{J}(q)\dot{q}$.

Impedance Range

The impedance range represents the ability of the device to render a wide range of impedances from free movement all the way up to a stiff wall. The inherent impedance of the mechanism or the actuators may reduce the impedance range, which means decreasing the range of possibilities being afforded (for example when the maximum stiffness that can be rendered is limited or when parasitic friction is present and a free movement should be rendered). The impedance range of a haptic device can be assessed as a function of the frequency, which is called the Z-width (Colgate and Brown, 1994).

The Z-width is bounded by the minimum impedance as lower limit. The minimum impedance represents the relation between the lowest damping forces for a given velocity input when rendering a free movement (i.e., the desired output force of the haptic device is zero). The minimum impedance over frequency can be measured by exciting the end-effector of the device while the haptic interface renders zero impedance or zero interaction force.

The upper limit of the Z-width, maximum impedance, is the highest possible gain that can be rendered without any human induced control instabilities by voluntary motion. The maximum impedance can be obtained by measuring the contact force and velocity produced when the user is tapping a very stiff wall. This excitation can be considered as an impact. Analyzing the resulting force and velocities using a system identification method provides the maximum impedance with respect to frequency (Samur, 2010). As it was mentioned in Section 3.1.2, the human hand motion is limited to 10 Hz, therefore, when using this method the Z-width obtained will be limited between 0 and 10 Hz.

Sensor/Actuator Asymmetry

A DOF of a force feedback device can be either active (equipped with actuators to provide force feedback) or passive (equipped only with sensors to measure the movement). When both types of DOF are present in one device, there is the so-called sensor/actuator asymmetry. This type of design is often chosen to reduce the complexity of the device while keeping full mobility (six or seven DOF per hand). Therefore, only a subset of the DOF provides force feedback, usually for the translational forces, while the remaining DOF are equipped only with position sensors.

Some examples of commercial devices presenting this actuator/sensor asymmetry are the Phantom Omni (*Sensable Technologies*, Woburn, MA, USA) with six sensors and three actuators, and the omega.7 (*Force Dimension*, Nyon, Switzerland) with seven sensors and four actuators. As it was mentioned in Section 2, these devices can be suitable for many applications including surgical robotic platforms, and their cost is considerably low compared to the fully actuated versions (Seibold et al., 2008).

In their pioneering work, Barbagli and Salisbury (2003) considered the effect of sensor/actuator asymmetry in haptic devices. Their results reveal that sensor/actuator asymmetry may lead to non-conservative forces in specific situations and therefore can decrease

realism. Semere et al. (2004) performed an experimental study to determine the effect of this sensor/actuator asymmetry during a blunt dissection. One of the conclusions to be drawn from their work is the improvement of the performance after adding partial force feedback. In a later study from the same group (Verner and Okamura, 2007), performance and applied forces during a peg-in-hole task were analyzed to evaluate the effect of the grip force. In this case, feedback on the grip force helped the subjects to apply the minimum force required to hold the peg. Regarding the addition of torque feedback, the results of recent studies differ depending on the application. Verner and Okamura (2009) reported that for simple tasks such as drawing or writing in a 3D virtual environment, the performance with force feedback alone was similar to the performance obtained when the device rendered both force and torque feedback. However, in other applications in which forces and torques are decoupled, the torque information might be crucial. For instance, it is proven that the torque feedback provided by the steering wheel of the car has a direct implication on the driver performance since it carries information related to the vehicle dynamics (Toffin et al., 2007). Furthermore, if the visual information is limited or unreliable, users mainly rely on the haptic information (Ernst and Banks, 2002). As an example, during screw insertion in a teleoperated spinal-fusion surgery, both torque and force feedbacks are necessary to successfully achieve the task (Lee et al., 2009). The results of these studies show that the effect of sensor/actuator asymmetry mainly depends on the task to be carried out.

3.3 Quantifying the Level of Telepresence

In this section, the general methods that have been used to assess telepresence are briefly described. The assessment of the telepresence of a teleoperated robotic system is complex because it depends on both the system and the user. Therefore, both objective and subjective measurements are needed for a complete evaluation. An objective measurement of telepresence is the performance of the operator on a given task (reaction time to a given stimulus, task-completion time, error rate, etc.). This type of measurement should be chosen depending on the nature of the task and how the quality of the results is assessed in that specific application. For instance, accuracy can be more important than completion time (brain surgery) or the opposite (reaction to an alarm). A subjective measurement can generally only be acquired through a questionnaire inquiring about the user's feelings and preferences. Post-experiment questionnaires to address these items were given in each of the studies performed within this thesis.

In some applications such as neuroscience or the treatment of phobias with VR setups, physiological measurements such as heart rate, Electroencephalography (EEG), breathing rate, galvanic skin response are useful: as they are not affected by the subject's bias, they can be considered as objective, contrary to behavioral measurements which are more subjective. (Riva et al., 2003). Physiological measurements have not been addressed in this work. As it will be shown in Section 8.6, electromyography measurements have been performed but with a different goal: the ergonomic assessment of a prototype.

Another way of assessing agency and hand ownership investigating visuo-tactile integration is the so-called **Cross-modal Congruency Effect (CCE)** (Pavani et al., 2000; Zopf et al., 2010). During a typical **CCE** experiment the subject holds with both hands a foam block that integrates visual cues (lights) and vibrotactile cues near the thumbs and index fingers. Subjects are then asked to identify where they receive the vibrotactile stimulus (index or thumb) while ignoring the visual stimuli (Spence et al., 2004; Aspell et al., 2009). The latency of response due to the incongruence between the two stimuli indicates the level of agency. Recently, **CCE** have been tested in a robotic environment under active movement conditions (Rognini et al., European Journal of Neuroscience, under revision). This work found a modulation of **CCE** related to changes in ownership and agency of one's own moving upper limbs.

Since a high degree of **transparency** is a necessary but not sufficient requirement for **telepresence**, it becomes also an indirect measurement of it. A measurement of transparency usually requires comparing the real information of the remote environment with the information rendered to the operator. When an evaluation of the whole teleoperation system cannot be performed, as is the case in this work, the best approach is the quantification of the mechanical artifacts that could affect transparency: inertia, friction, backlash, workspace, etc.

3.3.1 Psychophysical Assessment

The most conventional performance metrics are accuracy or error rates measurements and task completion time adapted to the nature of the task. In some cases this type of measurement might not be sufficient to quantitatively compare the effectiveness of different feedback types or haptic devices. Psychophysical measurements characterizing the human-interface interaction have been broadly applied for this purpose (Hannaford et al., 1991; Samur, 2010; Wall and Harwin, 2000; Chun et al., 2005). In this thesis two psychophysical methods have been used: the **Absolute Identification Paradigm (AIP)** and Fitts law.

Absolute Identification Paradigm

The **AIP** is used to assess the information transmission capacities of different feedback types for a specific identification task. The measurement of the **Information Transfer (IT)** quantifies the amount by which uncertainty has been reduced and is easily applicable to experiments in which subjects must differentiate one stimulus from a set of alternatives (Tan et al., 2010). This paradigm has been used to compare the performance of various haptic devices in tasks in which the user should identify different 3D shapes (Tan, 1997; Samur et al., 2007b). Tan (1997) applied the **AIP** to sphere size identification for human performance estimations and the results were presented in bits of **IT**. During a manual identification task they showed that humans could correctly identify a maximum of four sphere sizes, which corresponds to an **IT** of 2 bits.

In the **AIP**, to k stimuli $(S_n)_{1 \leq n \leq k}$, correspond k correct responses $(R_n)_{1 \leq n \leq k}$ in a one-to-one mapping. The stimuli are presented in a random order and the subject is instructed to respond to each stimulus S_n with the corresponding R_n . In general, this means that the user

must identify the stimulus.

The maximum likelihood estimate of Information Transfer (IT_{est}), for a particular response pair (S_i, R_j) is given as

$$IT_{\text{est}} = \sum_{j=1}^k \sum_{i=1}^k \frac{n_{ij}}{n} \log_2 \left(\frac{n_{ij} \cdot n}{n_i \cdot n_j} \right) \quad [\text{bit}] \quad (3.2)$$

where n is the total number of trials, n_{ij} is the number of joint events in which the pair (S_i, R_j) occurs, n_i represents how many times the stimulus S_i was presented and n_j represents how many times the subject gave the response R_j (Tan, 1997).

Limitations: the IT obtained with this method is limited to the number of stimuli presented during the experiment, which is generally low in order to allow the subjects to remember the different possibilities available during the test (i.e the four sphere sizes used by Tan (1997)). This means that the real information transfer capability of the device might be much higher than the one obtained by this method. However, using AIP to test different devices under the same experimental conditions allows one to quantify the loss of information of each of them and compare them. Therefore, AIP is a useful method to compare the perception performance of the user while using different devices but it is not accurate enough to quantify the absolute performance of the device itself.

Fitts Law

Fitts (1954) applied the concept of information theory to the human psychomotor behavior. He determined that the Movement Time (MT) to displace a physical stylus from a home position to a stationary target is related to the movement amplitude (A) and the target size (W). These two dimensions, described in Fig 3.1, define the Index of Difficulty (ID) of the motor task in bits.

Fitts defined the relation between ID and MT as follows:

$$MT = a + b \cdot ID \quad [\text{s}] \quad (3.3)$$

$$ID = \log_2 \left(\frac{A}{W} + 1 \right) \quad [\text{bit}] \quad (3.4)$$

To make the analogy to communication theory, the user is said to transmit a certain amount of “bits of information” while performing this movement. If the number of bits is divided by the MT, the transmission rate (in bit/s) can be determined, see Eqn. 3.5. This transmission rate is the so-called Index of Performance (IP):

$$IP = \frac{1}{b} \quad [\text{bit/s}] \quad (3.5)$$

The maximum IP corresponds to the limit where $b \rightarrow 0$, i.e. when the regression line between MT and ID is horizontal (MT is independent of ID). This means the user performs the task in the same time whatever the ID of the task.

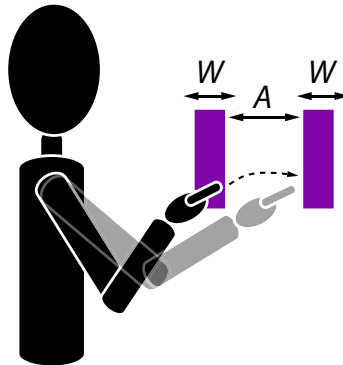


Figure 3.1: Motor task proposed by Fitts. The distance between home and target (A) and the width of the target (W) are the variables that define the Index of Difficulty (ID) of the task.

Paul Fitts conducted three different experiments in his study: the above-mentioned stylus-tapping task with two different stylus weights (1 oz and 1 lb), the disc transfer task and the pin transfer task. The latter two tasks were more demanding in terms of target difficulties, and resulted in higher intercept values (a) for similar values of IP .

This law has already been used in a variety of studies of human-computer interaction such as the performance evaluation of a kinesthetic device (Hannaford et al., 1991), the development of a systematic evaluation for haptic interfaces (Samur et al., 2007b), the comparison of visuo-haptic workstations for surgical simulators (Chun et al., 2005). Besides, it has been successfully applied to assess the benefits of force feedback in human's performance (Wall and Harwin, 2000) and to adjust the difficulty of an exercise for upper-extremity rehabilitation (Zimmerli et al., 2012).

Several research groups have performed refinements of Fitts model and reformulations of the ID in order to adapt it to more complex tasks involving more degrees of freedom (MacKenzie and Buxton, 1992) or different speed-accuracy tradeoffs (Zhai et al., 2004).

Limitations: Fitts Law has been broadly applied to evaluate the performance of haptic interfaces. However, similarly to the AIP method, Fitts Law does not provide an absolute measurement of the performance of a limb or a device, it is rather a comparative tool for studying different devices or interaction techniques. One can conclude that a device with a higher index of performance would be faster and thus it is presumably better.

Another important point to discuss is that this empiric law initially explained the user's behavior during a motor task performed almost in open loop (force feedback gave information about the stylus weight and when the user tapped the target, and therefore it only affected the intercept value). However, its adaptation to a peg-in-hole task in which the user has to insert a peg in a target hole, the force feedback is not very significant during the movement but it is present during the whole peg insertion which is a sub-task performed in close-loop. Even

though this adaptation is sometimes subject to controversy, several of the above-mentioned studies have successfully adapted Fitts law to a peg-in-hole task, allowing them to compare users' performance using different interfaces (Samur et al., 2007b; Chun et al., 2005). The measured data in those experiments can often be fitted with a straight line with a correlation coefficient of 0.95 or higher. This indicates that the model is also accurate to predict task completion time with respect to the difficulty for a the peg-in-hole task.

3.3.2 VR-based Testbeds

In order to investigate the influence of different feedback modalities on the user's performance during teleoperated robotic surgery, the ideal setup would be to use the whole teleoperation system. However, it has been shown that when experiments are performed through a teleoperated robotic system, the results are affected by the technical limitations of the slave robot. In the experiment performed by Feller et al. (2004), the subjects palpated a phantom tissue using direct manipulation and a teleoperated robot. Their results showed that performance using the robotic system was highly dependent on the distal exploration force. Therefore, the scale of forces between master and slave, the applied forces and the tactile sensors can greatly influence the results. In a similar experiment, Talasaz et al. (2010) affirmed that their tactile sensor was sensitive to the inconsistency of applied force provoking false positives when trying to find hidden hard lumps in a bovine liver. The same research group found that when using a robotic system to find hidden lumps, the applied forces decreased by 35%. However, they also found that this result was affected by the control scheme of the robot (force control performed better than position control) (Trejos et al., 2009).

Another approach is to develop a VR-based testbed that simulates the task to be accomplished and behaves as if the performance of the "slave part of the system" was perfect. The use of VR-based testbeds allows us to control and preserve the same experimental conditions for all subjects (e.g. tissue properties, instrument orientation, etc.). Besides, it offers the possibility to randomize the order of the feedback type and other factors during the experiment. Consequently, subjects cannot know which feedback or environment will be displayed next, avoiding a bias in their attention. For these reasons, the assessment experiments that will be presented in Chapters 4, 5 and 8 are all performed on VR-based testbeds.

The degree of simplifications of each testbed depends on the surgical task. VR-based surgical simulations are complex because the interaction force between a surgical instrument and an organ is generally nonlinear. In some cases, the force while indenting the surface of a soft tissue can be simplified to a linear model. However, when the instrument-organ interaction involves cutting or piercing the organ this simplification is no longer valid as the tissue itself is being modified. Several approaches have been proposed in the literature to deal with these situations. For a cutting task, Mahvash and Hayward (2001) proposed an approach inspired from fracture mechanics methods to calculate the interaction force by measuring the instrument displacement. This way the problem was reduced to the existence of three distinct interaction phases. To provide an accurate force model of each phase, the cutting forces were previously measured in a real cutting task. Similarly, Barbé et al. (2007a) and Okamura et al.

(2004) measured the interaction forces during a needle insertion in soft tissue to propose a multiphase force model based on energy thresholds and needle displacement. For even more accurate simulations, fast modeling algorithms (Wang, 2009), multi-rate virtual environment solving local models at different frequencies (Mahvash and Hayward, 2005) and simulations based on finite element analysis with a hierarchical mesh have also been proposed (Astley and Hayward, 2000).

Chapter 4

Influence of Force and Torque Feedback on Accuracy and Execution Time in a VR-based Suturing Task

To design the optimal haptic device for a surgeon's console, the catalogue of solutions should be task-specific. Therefore, the surgeon's actions must be decomposed into basic hand gestures in order to identify which active **DOF** are crucial, and which **DOF** can be inactive, to decrease overall system complexity and cost. The most frequent tasks executed by surgeons during a common surgical procedure are resection, grasping, suturing, ablation and injection (Nio et al., 2002). Most of these tasks are carried out by translating the hands in the three dimensions. The orientation of the tool remains almost invariable during the translations. This implies that the surgical device must have seven **DOF** to position tools (three for translations, three for orientations and one for the grasping movement). However, it might be necessary to provide force feedback only in the translational **DOF** and in the grasping movement, but no torque feedback since the orientation is rarely changed while the task is performed. Nevertheless, as illustrated in Fig. 4.1, while suturing, to insert the arc-shaped needle into the tissue, surgeons execute a pure rotation of their wrist around its pronosupination axis (Iwamoto et al., 1993; Seki, 1988). Therefore, torque feedback could help the surgeon to correct the tool trajectory and to apply the correct forces, thus improving suturing quality.

There are many surgical procedures where sutures are essential, for example, the repair of liver lacerations or during cardiac procedures. Besides, when suturing less delicate wounds, such as in dermatologic surgery, both cosmetic and functional results can be compromised if the execution is poor. Kitagawa et al. (2005a) investigated the effect of sensory substitution in suture-manipulation forces for surgical robotic systems. In this study, applied forces during a knot-tying task were measured in several sensory substitution scenarios. Results showed that when force feedback was substituted through visual or auditory modes, the applied forces

approximated suture tensions achieved by manual suture. However, the trajectory of the needle during the insertion was not analyzed.

This chapter presents a task study to determine the minimum number of active **DOF** that the surgeon’s haptic console should have to improve the accuracy of the needle insertion and thus to improve suturing performance. Two rounds of experiments were performed with 10 subjects, including six with medical background. The main results showed that feedback conditions, including force feedback, significantly improved the accuracy independently of the operator’s suturing experience. There was, however, no further significant improvement when torque feedback was added. Consequently, it was deduced that force feedback in translations can improve subject’s dexterity, while torque feedback might not further benefit in such a task.

This study has been published in Santos-Carreras et al. (2010a). It should be pointed out that for the sake of consistency in the methodology throughout the thesis, the statistical analysis done in this chapter is slightly different from that of the article. In this chapter, repeated measures **Analysis of Variance (ANOVA)** is used without the factor of “individual subject” as it is well known to be always significant and does not provide any additional contribution to the conclusions. Nevertheless, the main results and conclusions are in agreement with those of the article.

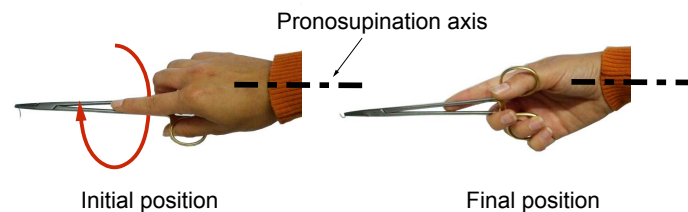


Figure 4.1: Wrist rotation around the axis of the forearm during needle insertion (pronosupination)

4.1 Methods and Protocol

4.1.1 Hardware

Specifications

For this specific task, four **DOF** were required; three translations to position the suturing needle on the suture location and an extra **DOF** to rotate the arc-shaped needle around its center. According to wrist mobility anthropometric data, at least 220° should be provided to allow for a full rotation around the pronosupination **DOF** of the wrist (Pheasant and Haslegrave, 2006).

The forces measured during needle insertion and soft tissue indentation reported by Okamura et al. (2004) and Samur et al. (2007a) were taken into account to select the actuation of

the device. The maximum force on the needle tip found by Okamura et al. (2004) was 2.3 N. Therefore, for a conventional arc-shaped needle as the one used by Iwamoto et al. (1993) (with an arc diameter of 14.5 mm) the maximum peak torque that the motor should provide is 30 mN.m

Prototype

The haptic device used in the experiment was an omega.3 (Force Dimension, 2011). A dedicated handle allowing the extra DOF for the pronosupination of the wrist was developed and attached to the omega.3 device (Fig. 4.2, left). The handle used was a real needle holder to preserve the ergonomics of a normal suture. To guarantee the same performance of the haptic device for all the suture locations, the suture points were located within the boundaries shown in red in Fig. 4.2 (right).

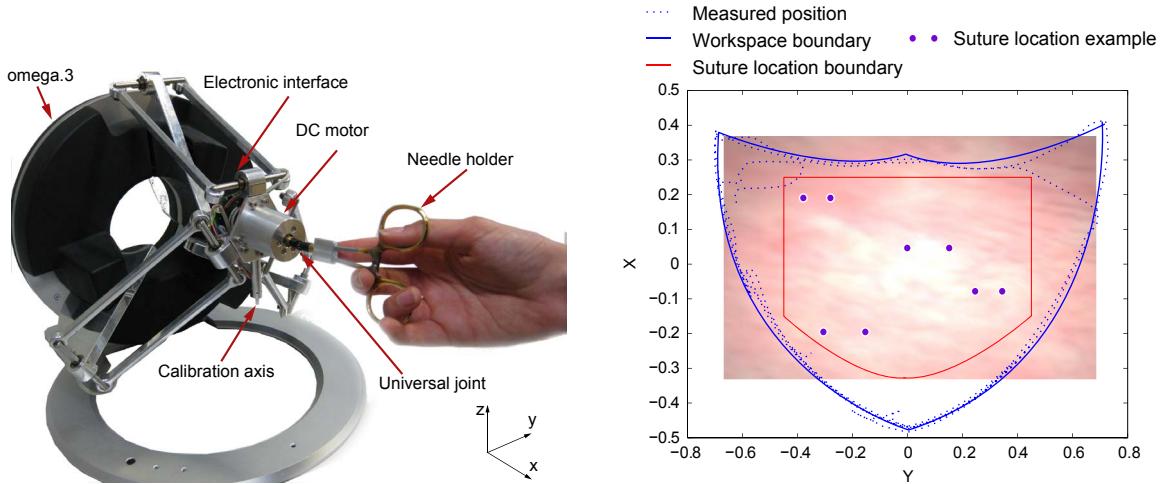


Figure 4.2: (left) The customized handle added to the omega.3, provides torque feedback in the pronosupination DOF of the wrist; and (right) suture location boundaries (in red) with respect to the omega.3 workspace (in blue) in the horizontal plane passing by its center ($Z=0$).

An RE25 motor (*Maxon Motor AG*, Sachseln, Switzerland) with a magnetic encoder (1000 Counts Per Turn (CPT)) was chosen for the dedicated handle. The nominal torque of this motor is 29.2 mN.m, fulfilling the force specifications mentioned before.

The torque feedback module was carefully designed to minimize the mechanical artifacts that could affect the device transparency. As shown in Table 4.1, the actuator and the transmission components present very low friction, inertia and backlash. In addition, in order to preserve the performance of the entire device, the mass of the torque feedback module was adjusted in the compensation algorithms of the omega.3. The torque module was individually calibrated to ensure repeatable and optimal precision and performance.

An electronic interface was developed in order to avoid the requirement of an additional

Table 4.1: Characteristics of the torque feedback module components

Parameters	Motor	Universal joint	Handle
Radial play (mm)	0.025	Backlash free	Backlash free
Axial play (mm)	0.05	Backlash free	Backlash free
Weight (g)	130	0.7	23
Inertia (g.cm ²)	10.5 (rotor)	0.03	–

USB connection. This solution permits the use of the original motor amplifiers of the haptic device and consequently the synchronization with the rest of the actuators could be guaranteed.

Since the aim of this experiment was to determine if the specific torque along the pronosupination **DOF** improved performance, the other two rotations for the wrist orientation were kept invariant in the simulation. Therefore the pitch and yaw orientations were not tracked by any position sensor. As shown in Fig. 4.2, the suture points were always parallel to the base of the omega.3 to avoid a transparency decrease due to the constrained rotations.

Preliminary trials showed that a rigid horizontal tool results in an unnatural wrist posture. For this reason, a universal joint was added between the actuator and the needle holder to allow for small deviations in the subjects' wrist orientation (Fig. 4.2, left). Nevertheless, subjects were instructed to keep the orientation of the other rotation axis essentially unchanged. Alignment deviations of a few angular degrees were tolerable in the framework of this experiment.

4.1.2 VR-based Testbed

The **VR**-based testbed was kept as simple as possible to reduce the influence of unknown factors such as: differences on the tissue depending on the organ, the shape of the tissue, etc. In the experiment, sutures were performed with only one hand, although surgeons usually grip the tissue with one hand and suture with the other. The main motivation for this choice was to avoid the influence of how the tissue was grasped. The virtual tissue was flat, differing from a real suture task where surgeons insert the needle into the edge of the grasped tissue.

The **VR**-based testbed consists of a soft tissue and a needle holder with a fixed arc-shaped needle (Fig. 4.3). The needle holder is a virtual copy of the real holder used for the experimental handle. The surgical needle is an arc-shaped needle, commonly used for skin, peritoneum and muscle sutures. The shadow of the tool on the tissue was added to provide additional visual perception of depth to the subject. The shadow was found to be a crucial cue for subjects to target the given entrance point of the suture during the experiment.

The soft tissue was modeled as a mass-spring-damper mesh and the needle arc was decomposed into 10 connected segments. A bounding sphere was created around the needle tip using the length of the spring of the soft tissue. Whenever a tissue node was located inside

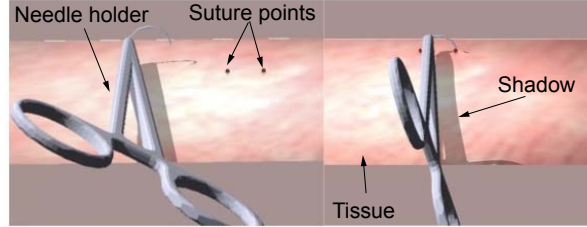


Figure 4.3: Virtual suturing testbed. Users used the shadow to position the needle near the indicated entrance point. The suture was performed towards the indicated exit point.

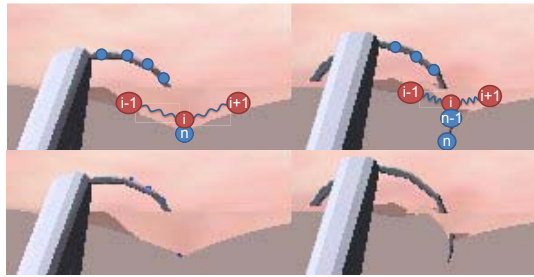


Figure 4.4: Simulation of the needle insertion, where n represents the needle nodes and i represents the tissue elements.

this bounding sphere, the neighboring masses became collision candidates.

The collision detection had two different modes depending on the needle orientation. The first collision mode simulated the interaction of the concave part of the needle with the tissue (when needle insertion cannot be performed). The second collision mode simulated the needle insertion. This was a complicated procedure to simulate with several states depending on the number of needle nodes inserted and the needle trajectory (e.g. penetrating or exiting the needle at the entrance point). We used a similar procedure as the one proposed by [Fei et al. \(2008\)](#), to simulate the tissue-needle adhesion. As illustrated in Fig. 4.4, the pierced mass of the tissue element i initially follows the closest needle node n . When the length of the adjacent springs overcomes a threshold, the tissue element i follows the next needle node $n-1$.

An impedance type control scheme was employed (Fig. 4.5). With this approach, the subject feels the forces from the dynamics and statics of the simulated environment in response to moving the device ([Hayward and MacLean, 2007](#)). Therefore, subject movements were measured and thereafter the interaction with the virtual tissue for that specific needle movement was calculated. The torques that should be generated by the actuators were then transmitted to the omega control board. The simulation was run on a Mac Book 5.1 laptop with an Intel Core 2 Duo 2.4GHz CPU. The laptop graphic card was a NVIDIA GeForce 9400M 256M GPU. The haptic and graphic loops were updated at 1 kHz and 30 Hz respectively.

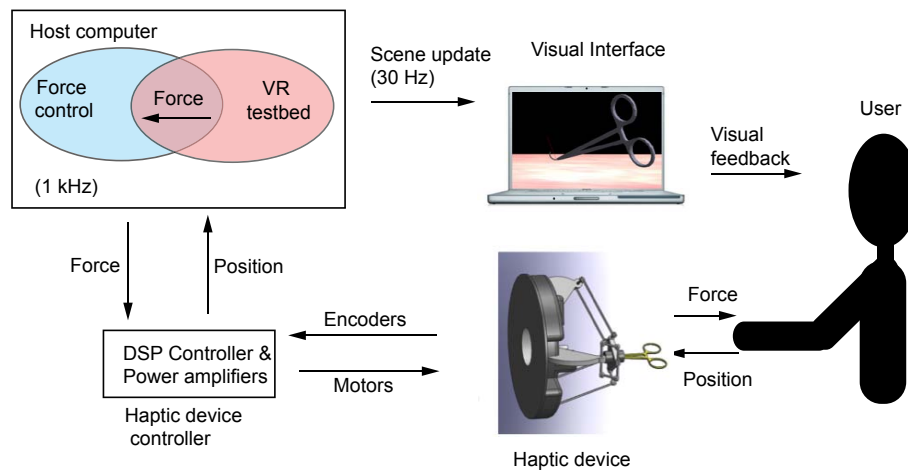


Figure 4.5: Control scheme of the overall experimental setup.

Needle Insertion Model

The experiment consisted of a pinpoint task in which the needle should pass through two points. Between the input and output points the needle was hidden by the tissue. During the time when the needle could not be seen, the only available information about the action was the subjects' self-perception of the movement and the [haptic feedback](#) (if provided by the device).

The interaction between a needle and a living tissue is very complex:

1. the different layers of tissue are inhomogeneous and so the mechanical properties cannot be described by an elastic isotropic model;
2. the characteristics of the tissues are organ-dependent; and
3. the insertion forces change with the needle shape.

This inherent complexity in living tissues has been simplified in the literature. Most of the current needle insertion models based on measurements of straight needle insertion ([Simone and Okamura, 2002](#); [Barb  et al., 2007a](#); [Okamura et al., 2004](#); [Abolhassani et al., 2007](#); [Barb  et al., 2007b](#)). In these experiments it was found that a needle insertion follows at least three phases represented in [Fig. 4.6](#).

- (1) The needle makes contact and deforms the tissue.
- (2) Once the energetic threshold is overcome, the needle perforates the surface; the damping forces attract the tissue along the needle shaft.
- (3) The needle is extracted from the tissue; again the tissue adheres to the needle shaft and follows its movement.

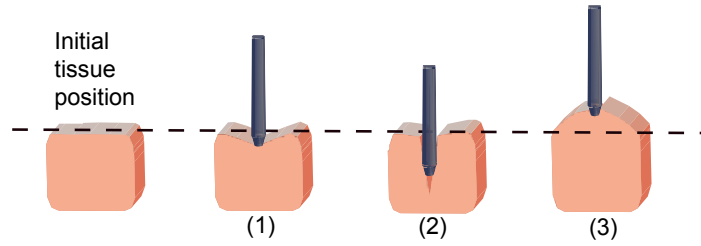


Figure 4.6: One-DOF needle insertion phases identified by Okamura et al. (2004), Barbé et al. (2007a) and Barbé et al. (2007b).

For this experiment, the needle insertion followed the same phases. Forces rendered to the subject are calculated similarly to the models proposed by Okamura et al. (2004) and Barbé et al. (2007a). The needle insertion force model is then a combination of stiffness, damping and puncture forces that takes into account the needle depth in the tissue. However, in both studies, needle insertion was performed along a straight path. For an arc-shaped needle, in which the path is almost circular, this one-DOF-translational-model was mapped along a circular trajectory.

The suture movement is performed in the YZ plane. Consequently, the components of the force in this plane \vec{F}_y and \vec{F}_z pass through the needle insertion phases described in Fig. 4.8 (left). The force model along the X axis does not vary because the needle insertion is always perpendicular to it (Fig. 5.10). \vec{F}_x simulates the reaction forces to lateral needle displacement, as suggested by Kataoka et al. (2002). In real sutures, these forces help to keep the needle in place once it has been inserted (Fig. 4.8, right). The torque, $\vec{\tau}_x$, is calculated by multiplying the needle tip force, \vec{F}_r , which is tangential to the needle arc, by the needle radius.

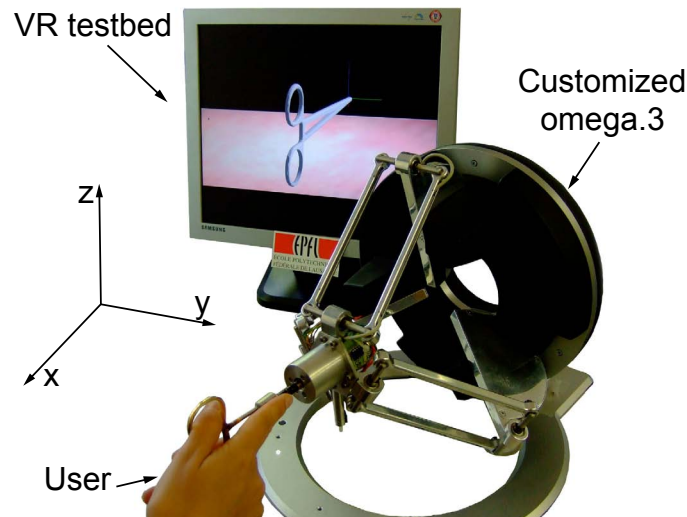


Figure 4.7: Customized omega.7 device used in the experiment and VR testbed.

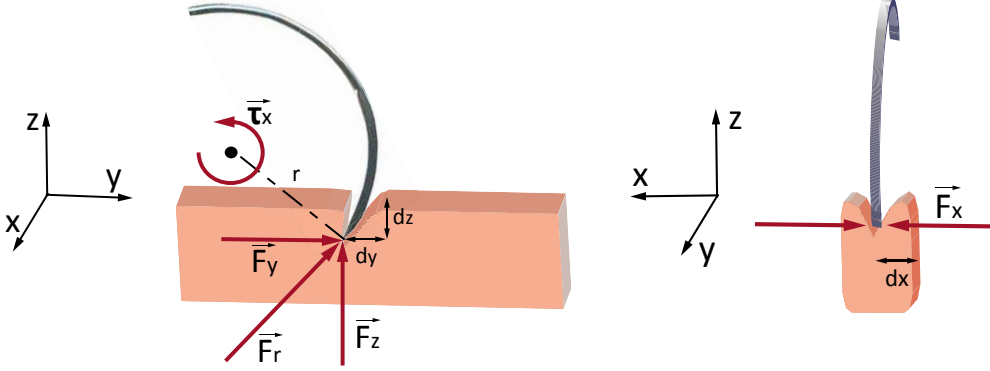


Figure 4.8: Interaction model: (left) \vec{F}_y and \vec{F}_z components of the rendered force \vec{F}_r and torque $\vec{\tau}_x$, and (right) force along the X axis.

With these definitions:

- $\vec{d}(d_x, d_y, d_z)$ is the tissue deflection;
- l_1 is the thickness of the first layer, $(\vec{d}_z - \vec{l}_1)$ represents the amount of needle penetration into the second layer with respect to the first;
- K values represent the stiffness;
- $B_{A,i}$ ($A = X, Y, Z, i = 1, 2$) is the damping coefficient per unit of length along the A axis, for the insertion phase i ; and
- $\vec{v}(v_x, v_y, v_z)$ is the needle tip velocity.

Before puncture occurs ($d < d_{threshold}$), the force model is described by:

$$\text{Shear component: } \vec{F}_y = K_{y1} \cdot \vec{d}_y \quad (4.1)$$

$$\text{Normal component: } \vec{F}_z = K_{z1} \cdot \vec{d}_z \quad (4.2)$$

After puncture, ($d > d_{threshold}$):

$$\text{Shear component: } \vec{F}_y = K_{y2} \cdot \vec{d}_y + (B_{y1} \cdot \vec{l}_1 + B_{y2} \cdot \vec{d}_y) \cdot \vec{v}_y \quad (4.3)$$

$$\text{Normal component: } \vec{F}_z = K_{z2} \cdot \vec{d}_z + (B_{z1} \cdot \vec{l}_1 + B_{z2} \cdot (\vec{d}_z - \vec{l}_1)) \cdot \vec{v}_z \quad (4.4)$$

Forces when extracting the needle:

$$\text{Shear component: } \vec{F}_y = (B_{y1} \cdot \vec{l}_1 + B_{y2} \cdot \vec{d}_y) \cdot \vec{v}_y \quad (4.5)$$

$$\text{Normal component: } \vec{F}_z = (B_{z1} \cdot \vec{l}_1 + B_{z2} \cdot (\vec{d}_z - \vec{l}_1)) \cdot \vec{v}_z \quad (4.6)$$

The force model along the X axis is constant:

$$\vec{F}_x = K_x \cdot \vec{d}_x + B_x \cdot \vec{v}_x \quad (4.7)$$

Torque is calculated from the resulting force as:

$$\vec{F}_r = \vec{F}_y + \vec{F}_z \quad (4.8)$$

$$\vec{\tau}_x = \vec{r} \times \vec{F}_r \quad (4.9)$$

According to the visual simulation, when the needle tip deflects the tissue before the puncture occurs (before switching to the next needle node) the forces and torque rendered to the subject are determined by Eqn. (4.1), (4.2) and (4.9). In that phase, the Y and Z stiffnesses, K_{y1} and K_{z1} , are higher and then suddenly decrease when the energetic threshold is overcome. Afterwards, the force model is mainly due to damping forces that depend on the amount of needle penetration into the tissue, as is described by Eqn. (4.3) and (4.4). Therefore, the force model is non-linear with the Y and Z stiffnesses that are higher before the puncture and then suddenly decrease. When the subject inverts the trajectory, which means that the needle is extracted through the entrance point, the force model changes to the extracting phase.

The magnitudes of K and B were similar to the measurements of an ex-vivo liver puncture reported by Okamura et al. (2004) and the parameters used by Gerovichev et al. (2002). However, during screening trials, subjects suggested that initial tissue stiffness felt too high after puncture. When the spring force is released, there is an undesired overshoot in the subject's hand movement. Subjects push against a boundary that is suddenly removed, thus they are not able to stop immediately due to both reaction time and arm impedance. The same phenomenon was identified by Gerovichev et al. (2002) and Barbé et al. (2007a) and is a factor that must be compensated by the control scheme when performing teleoperated needle insertion. Therefore, the stiffness of the first phase was slightly reduced to minimize this effect.

In Fig. 4.9, the rendered forces and the needle tip position in each axis during a needle insertion trial are shown. The peak force that appears at the beginning of the insertion, mainly along the Z axis, is due to the initial tissue stiffness before the puncture occurs.

This interaction model was assessed and validated by surgeons, who affirmed that there was a realistic correlation between forces and the needle insertion.

4.1.3 Suture Performance Assessment

Iwamoto et al. (1993) and Solis et al. (2008) defined the ideal suture as the one where the needle emerges exactly at the exit point with the intended tissue bite producing the least possible suture-trauma (Fig. 4.10, top-left). To minimize trauma and to reach the expected tissue bite, the needle must advance along its curvature (Fig. 4.10, top-right). The position error highly depends on the insertion angle of the needle while entering the tissue. The choice of the optimal insertion angle is generally related to the surgeon's experience (Seki, 1987). According to these publications the pinpoint accuracy in the suturing technique can be measured by the distance deviated from the optimal exit point. Therefore, in this experiment, suture point error is calculated as the norm of the 3D distance vector between the given suture

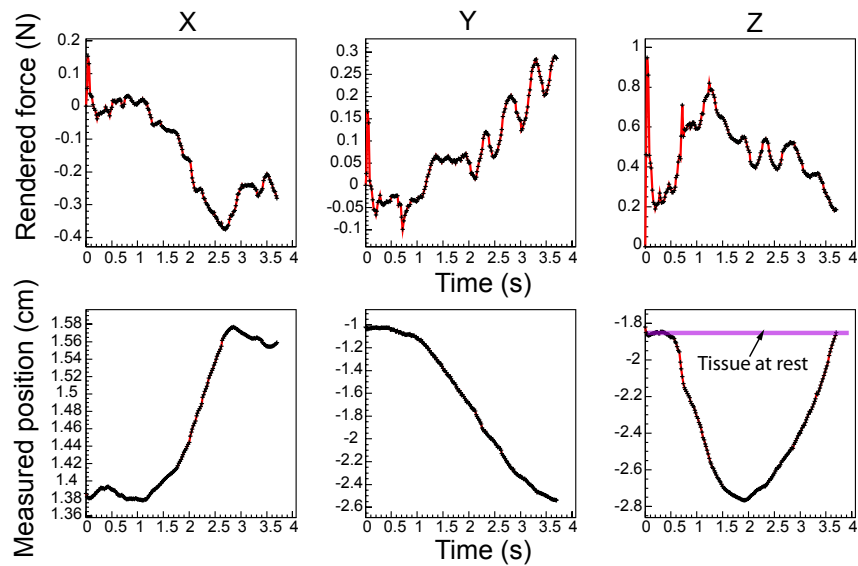


Figure 4.9: Interaction forces and needle tip position along each axis for a suturing trial. The initial peak of the force curve, especially along the Z axis, is due to the higher tissue stiffness before puncture.

point and the suture point reached by the subject (“err” in Fig. 4.10, top-left). In addition to the position error, maximum penetration depth and task-completion time were measured.

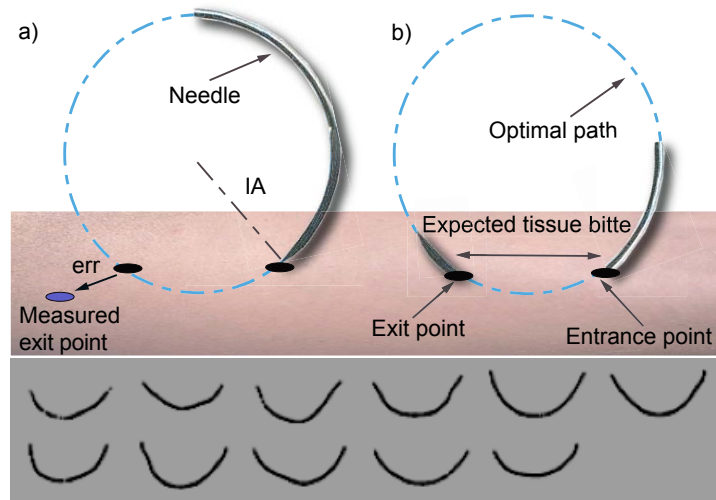


Figure 4.10: (top) Optimal insertion of an arc-shaped-needle, IA corresponds to the insertion angle of the needle (Solis et al., 2008; Iwamoto et al., 1993; Seki, 1987) and (bottom) real surgeons’ suture tracks recorded on X-ray film by Iwamoto et al. (1993).

4.1.4 Experimental Protocol

After the first round of experiments, surgeons highlighted two issues in the setup that could affect the performance of the suture. The surgeons first pointed out that they preferred to be standing to perform the experiment. The second point was that the needle should be held at one third of its length (Fig. 4.11, right) instead of at the extremity (Fig. 4.11, left). Therefore, a second experiment with a different configuration taking into account these remarks was performed to study if there was any influence on the results.



Figure 4.11: (left) Needle held at the extremity and (right) needle held at one third of its length.

Subjects

The two configurations of the experiment were conducted with 10 subjects each, aged 25-35, all right-handed. The subject groups were composed of 7 males and 3 females for the first configuration, and 5 males and 5 females for the second one. In both configurations there were three subjects with suturing experience.

The experimental protocol is a full factorial design with the following factors and levels:

1. feedback type (three levels);
 - (a) visual feedback only (V);
 - (b) visual and force feedback (VF); or
 - (c) visual, force and torque feedback (VFT).
2. suture bite (two levels);
 - (a) 12 mm; or
 - (b) 14 mm.
3. suture location (five levels).

Before the experiments, subjects performed a training phase to familiarize themselves with the test: (1) subjects were asked to explore the tissue by changing the feedback type during an unlimited time, and (2) a training phase similar to the experiment was carried out. The aim of this part of the training was to make subjects familiar with the task so that there would be no further learning effect during the experiment.

The VR testbed represented a section of visco-elastic tissue on which the ideal suture entrance and exit point were indicated (Fig. 4.3, right). Subjects were asked to introduce the arc-shaped needle as precisely as possible in the indicated location. The subject began by placing the needle at the reference entrance point and then performed the suture movement targeting the exit point (Fig. 4.3, left). A visual cue appeared over the tissue to indicate that the suture was completed. Subjects were instructed to release the tissue and lift the tool towards this visual sign to make a pause. After three seconds the visual cue disappeared and the next suture points were displayed. During the experiment, all combinations of distance between points and feedback type were repeated 5 times resulting in a total of 30 trials per subject. Subjects were aware that time was measured; however, they were instructed to perform the suture as accurately as possible.

As mentioned in Section 4.1.4, the *entrance* and *exit point error*, *maximum penetration depth* and *task-completion time* were measured during the experiment. At the end of the experiment, a questionnaire was given to the subject. In this questionnaire, the subject's background, the task difficulty and their impression on the different feedback types were enquired.

4.2 Results

Repeated measures ANOVA was performed to study the influence of each factor on the subject's performance. The results of the ANOVA for the 1st experimental configuration are summarized in Table 4.2.

Table 4.2: ANOVA for the 1st experimental configuration: subjects were seated and the needle was held from the extremity

Parameters	Distance	Feedback type	Interaction (distance, feedback)
Exit point error	$F(1, 9) = 1.856$ p = 0.206	$F(2, 18) = 45.910$ p < 0.001	$F(2, 18) = 1.209$ p = 0.321
Entrance point error	$F(1, 9) = 1.085$ p = 0.324	$F(2, 18) = 0.198$ p = 0.821	$F(2, 18) = 0.940$ p = 0.408
Max. penetration depth	$F(1, 9) = 0.451$ p = 0.518	$F(2, 18) = 8.693$ p = 0.002	$F(2, 18) = 1.478$ p = 0.254
Task-completion time*	$F(1, 9) = 1$ p = 0.349	$F(1.19, 10.74) = 0.596$ p _{corr} = 0.063	$F(1.57, 14.12) = 0.784$ p _{corr} = 0.404

* This factor did not pass Mauchly sphericity test, thus a Greenhouse Geisser sphericity correction was performed.

The feedback type had a significant influence on the *exit point error* (p < 0.001) and *maximum penetration depth* (p = 0.002).

The mean values for each feedback type are shown in Fig. 4.12. The high standard deviation is due the high variability in performance among subjects. In order to assess whether the

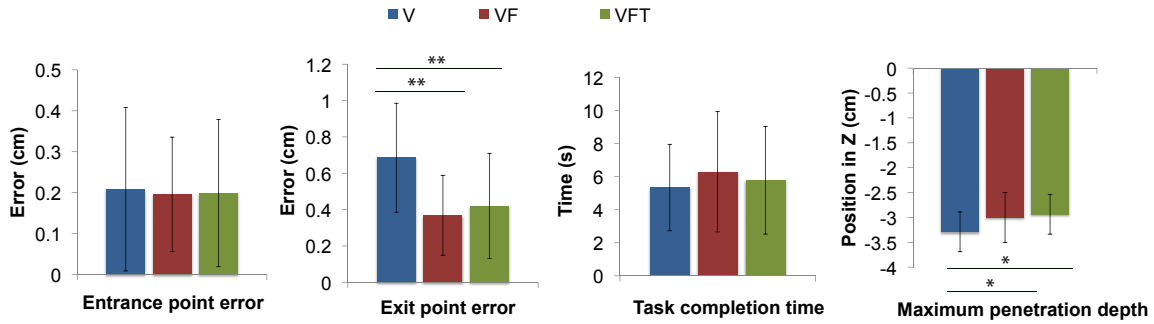


Figure 4.12: Mean values for each parameter with respect to the feedback type (1st configuration). Error bars represent the standard deviation. Lines with stars above connect the mean values that are significantly different according to the Bonferroni post hoc test (** for $p < 0.001$ and * for $p < 0.05$).

means of the three groups were statistically different from each other, a Bonferroni post hoc test for multiple-comparison was performed. The Bonferroni test showed that the VF and VFT feedback types significantly reduced *exit point error* ($p_{V-VF} < 0.001$, $p_{V-VFT} < 0.001$) and *maximum penetration depth* ($p_{V-VF} = 0.015$, $p_{V-VFT} = 0.002$) when compared with the V feedback. Nevertheless, the VF and VFT were not significantly different from each other ($p_{VF-VFT} = 1.000$ for both measurements). In addition, from the individual results shown in Fig. 4.13, we observed that the *exit point error* presented the same tendency for all subjects, with respect to the feedback type: error with visual feedback only (V), was always higher than for feedback types including force feedback (VF and VFT). This proves that feedback types including force feedback significantly reduced *exit point error* and *maximum penetration depth* across all subjects independently of their individual ability. However, the addition of torque feedback did not result in any significant change.

Results of the ANOVA for the 2nd configuration are shown in Table 4.3. As in the previous experiment, the distance between suture points did not have a significant effect on any of the measurements. The feedback type had a significant influence on the *exit point error* ($p < 0.001$) and *maximum penetration depth* ($p < 0.001$).

The mean values of each measurement for every feedback type are illustrated in Fig. 4.14. Once again a Bonferroni post hoc test found a significant decrease on the *exit point error* and the *maximum penetration depth* when force feedback was present compared with only visual feedback V ($p_{V-VF} < 0.001$, $p_{V-VFT} < 0.001$ and $p_{V-VF} = 0.001$, $p_{V-VFT} < 0.001$ respectively). No significant differences between the mean values of VF and VFT were observed; $p_{VF-VFT} = 0.505$ for the *exit point error* and $p_{VF-VFT} = 1.000$ for the *maximum penetration depth*.

In Fig. 4.15 we observed the same tendency for all subjects with respect to the feedback type, as it was found 1st configuration. In order to study the influence of the experimental configuration, repeated measures ANOVA was again performed, merging data from both experiments and adding one extra factor: experimental configuration. Results are shown in

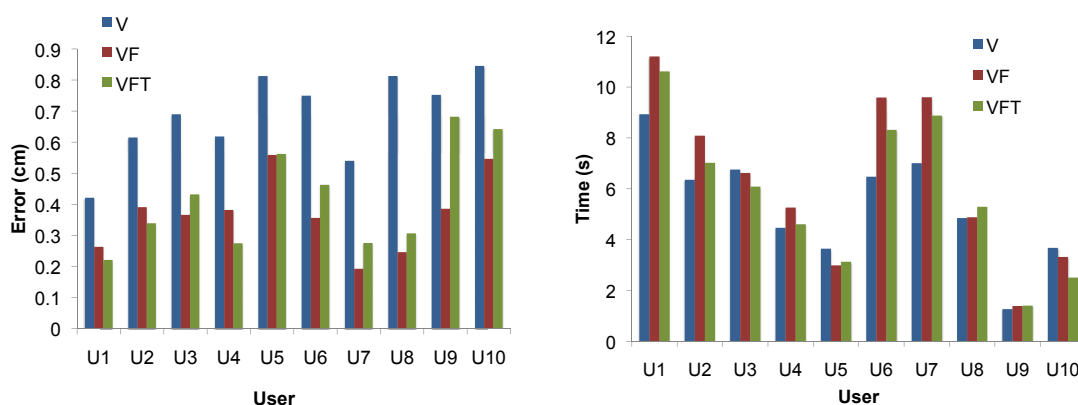


Figure 4.13: Results per subject and for each feedback type (1st configuration): (left) exit point error per subject and (right) task-completion time per subject. U8, U9 and U10 correspond to subjects with suturing experience. Note that when force feedback was present the *exit point error* was highly reduced.

Table 4.3: ANOVA for the 2nd experimental configuration: subjects were standing and held the needle at one third of its length.

Parameters	Distance	Feedback type	Interaction (distance, feedback)
Exit point error	$F(1, 9) = 0.697$ $p = 0.420$	$F(2, 18) = 32.324$ $p < \mathbf{0.001}$	$F(2, 18) = 1.563$ $p = 0.236$
Entrance point error	$F(1, 9) = 0.794$ $p = 0.396$	$F(2, 18) = 1.617$ $p = 0.226$	$F(2, 18) = 1.319$ $p = 0.292$
Max. penetration depth	$F(1, 9) = 1.117$ $p = 0.318$	$F(2, 18) = 15.557$ $p < \mathbf{0.001}$	$F(2, 18) = 3.867$ $p = \mathbf{0.04}$
Task-completion time	$F(1, 9) = 0.968$ $p = 0.351$	$F(2, 18) = 2.755$ $p = 0.091$	$F(2, 18) = 0.705$ $p = 0.509$

Table 4.4. Experimental configuration (seated or standing and how the needle was held) seemed not to have a significant influence on the results. Overall, the results of the 2nd configuration confirmed the conclusions obtained in the first round. Only the entrance point error increased slightly due mainly to the subject's posture. During the 1st configuration, subjects were seated and thus had more stability while manipulating the device. Once again, neither distance between suture points nor the type of feedback seemed to have any effect on entrance point accuracy. This is consistent since the placement of the needle near the entrance point is totally based on visual cues.

As it can be seen in Fig. 4.13 (left) and Fig. 4.15 (left), surgeons' results are quite similar to those of the untrained subjects. However, Fig. 4.13 (right) and Fig. 4.15 (right) show that surgeons generally perform the sutures faster than other subjects. Normalized distributions of the results for the *exit point error* and *task-completion time* are shown in Fig. 4.16. We observed that surgeons' the distribution for *task-completion time* was shifted to lower val-

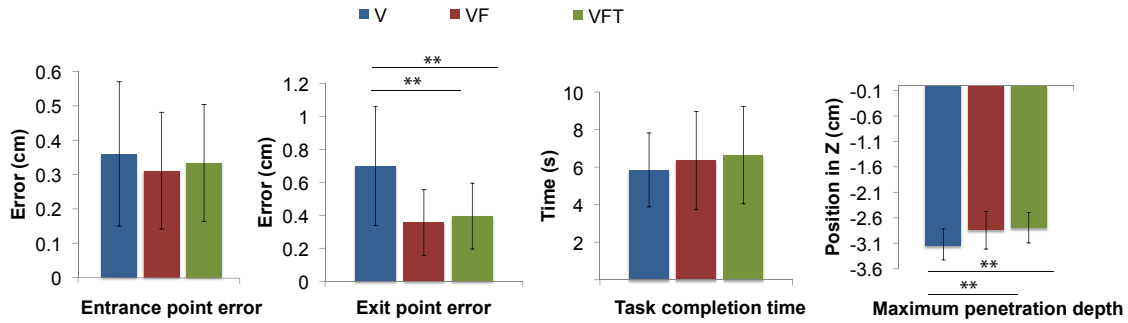


Figure 4.14: Mean values for each parameter with respect to the feedback type (2nd configuration). Error bars represent the standard deviation. Lines with stars above connect the mean values that are significantly different according to the Bonferroni post hoc test (** for $p < 0.001$ and * for $p < 0.05$).

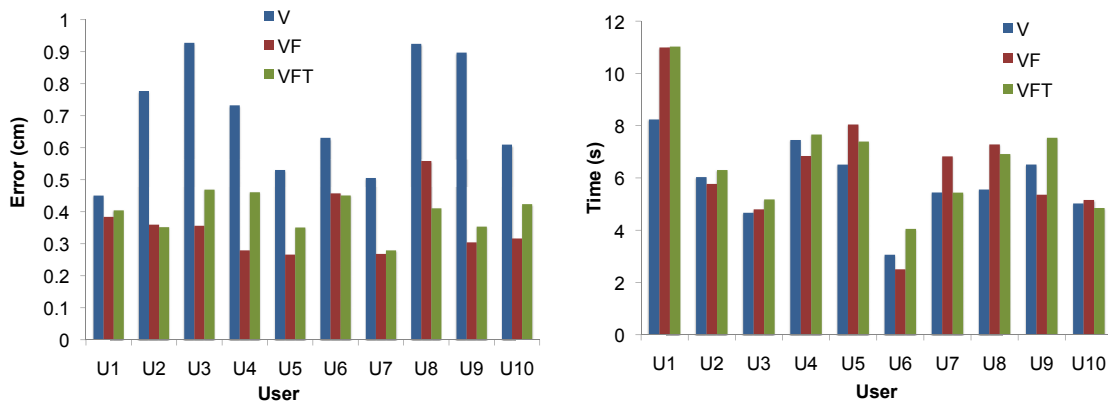


Figure 4.15: Results per subject and for each feedback type (2nd configuration): (left) exit point error per subject and (right) task-completion time per subject. U8, U9 and U10 correspond to subjects with suturing experience. Note that when force feedback was present the *exit point error* was highly reduced

ues compared to inexperienced subjects distribution. Nevertheless, their error distribution is similar to the distribution of inexperienced subjects. These results show that inexperienced subjects were specially concentrated on accuracy because they have never performed real sutures and they ignore how fast this task is generally achieved. This means that non-surgeons have a different subjective accuracy-speed tradeoff, which biases the results. Therefore, inexperienced subjects can perform sutures with similar accuracy as a surgeon but requiring more time. In addition, it should be taken into account the effect of subject's impedance on the overall performance. Several studies have shown that subjects can learn to compensate for the forces in a feed-forward manner by learning an internal model of the dynamics involved in that specific task (Shadmehr and Mussa-Ivaldi, 1994). Since surgeons have already performed the suture gesture and know the force profile of a needle insertion, they might have learned the

Table 4.4: ANOVA comparing the influence of the experimental configuration

Parameters	Distance	Feedback type	Experiment configuration
Exit point error	$F(1, 9) = 2.121$ $p = 0.179$	$F(2, 18) = 63.816$ $p < \mathbf{0.001}$	$F(1, 9) = 0.032$ $p = 0.860$
Entrance point error	$F(1, 9) = 0.794$ $p = 0.396$	$F(2, 18) = 1.462$ $p = 0.258$	$F(1, 9) = 11.611$ $p = \mathbf{0.007}$
Max. penetration depth *	$F(1, 9) = 2.524$ $p = 0.146$	$F(1.22, 11.02) = 17.758$ $p_{\text{corr}} = \mathbf{0.001}$	$F(1, 9) = 1.575$ $p = 0.241$
Task-completion time *	$F(1, 9) = 10.619$ $p_{\text{corr}} = \mathbf{0.009}$	$F(1.24, 11.20) = 5.802$ $p_{\text{corr}} = \mathbf{0.028}$	$F(1, 9) = 1.575$ $p = 0.671$

* These factors did not pass the [Mauchly sphericity test](#), thus a [Greenhouse Geisser sphericity correction](#) was performed.

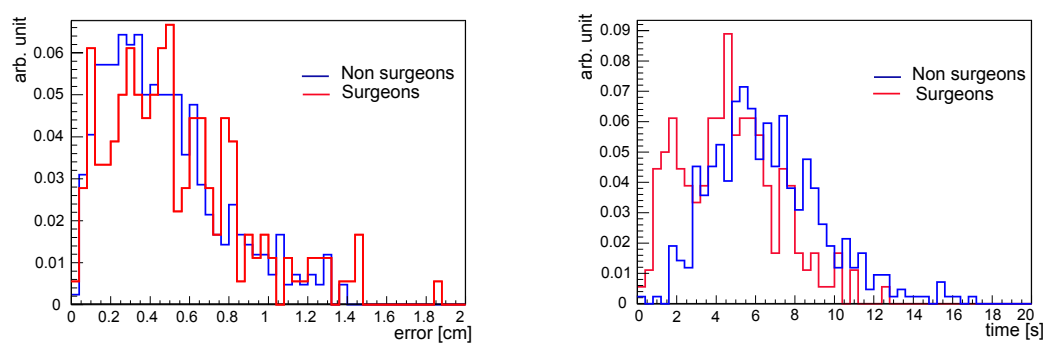


Figure 4.16: Normalized distributions of *exit point error* (left) and *task-completion time* (right). A clear distinction can be seen between surgeons and non surgeons distributions for the *task-completion time*, the error distribution of the surgeons' is similar to the distribution of inexperienced subjects.

optimal impedance that should be applied. Therefore, they can adapt their arms impedance faster to the force changes.

4.3 Post-experiment Questionnaire

At the end of the experiment, subjects had to answer the questionnaire presented in Section 4.3.1. In this questionnaire, subject's background, the task difficulty and their impression of the different feedback types were enquired.

4.3.1 Questions

1. Age and gender.
2. Have you ever performed real suturing? Never, Some times or Often.
3. Do you have previous experience with haptic devices? Yes, Some or None.
4. How difficult did you consider the suturing task? Very difficult, Difficult, Medium, Easy or Very easy.
5. Were you aware of all the feedback changes during the experiment? Always, Sometimes or Never.
6. What do you feel as the more natural feedback? Visual Feedback, Force feedback or Force + Torque feedback.
7. Which feedback is less tiring for you? Visual Feedback, Force feedback or Force + Torque feedback.
8. Do you think that you could perform perfectly the suture with only visual feedback? Yes or No.
9. Comments

4.3.2 Results

By analyzing the answers to the questionnaire, it was found that the majority of the subjects found the task difficult in both configurations, but they commented that the second configuration caused more fatigue because they were standing up during the entire experiment. Most of the subjects noticed when the feedback type was changed from one trial to another but more than half commented that sometimes they did not distinguish between force feedback alone and force plus torque feedback. During the post-experiment questionnaire, most of the subjects asserted that they preferred the feedback types providing force and torque feedback. It was perceived more natural and intuitive than with only the visual feedback and thus it was felt as less tiring.

4.4 Discussion and Conclusions

The aim of this study was to investigate the influence of force and torque feedback on accuracy and execution time in a VR-based suturing task. To do so, the deviation to the optimal suture points, task-completion time and maximum penetration depth into the tissue for three feedback types were compared: (1) visual feedback only, (2) visual and force feedback and (3) visual, force and torque feedback.

Based on the results, the following conclusions were extracted:

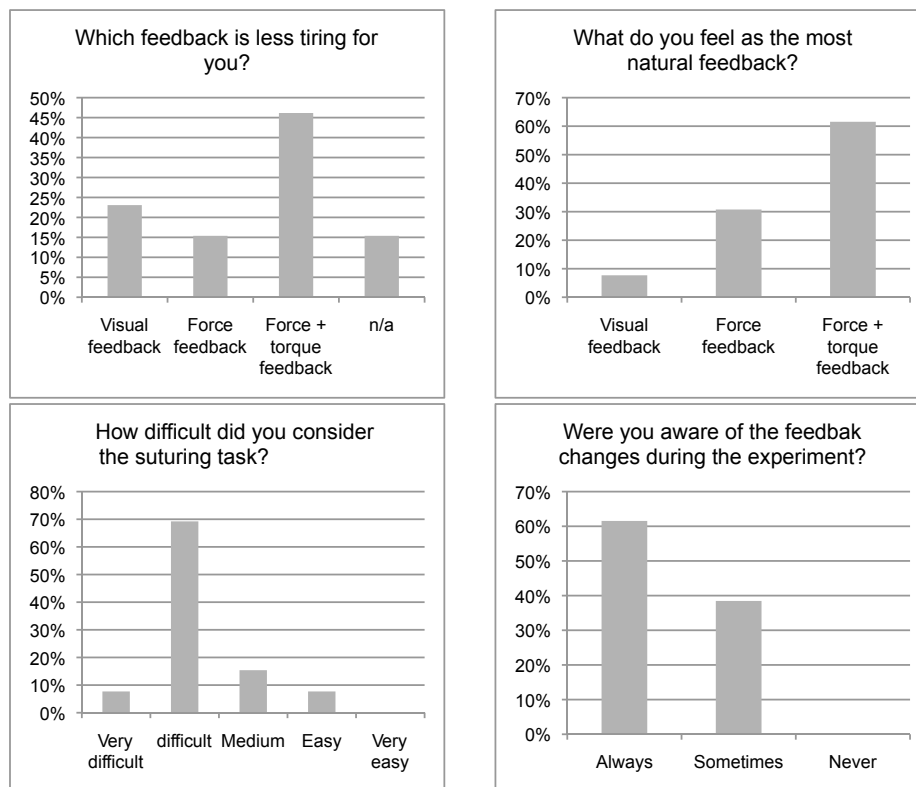


Figure 4.17: Bar plots with the questionnaire answers. The suturing task was generally perceived as difficult. The feedback types rendering force feedback were felt as more natural, especially when both force and torque were present.

- Experimental results regarding the exit point error confirmed the assumption that force feedback can clearly improve the accuracy in a suturing task.
- Without force feedback, subjects tended to penetrate too deeply into the tissue.
- The addition of torque feedback – in this particular context – did not improve suturing quality when compared to the addition of force feedback alone. This result supports the assumption that it might not be worth adding an extra actuator to provide torque feedback on the pronosupination [DOF](#).
- These results were independent of the subject factor as all subjects presented the same tendency with respect to the feedback type.
- Force feedback improved accuracy significantly, for surgeons as well as non-surgeons. Generally, surgeons carried out the task considerably faster independently of the feedback.

In real suturing tasks, the tissue helps to stabilize the needle trajectory by damping the movement. In addition, subjects exploit force information to correct their path and the applied force. Force feedback helps to stabilize the movement as tissue does in the real case.

Consequently, force feedback clearly improves accuracy when compared to a free movement, which corresponds to the visual feedback alone in this experiment.

The majority of experienced subjects stated that they would be able to execute the task with only visual cues, as they do on current teleoperated systems such as the da VinciTM Surgical System (Guthart and Salisbury, 2000). Nevertheless, their results showed that their error is almost halved when force feedback is provided (the surgeons correspond to the subjects U8, U9 and U10 in both Fig. 4.13 and Fig. 4.15). On the other hand, on a robotic surgery platform without force feedback, when the teleoperated robot inserts the needle, the real tissue stabilizes it. However, contrary to a real suture, interaction forces are not transmitted to the surgeon, who might deviate, thereby applying undesired forces to the tissue. If the tremor filter does not cancel out these deviations, there will be significant risks of damaging fragile tissues. The results of this study clearly showed that force feedback significantly improved accuracy independently of subjects' experience, which can potentially speed up the surgeon's learning process. Torque feedback in return, may not bring enough improvement to justify the additional complexity and cost that it implies.

Most of the subjects preferred when force feedback was given. It was perceived as being more natural and intuitive than working with only visual feedback. Force feedback generally made subjects feel more secure with the task as they had feedback to confirm their actions. This could also imply that the availability of force feedback might reduce the visual workload.

Chapter 5

Tactile Feedback during Surgery. Task Example: Assessment of the Vascularization of a Tissue

Several surgical tasks highly depend on the sense of touch. Force feedback is often not sufficient to provide specific tactile information to the surgeon. During open procedures surgeons often palpate tissues to perceive the local pulse of hidden vessels or arteries in order to localize them and avoid their rupture while dissecting nearby tissue. Feeling the temperature of the tissue can help the surgeon to assess the blood oxygenation of a tissue and to detect an early stage necrosis. Local stiffness is used to determine the extension of small lumps and tumors that should be extirpated. Being able to feel the roughness of the tissue, the surgeon can evaluate the degree of fibrosis of a surgical adhesion.

Nowadays, many research groups attempt to restore the tactile information that the surgeon has lost in robotic surgery. Some of these developments have been already discussed in Section 2. However, most of them aim to render local stiffness allowing the surgeon to telepalpate an organ or tissue to find hidden lumps (Ottermo et al., 2008; King et al., 2009; Gwilliam et al., 2012). The work presented in this chapter aims at restoring the tactile information involved in a palpation task to assess the vascularization of a tissue. Therefore, the development of a novel tactile display that could realistically render a vessel-like pulsation under the user's fingertip was necessary. Furthermore, the tactile display should fulfill certain requirements in terms of size and weight in order to be integrated into a haptic device.

This study mainly followed two phases. First, a tactile pulse display was developed and its technical performance was assessed (Section 5.1). Two psychophysical experiments were carried out to evaluate the performance of the tactile display when rendering a pulsating pattern with different orientations. In the second phase, the tactile pulse display was integrated into a haptic device (Section 5.2). Two psychophysical experiments were performed to investigate the effect of different feedback types on the subjects performance. The tasks were: (1) exploring a tissue to find a hidden artery and (2) identifying the orientation of a hidden

artery. Results showed that adding tactile feedback significantly reduced task completion time in both tasks. Moreover, for high difficulty levels, subjects performed better with the feedback condition combining tactile and visual cues. As a matter of fact, the majority of the subjects in the study preferred this combined feedback because the redundant information increased their confidence.

5.1 Tactile Pulse Display

The results of the first phase of this study have been published in Santos-Carreras et al. (2010b), it should be noted that the statistical analysis of this chapter slightly differs from the article. The repeated measures ANOVA is used without the factor “individual subject”, as it is well known to be always significant and does not provide any relevant information to the conclusions. The main results and conclusion are still in accordance with those of the article.

5.1.1 Implementation

As the final goal of the tactile display was to be integrated in the surgeon’s console it must OR compatible thus, the display should be single-use or easy to clean and use safe voltage levels. These constraints implied that many of the actuation methods already used in tactile displays such as electro-reohological fluids (Klein et al., 2005), DC motors (Ottermo et al., 2004) and piezoelectric actuators (Pasquero et al., 2004; Winfield et al., 2007; Wang and Hayward, 2010) were not applicable in this particular case.

Since it was assumed that the surgeon holds a haptic device through the display, which needs a certain pressure, the forces produced by the actuators of the display have to be, at least, of similar magnitude. In addition, the tactile display should be compact and light to be integrated into a haptic device. Consequently, displays based on pneumatic actuation are preferred due to their OR compatibility, lightweight and because they can realistically simulate artery pulsation. Moreover, the majority of ORs normally feature a pressurized air access point. This technology has already been successfully used to actuate tactile displays that can render local pressure distribution in the fingertip (King et al., 2009; Moy et al., 2000).

Manufacturing

Since pneumatic actuation is employed, the actuator density on the display is limited. Therefore, finding an optimal actuator arrangement is an important factor in the display design. King et al. (2008a) used a 3×2 matrix with 1.5 – 4 mm in diameter to render pressure levels. In the present study, the pressure level and the orientation of the artery relative to the tactile sensor is more important than the texture, or the exact shape of the artery, which is generally known, that is why a $2 - 1 - 2$ configuration was used, as shown in Fig. 5.1 (left). This pattern allows one to represent vertical, horizontal and diagonal lines by actuating different groups of balloons, while keeping the display compact (fingertip size). It was found in previous

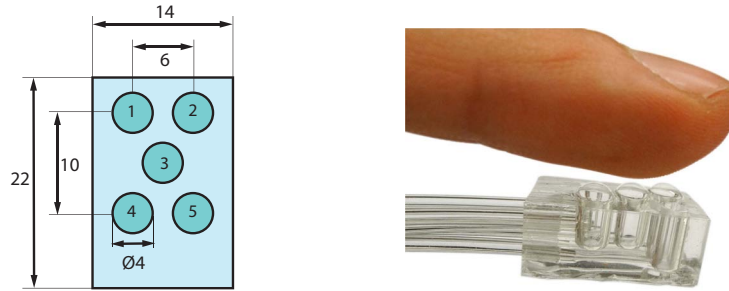


Figure 5.1: (left) balloon arrangement (dimensions in mm) and (right) tactile pulse display rendering a diagonal line.

psychophysical studies that a minimum distance of 4 mm should be guaranteed to allow the discrimination between two pneumatic stimuli applied to the fingertip (Kim et al., 2006). We used 4 mm balloons separated by 6 mm. All dimensions of the display are indicated in Fig. 5.1 (left).

The display was manufactured in Polydimethylsiloxane (PDMS) material (Sylgard 184, Dow Corning) that is often used in micro fluidic applications. The tactile array consists of five air chambers of 4 mm in diameter in a PDMS block, covered by a 300 μm thin film of the same material. When pressure is applied at the input of the air chamber, the thin membrane is inflated to a balloon-like shape (Fig 5.1, right).

The manufacturing process was similar to that of King et al. (2008b). By using a mold to manufacture the thin film we were able to ameliorate the homogeneity of the film as compared to King et al. (2008b) guaranteeing a uniform balloon-inflation. The two PDMS parts were then bonded using a layer of uncured PDMS, which has been shown to be one of the strongest bonding techniques for PDMS (Eddings et al., 2008; Satyanarayana et al., 2005). The resulting connection proved to be very durable, supporting pressures up to 3 bar.

Control Unit

The purpose of the pressure control unit was to distribute a global input pressure to the five balloons and regulate the pressure in each balloon independently between 0 and 2 bar. Other solutions actuated through electromagnetic pressure regulators or proportional valves were discarded based on cost, complexity and volume criteria. The proposed control scheme for each balloon is composed of a one 3-way solenoid valve regulated by a Pulse Width Modulation (PWM) signal and a pressure sensor. The selected valves (Parker X-Valves) require low power (less than 1 W), are very compact and are directly mounted on the Printed Circuit Board (PCB) (Fig. 5.2).

The control unit consists of two circuits: the first one includes the microcontroller, power, Universal Serial Bus (USB) communication and programmer, while the second one contains the power circuitry for the valves. A digital signal controller (dsPIC33FJ128MC706) was chosen as microcontroller. The communication with the computer is performed over the Universal

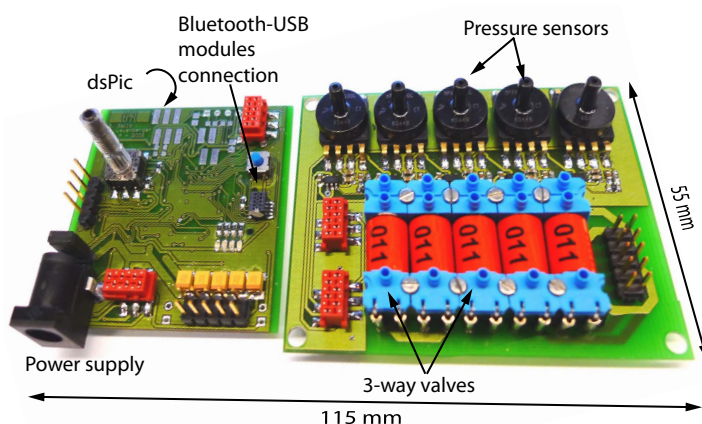


Figure 5.2: Control electronics of the pulse display integrating the PCB mounted valves.

[Asynchronous Receiver Transmitter \(UART\)](#), and then converted to [USB](#) connection. Each valve is driven using a MOSFET that can support continuous currents up to 1.2 A, thus guaranteeing the required power (1 W). An important part of the pressure regulation was implemented on the microcontroller firmware. The nominal opening time of the chosen valves was too high (around 20 ms). Therefore, the opening time was reduced down to 0.3 ms by using a higher control voltage at the beginning of each opening cycle. The valve was powered through a transistor that was switched through a [PWM](#) signal with a high-enough frequency to keep the current flowing through the solenoid, in this case 60 kHz. This signal allowed modulating the mean valve voltage from 3.3 to 7 V.

5.1.2 Technical Performance

Control Resolution

Taking into account the delays of the valves, the effective resolution is 92 levels of pressure between 0 and the input pressure. However, as it can be seen in Fig. 5.3 (left), non-linearities were observed during valve opening probably due to a small spool overlap with the output. Therefore, a conventional [Proportional Integral Derivative \(PID\)](#) was not sufficient to control the air pressure with precision. Stable and accurate control could only be achieved for either low or high pressures, but never both with the same [PID](#) settings producing either insufficient or unstable outputs for the rest of the pressure range (Fig. 5.3, right).

The pressure output was measured for a range of pulse widths of the valve control signal, analyzed and then linearized in two regions to generate the feedforward model. The feedforward control was combined with feedback [PID](#) control because a second loop was still required to track reference changes and to suppress the unmeasured disturbances that are always present in any real system. As shown in blue in Fig. 5.3 (right), with the feedforward control the output pressure could precisely follow the [PWM](#) command along all the pressure range.

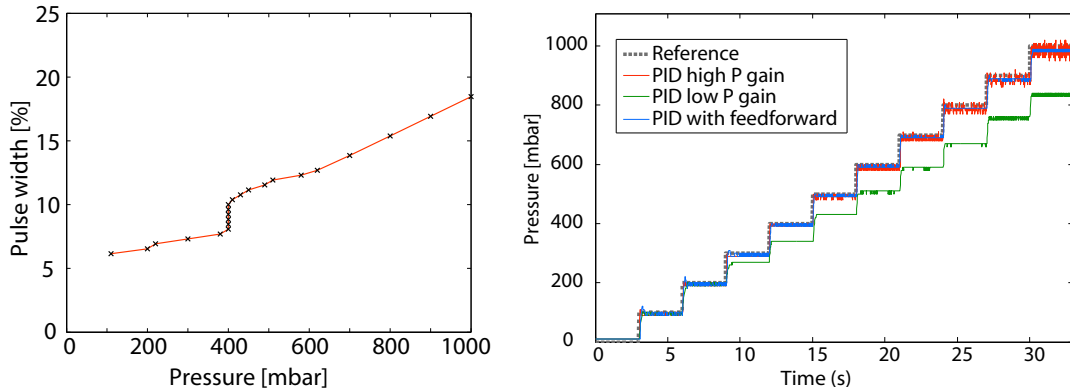


Figure 5.3: (left) Pressure output with respect to the PWM signal sent to the valve. Note the non-linearity produced at 400 mbar. (right) Pressure output for different control approaches over the working range of the display. Note that when a simple PID is applied, the output produced cannot follow the reference signal properly for both high and low pressures due to the non linearity.

Balloon Deformation versus Pressure

The tactile pulse display was characterized using a pressure regulator (FESTO MPPE3-1/4-6-010). The pressure inside the balloons was controlled over a range of 0 – 2 bar in steps of 0.2 bar and the corresponding deflection was measured for each pressure value. Results showed that the balloons deformation was approximately linear for pressures up to 1 bar and that the deformation was uniform for all the balloons as shown in Fig. 5.4. The non-uniform deformation of the 4 mm diameter balloons that was reported in King et al. (2008a), was solved in the present design thanks to the new method used to produce the thin film.

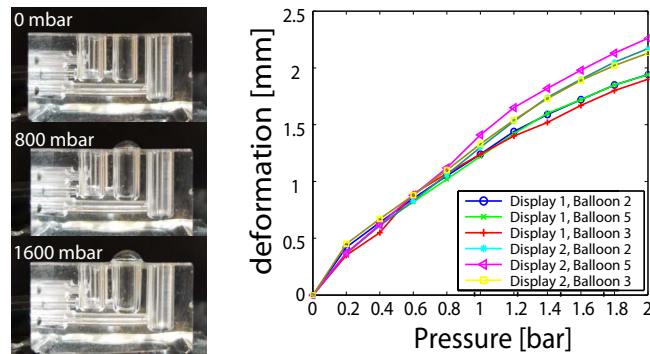


Figure 5.4: The deformation of a balloon for several pressures is shown. The plot on the right corresponds to the deformation of the three different types of balloons (different chamber size) from two different displays plotted against pneumatic pressure. The pressure-to-deformation ratio can be considered as linear up to 1 bar.

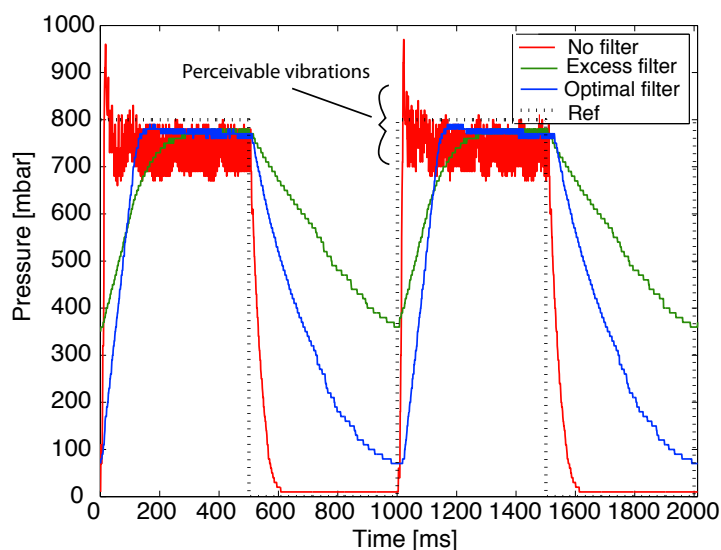


Figure 5.5: Pressure output plot for a 1 Hz-square signal as a reference and with three different mechanical low-pass filters to remove output vibrations.

Bandwidth

The oscillations in the pressure profile due to the [PWM](#) of the pneumatic valves were damped using a mechanical low-pass filter implemented by reducing the tubes diameter at its entrance. This damping increased both fill and exhaust times and consequently reduced the device's bandwidth to 5 Hz (Fig. 5.5). This frequency is still high enough to render a pulsating artery. Note that tachycardia corresponds to about 190 [Beats Per Minute \(BPM\)](#), which is equivalent to 3.1 Hz.

Pulse Simulation

The pulse model rendered by the display imitates the radial artery pressure profile described in [Chen et al. \(1997\)](#). Since the small expansion produced when the diastolic phase starts is generally not perceivable, we proposed the simplification shown in Fig. 5.6 (left). The pressure profile of a simulated pulse with a pressure peak of 800 mbar is shown in Fig. 5.6 (right).

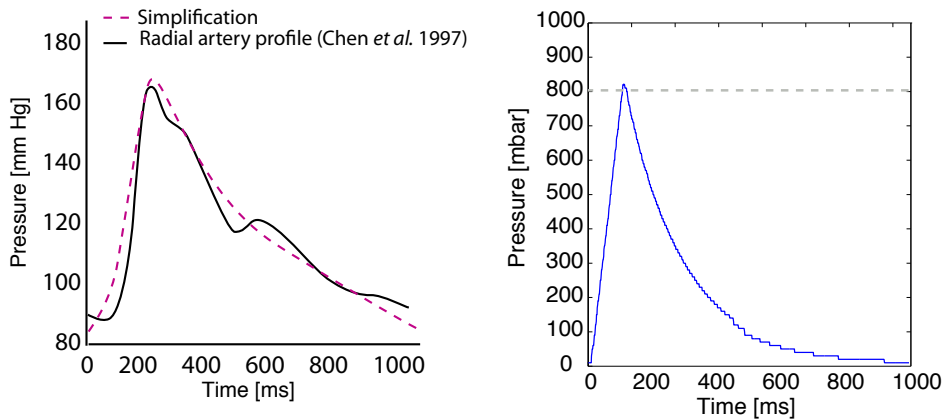


Figure 5.6: (left) Radial artery pressure profile described in (Chen et al., 1997) and proposed simplification; and (right) measurement of the pressure profile output on the display. Note the stair-shaped plot is due to the transmission limit of the pressure data (8 bits).

5.1.3 Psychophysical Evaluation

Two psychophysical experiments were conducted with 14 subjects. The subject group consisted of four women and ten men, aged between 22-38 years, nine of them were right-handed and five left-handed. None of the subjects had prior experience with tactile displays.

Magnitude Estimation

A psychophysical ratio scaling method called *magnitude estimation* was performed to determine the mathematical relation between the physical stimuli presented to subjects (balloon pressure) and the human tactual sensory experience. This experiment represents a fast and quantitative way of assessing sensations. During this experiment, subjects were requested to assign a number accordingly to the magnitude of the sensation produce by each presented stimuli.

Experiment Protocol

Only one balloon in the center of the array was used during this test. The number of pressure levels was kept low, using only seven levels, to allow subjects to easily compare the feeling produced by the different stimuli. For each inflation level, the balloon was actuated to simulate six heartbeats at a rate of 1.25 Hz (corresponding to 75 BPM). The different pressure levels were presented in a random order and were repeated five times, resulting in a total of 35 trials per subject. After six pulsations, the subject had to score the magnitude of the presented stimulus. In order to avoid biasing the results, neither a scale nor a reference pressure level was given, as it is generally recommended for this kind of experiments (Gescheider,

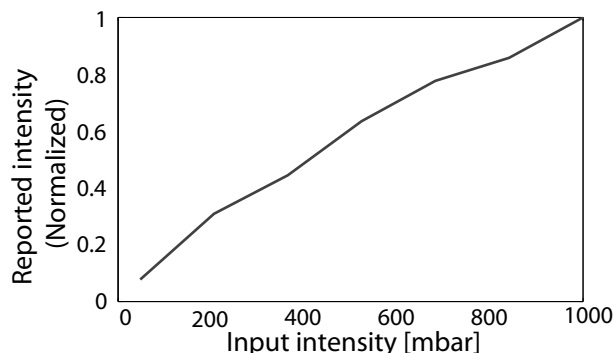


Figure 5.7: Magnitude estimation as a function of balloon pressure on the tactile display.

1997). Therefore, subjects were free to assign the number that best matched the perceived magnitude of the stimuli.

Results

To establish a function showing how intense the different pressure levels were perceived (psychophysical magnitude function), the data from fourteen subjects was combined by calculating its geometric mean and then plotted against the real stimulus value (Fig. 5.7). The geometric mean indicates the central tendency of the set of measurements and is computed as follows:

$$\text{Geometric mean} = 10^{\frac{\sum \log X}{N}}, \quad (5.1)$$

where X is a score value and N is the number of scores.

The resulting function was almost linear, with a positive slope and did not present any saturation (Fig. 5.7). Consequently, the perception of balloon pressure can be taken as proportional to the input pressure, which ranges from 0 to 1000 mbar corresponding to a deformation of 0 to 1.4 mm. The fact that no saturation was observed indicates that, in terms of psychophysics, the input pressure could be increased to expand the working range. However, technically this might be only feasible to a certain value due to the mechanical limits of the display. The majority of the subjects were able to distinguish from four to six different levels of pressure, which was consistent with the five levels reported by King et al. (2008a).

Pattern Identification

A second experiment was carried out to evaluate the display performance in terms of spatial representation. During this experiment, the number of correct answers while identifying different patterns was evaluated for three different balloon pressures.



Figure 5.8: Experimental protocol for pattern identification experiment.

Experiment Protocol

This experiment follows a factorial design with two different factors: pressure (3 levels), and pattern (6 levels). The six patterns used in the experiments are shown in Fig. 5.8. As in the previous experiment, each balloon was actuated simulating six heartbeats at a rate of 1.25 Hz (75 BPM). The patterns were presented in a random order and at three different pressure levels (200 mbar, 400 mbar and 900 mbar). Each pattern-pressure combination was repeated five times, resulting in a total of 90 trials per subject. During the experiments, subjects had a sheet in front of them with the numbered possible patterns (Fig. 5.8). Then they were asked to identify the pattern as soon as they were sure about their answer. Subjects were aware that number of pulsations they had to feel before answering was being recorded. However, it was pointed out that correctness was more important than response time. If the subject did not provide an answer, it was considered as a wrong answer.

Results

Repeated measures ANOVA was performed with the aforementioned factors: pattern and pressure level. The results are summarized in Table 5.1. The pressure factor had a highly significant effect on all measurements ($p_{corr} = 0.015$ for correctness and $p < 0.001$ for time response). Pattern factor was significant for the response time ($p = 0.006$).

Mean values for correctness and response time are shown in Fig. 5.9. The presented patterns were correctly identified in 96.3% of the cases. A percentage of 92.6% of the patterns presented at a pressure of 200 mbar were correctly identified, 98.8% at 400 mbar and 97.4% at 900 mbar. A Bonferroni post hoc test for multiple comparisons was performed to determine if there were significant differences at various pressure levels in answer correctness ($p_{200-400} = 0.007$, $p_{400-900} = 1.000$ and $p_{200-900} = 0.048$) and in response time ($p_{200-400} = 0.058$,

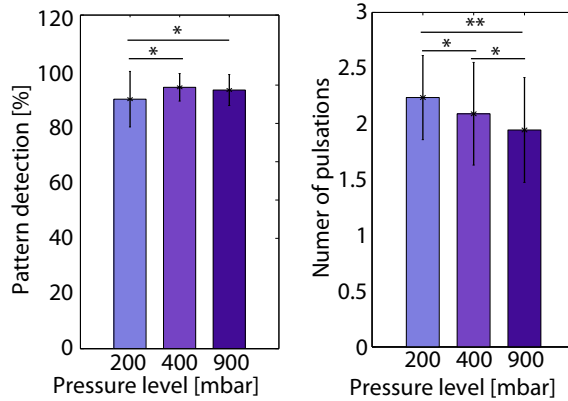


Figure 5.9: Mean values of answer correctness during the pattern identification and the number of pulsations that the subject required before answering in each trial. Lines with stars above, connect mean values that were found to be significantly different in the Bonferroni post hoc test (* for $p < 0.05$ and ** for $p < 0.001$). Pressure higher than 400 mbar seemed to enhance pattern perception thus speeding up the identification and increasing the number of correct answers.

$p_{400-900} = 0.058$ and $p_{200-900} < 0.001$). As it is shown in Fig. 5.9 pressure above 400 mbar significantly improved pattern recognition and decreased response time. No significant improvement was found for higher pressures in terms of correctness. Nevertheless, when the pattern was rendered at 900 mbar the response time was significantly reduced. We assume that there was no improvement in answer correctness for pressures above 400 mbar because the detection threshold might already be overcome at 400 mbar. According to [Stevens and Patterson \(1995\)](#), the minimal detectable indentation that can be differentiated from a uniform plane is at 0.2 mm. In this case, due to the smooth edges of the balloons the threshold might be higher. For this reason, the patterns displayed at pressures below 400 mbar are not easily identified. As can be seen in Fig. 5.4 at 400 mbar the produced deformation is around 0.5 mm but it should be noted that when the balloon is in contact with the fingertip, the deformation is slightly lower. Pressures above this threshold do not provide the users any additional information. However, subjects were more confident with their answers at 900 mbar, thus lowering their response time and improving their speed-accuracy results. The Bonferroni post hoc test the pattern 1 (horizontal top line) was recognized faster than the pattern 6 (diagonal from

Table 5.1: Results of the repeated measures ANOVA for the pattern identification test

Parameter	Pressure	Pattern	Interaction
Correctness *	$F(1.41, 18.40) = 6.125$ $p_{\text{corr}} = \mathbf{0.015}$	$F(1.92, 25.02) = 2.374$ $p_{\text{corr}} = 0.115$	$F(10, 130) = 0.627$ $p = 0.633$
Resp. time	$F(2, 26) = 12.399$ $p < \mathbf{0.001}$	$F(5, 65) = 3.634$ $p = \mathbf{0.006}$	$F(10, 130) = 0.740$ $p = 0.685$

* This factor did not pass the [Mauchly sphericity test](#), thus [Greenhouse Geisser sphericity correction](#) was performed.

top-left to bottom-right) with a $p_{P1-P6} = 0.0535$, that is the reason why pattern was found to be a significant factor in the repeated measures ANOVA. However, no significant differences were found among all the other patterns.

5.1.4 Discussion and Conclusions

The tactile pulse display provides notable flexibility, a simple manufacturing process, and cost-efficiency. In addition, an ad-hoc control unit was developed resulting in a compact, portable and multi-platform overall system. The performance of the PDMS block, in terms of output displacement related to pressure input, fulfilled all the initial requirement, with in particular, a linear response to pressure input. Moreover, the characterization of the control-unit showed that the bandwidth for an optimal operation, without undesired vibrations, is high enough to simulate a pulse pressure profile. The manufacturing process of the PDMS block is not expensive and could be simplified by using a mold-injection to fabricate both the main block and the thin elastic film. For this reason the display could be realized as single use unit.

The function obtained with the magnitude estimation experiment is nearly linear, meaning that the user's sensation can be considered as proportional to the input pressure. Furthermore, the function is free of saturation guaranteeing optimal performance at any pressure within the working range (0 to 1 bar). Besides, this function can be used to control the device, directly commanding the required level of user perception.

A second psychophysical experiment was performed in order to evaluate system performance in terms of spatial representation. The outcome of this test clearly shows that patterns are accurately identified, with an average of 96.3% of correct answers. It was observed that pressures of 400 mbar and above enhance the user's perception of the stimulus.

5.2 Influence of Tactile Feedback and Sensory Substitution on Palpation Performance

In this part of the chapter, the effect of different types of feedback (tactile and/or visual) on the performance during a palpation task is investigated. Subjects carried out two typical palpation tasks: (1) exploring a tissue to find a hidden artery and (2) identifying the orientation of a hidden artery. To do so we have developed an experimental setup based on a VR testbed that measures the users' performance under three different feedback conditions:

- visual feedback only "V",
- tactile feedback only "T" and
- visual plus tactile feedback "VT".

5.2.1 Experimental Setup

Hardware

A common palpation task performed in open surgery procedures provides simultaneous tactile and force feedback. Therefore, to evaluate the role of **haptic feedback** in this kind of task we used a device capable of conveying both essential feedbacks: tactile and kinesthetic. In order to reproduce a palpation task combining both of these modalities, a thimble was designed to attach the tactile pulse display previously described to the endpoint of an omega.3 force feedback device as shown in Fig. 5.10.



Figure 5.10: Omega.3 device customized with a thimble integrating the tactile pulse display.

The VR-based testbed ran on a Mac Book 5.1 laptop with an Intel Core 2 Duo 2.4 GHz CPU. The computer graphic card was an NVIDIA GeForce 9400M 256M GPU. The haptic and graphic loops were updated at 1 kHz and 30 Hz respectively and the communication with the omega.3 and with the tactile display controller were achieved through a USB connection (baud rate = 921.6 kb).

VR-based Testbed

As illustrated in Fig. 5.11, the proposed VR-based testbed is composed of:

- (a) a virtual model of soft tissue;
- (b) the model of a pointing hand that can be translated in space by the omega.3 haptic device;
- (c) a simulated tactile sensor;
- (d) a small window visually representing the tactile information; and
- (e) the tactile pulse display.

A second version of the setup with a left hand was used for left-handed subjects.

During the experiments, the exploration of tissue was performed with just one finger and the virtual tissue is flat with some bumps. The soft tissue was modeled as a mass-spring-

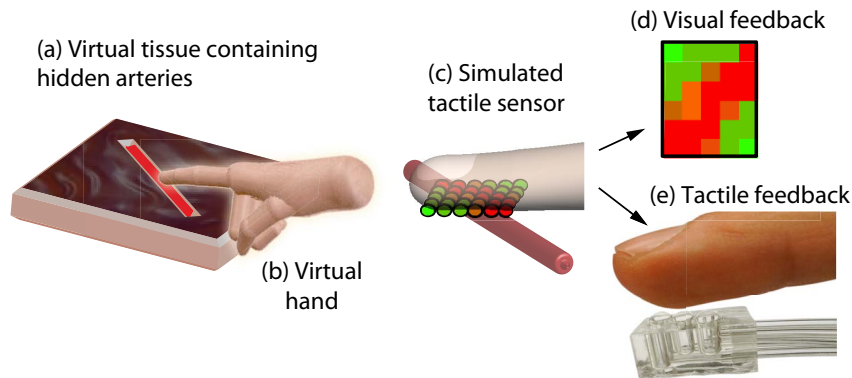


Figure 5.11: Components of the VR-based testbed and pulse rendering. A simulated tactile sensor with a 5×6 matrix of pressure sensitive cells is located below the virtual fingertip. The distance between the simulated sensor and the hidden artery determines the magnitude of the pulse rendered in each square of the visual feedback and in each air chamber of the tactile display.

damper mesh based on the GEL models provided by the CHAI3D library (Conti et al., 2007). The parameters of the mass-spring model of the virtual tissue were tuned to give the sensation of phantom tissue pads widely used in this kind of experiments (Wagner et al., 2007; Semere et al., 2004; Yamamoto et al., 2009; Kitagawa et al., 2005b). Furthermore, it is well known that physiological parameters such as tissue stiffness and damping vary widely from organ to organ, so that any attempt for higher mathematical precision in this context seemed in vain.

Pulse Rendering

The role of force feedback in this setup was to render the forces felt by the user's hand when touching the virtual tissue. Note that no haptic information regarding the hidden artery was given by the omega.3. Instead, the pulse from the hidden artery was provided through the tactile display and through a visual display (2D color map), presenting the local pressure distribution measured by the virtual tactile sensor.

To calculate the magnitude of the pulse information to be presented on the tactile and visual pulse displays, we simulate a tactile sensor located below the virtual fingertip. The simulated tactile sensor imitates the resistive tactile sensor developed by Schostek et al. (2006). The real tactile sensor consists of a matrix of 5×6 resistive cells providing a voltage value proportional to the pressure on each of them individually. Similarly, the measurement obtained from each simulated tactile sensor cells is inversely proportional to the distance of the artery to that particular cell as illustrated in Fig. 5.11 (c).

Although the setup is mostly bidimensional, the distance to the artery was calculated in 3D to increase the realism of the palpation task. The artery position was fixed in space and during the palpation the layer of tissue was compressed over it. Therefore, intensity of

the pulse information depended on both the distance to the artery and its diameter. If the subject pressed the tissue more firmly, he/she would get closer to the artery and thus, the pulse feedback would be stronger resulting in more pressure in the tactile display and more red intensity in the visual display.

The chosen visual feedback imitates the representation used by [Schostek et al. \(2006\)](#) in the use of their tactile sensor to detect arteries hidden in tissue. For this reason, the visual feedback shown in Fig. 5.11 (d), consists in a 5×6 matrix of squares that shows a color ranging from green to red representing the pressure calculated for the corresponding cell of the sensor. This type of 2D color map has been widely applied to represent the pressure distribution measured by a tactile sensor in other teletaction systems ([Trejos et al., 2009](#); [Gwilliam et al., 2010](#); [Talasaz et al., 2010](#)).

The resolution of the tactile display is lower as it is composed of only 5 air chambers. Therefore the pressure rendered by one of the tactile display's chambers corresponds to the average of the six adjacent cells of the simulated tactile sensor (Fig. 5.11 (e)). To geometrically match the measurement with the display, the air chamber in the center renders the center column of cells of the virtual tactile sensor. The frequency of the rendered pulse was 1.25 Hz, which corresponds to the average heart rate at rest (75 BPM), and was kept constant throughout all the experiments.

The maximum amplitude of the simulated pulse was 800 mbar, which corresponds to four times the real radial artery pressure (Fig. 5.6, right). This maximum will only be rendered if the user directly touches the artery, a case that never occurred in this experiment, as there was always some tissue between the virtual hand and the hidden artery. During the experiment the rendered pulse ranged between 200 and 700 mbar depending on the pressure exerted on the tissue and the size of the artery. The complete experimental setup is shown in Fig. 5.12.

5.2.2 Experiment 1: Exploration Task

In order to compare the users' performance under different feedback conditions, we first performed an experiment in which the user has to find a hidden artery of unknown size, orientation and location.

There is no obvious way to effectively measure user performance in a palpation task. When the effect of force feedback is studied, the force applied by the user during the palpation is a good mean of determining the possible effects on tissue ([Yamamoto et al., 2009](#); [Trejos et al., 2009](#); [Feller et al., 2004](#); [Talasaz et al., 2010](#)). Conventional performance metrics such as accuracy and completion time might not be sufficient to quantitatively compare the effectiveness of various types of feedback in a complex task.

Fitts law, discussed in Chapter 3, is not valid for the present experiment for two major reasons: (1) the target is not visible and thus the movement is not planned in advance, and (2) when the feedback to the user is transmitted by different senses (visual, tactile or both) the relationship between the difficulty of the task and the completion time might not be linear. This particular issue means that a model should be determined for every type of

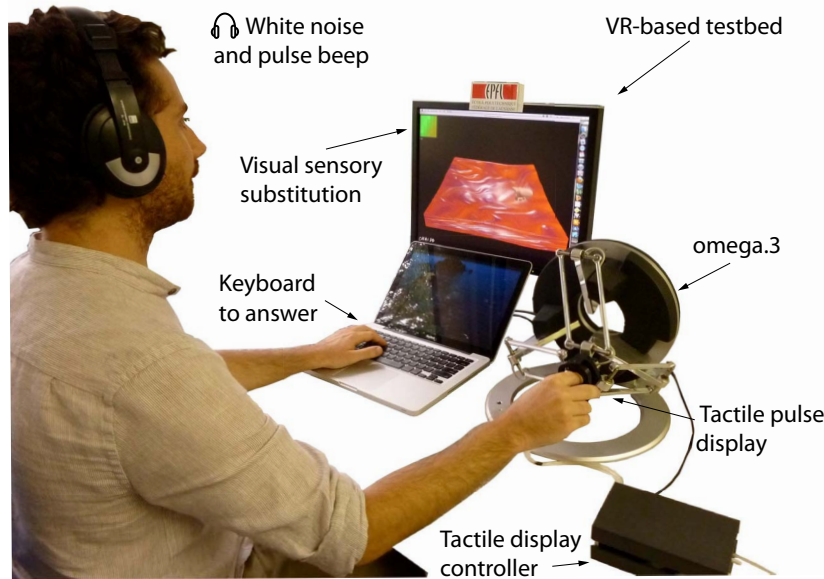


Figure 5.12: Experimental setup. Subjects wear headphones that play white noise and pulse beeps synchronized with the pulse feedback to drown out the noise of the pneumatic valves when the tactile display is active.

feedback making it impossible to compare the index of performance for the same task. In this experiment, we are quantitatively evaluating the user’s performance by task-completion time, and qualitatively evaluating the feedback’s performance by studying the subjects’ behavior across four different *ID*. In our experiments, the subject performs tactile exploration of a virtual tissue to find an invisible artery. This is the reason for increased difficulty when the area of the hidden artery decreases. Hence, what determines the *ID* is the ratio between the area that has to be explored (A_t) and the area occupied by the artery (A_a). The different indices of difficulty are fixed by changing the pulsating artery size with respect to the tissue area to be explored (Fig. 5.13). The highest *ID* corresponds to the smallest artery and vice versa.

Experimental Protocol and Subjects

In this experiment, the subject was asked to explore the virtual tissue and find the invisible artery hidden beneath it. He/She always began the experiment from the same point of the virtual environment. The point was indicated by a sphere fading away at the beginning of each trial (Fig. 5.14). Once the subject found the artery, he/she answered by pressing the “space” key on the keyboard and it is at that moment that the task-completion time was recorded. Thereafter the red sphere appeared a second time to indicate the starting point in the 3D space. The consecutive trial started after a rest period of 5 seconds, which was indicated by a change of the sphere’s color. Subjects were asked to slide over the tissue with

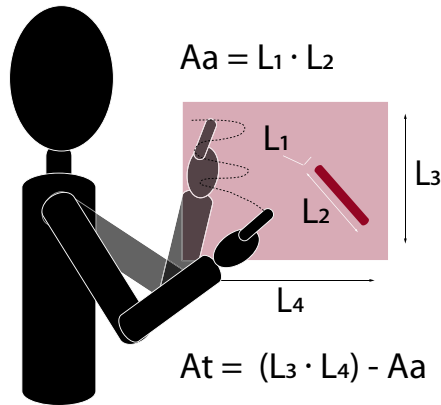


Figure 5.13: Exploration task experiment in which the subject performs the tactile exploration of a virtual tissue to find the hidden artery. Various difficulty levels are used in the experiment by changing the pulsating artery size with respect to the tissue area to be explored.

constant pressure. Subjects could choose their preferred direction and exploratory strategy. When the artery was not found subjects tended to re-explore applying more pressure to feel the weak arteries better. Subjects wore headphones displaying a white noise and a beep sound synchronized with the pulse signal to cover up auditory cues from the valve array. The experiment was constantly supervised to make sure that the subject only answered when the artery had been found otherwise that trial was discarded.

The artery position and orientation in the tissue were changed randomly but its depth was always constant. In order to sample a wide range of information, four combinations of arterial length (L_1) and width (L_2) were used to increase the task's difficulty (Table 5.2).

Table 5.2: Index of difficulty (ID) depending on artery dimensions.

Index of Difficulty	L_1 [cm]	L_2 [cm]	Aa [cm ²]
ID1	1.5	4.6	6.9
ID2	1.5	2.6	3.9
ID3	0.4	4.6	1.84
ID4	0.4	2.6	1.04

Force feedback was provided while interacting with the virtual tissue throughout all experiments. There are three types of feedback that can inform subjects when the virtual hand is in the proximity of a virtual artery:

- visual feedback only “V”,
- tactile feedback only “T” and
- visual plus tactile feedback “VT”.

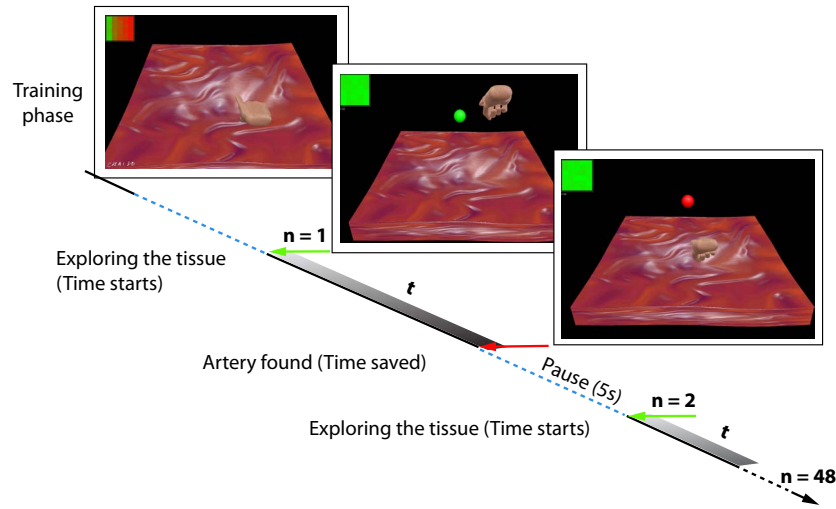


Figure 5.14: Experimental protocol for the exploration task. Subjects repeat the palpation task 48 times making a break of around 10 minutes after the 24th repetition. A red sphere indicates the starting point in the 3D space. After 5 seconds of pause the sphere turns green to indicate the start of the next trial. The feedback types (V, T and VT) are presented randomly.

The type of feedback available in each trial is randomized during the experiment. Subjects were not aware of the feedback they would receive each time to avoid a bias on their attention. Each combination of ID and feedback type was repeated 4 times. Thus, every subject performed a total of 48 trials. Subjects were allowed a few minutes of rest after 24 trials.

To avoid the influence of the learning curve on experiment results, the procedure started with a training phase until the subject obtained expert status. This was determined by comparing the task-completion times with the ones obtained during preliminary tests.

This experiment was performed with ten subjects who had no surgical experience (one woman and nine men), aged between 21 and 34 years old and all of them were right-handed. All participants gave written informed consent. The study protocol was performed in accordance with the ethical standards laid down in the Declaration of Helsinki.

Results

Repeated measures ANOVA with a critical value of $\alpha < 0.05$ was performed with two factors: feedback type and ID. The results are summarized in Table 5.3. The two factors and its interaction had significant impact on task-completion time.

In Fig. 5.15, the average values of task-completion time per feedback type are compared and analyzed for every difficulty level. When the complexity of the task is low, users perform significantly faster with the T feedback type. At these difficulty levels the addition of visual cues (VT feedback type) increased the task-completion time. However, at high difficulty

Table 5.3: Exploration task: repeated measures ANOVA for task-completion time

Feedback type *	ID *	Interaction *
$F(1.82, 16.44) = 6.410$	$F(1.47, 13.3) = 15.044$	$F(3.26, 29.35) = 3.519$
$p_{\text{corr}} = \mathbf{0.010}$	$p_{\text{corr}} < \mathbf{0.001}$	$p_{\text{corr}} = \mathbf{0.024}$

* These factors did not pass the [Mauchley sphericity test](#), thus [Greenhouse Geisser sphericity correction](#) was performed.

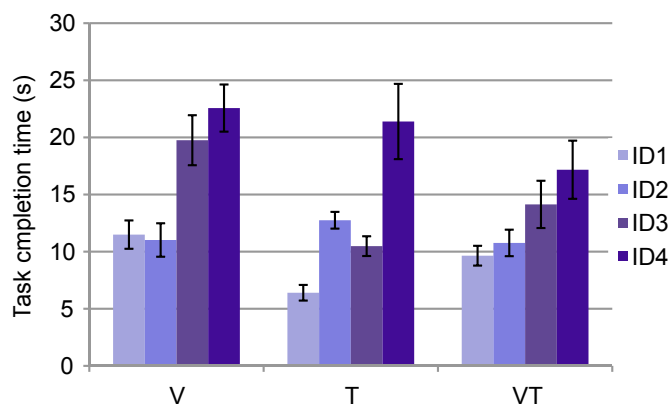


Figure 5.15: Average time that subjects spent palpating the tissue to find a hidden artery. Results are shown per feedback type and per ID. Note that task-completion times are generally lower when tactile feedback is available (T and VT). Error bars represent the standard error of the mean.

levels (ID) the users perform better with the VT feedback type. The Bonferroni post hoc test showed that the average task-completion time throughout all ID, was significantly reduced when tactile feedback was provided ($p_{V-T} = 0.015$ and $p_{V-VT} = 0.022$), see Fig. 5.16. The addition of visual feedback did not significantly affect task-completion time across difficulty levels ($p_{T-VT} = 1.000$).

Interaction between ID and feedback type is mainly due to an unexpected effect observed with the T feedback type for the ID3 and ID2. Most of the participants answered faster at ID3 than at the ID2 with this feedback type.

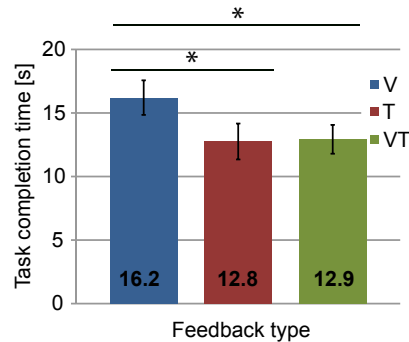


Figure 5.16: Global average values per feedback type. Lines with stars above, connect average values that were found to be significantly different in the Bonferroni post hoc test (* for $p < 0.05$ and ** for $p < 0.001$). Note that task-completion times are significantly lower when tactile feedback is available (T and VT). Error bars represent the standard error of the mean.

Discussion

The visual plus tactile feedback type (VT) presented better performance across different difficulty levels. For low difficulty levels the task-completion time is lower for tactile feedback alone than for visual feedback. We deduce that this is due to the difference in reaction time to visual and tactile stimuli. If the difficulty level is zero, which would correspond to an artery that occupies all the tissue, the task-completion time is due to the delay between pulses ($\approx 1s$), plus the reaction time to the given stimulus, and the time to press the key to answer. It can therefore be concluded that the reaction time to the given stimulus is the only component that can change from one feedback type to another. This result is thus coherent with other studies that have shown that reaction times to tactile stimuli are shorter than to visual stimuli (Sanders, 1998).

We also notice that for the lower difficulty levels, tactile feedback alone results in shorter task-completion times than the combination of tactile and visual feedback. However, when the palpation task becomes more difficult, the addition of visual feedback reassures subjects in their decisions and they are faster.

The task-completion time at low difficulty levels (ID1) and (ID2) is very similar for visual feedback only and visual plus tactile feedback. This finding suggests that for easy tasks when both types of feedbacks are present, subjects rely on more in visual feedback and thus task-completion times approach those obtained by visual feedback alone.

This is coherent with previous findings showing that vision strongly dominates the integrated visuotactile perception of the shape and size of objects (Rock and Victor, 1964). However, Ernst and Banks (2002) found that visual dominance occurs when the variance associated with visual estimation of the size of an object is lower than that associated with haptic estimation. In their study the estimation on the weight of an object was always closer to the visual information until the disturbances in visual information augmented. As the qual-

ity of visual feedback decreased the estimation started to be closer to the tactile information. Accordingly, we believe that the increase of difficulty level might augment the visual information's variance and thus tactile information would dominate at high difficulty levels reducing task-completion time. Results show that the two dimensions of the artery (L_1 and L_2) have a different effect on the difficulty of the task. As shown in Fig. 5.15, lowering the thickness (L_1) significantly increases the task-completion time for each feedback type. On the other hand, lowering the length (L_2) has only significant effect with tactile feedback. We hypothesize that reducing the length of the artery decreases the probability of passing over it while reducing the thickness of the artery decreases the intensity of the feedback (i.e. red level in the visual feedback or pressure on the tactile display). When the artery is thin and thus, the rendered pulse feedback is weaker, the tactile feedback is not affected as much as the visual feedback. This might be because the rendered pulse was weak but above the tactile detection threshold and thus the user felt the pulse. However, in the case of visual feedback, the change in color was weak, making it more difficult for the user's peripheral vision to perceive. This suggests that the model relating time and difficulty level might not be the same for visual and tactile feedback. Nevertheless, this effect is no longer present when both feedbacks are presented together. As it can be seen in Fig. 5.15, the trend of VT feedback across difficulty levels is almost linear.

5.2.3 Experiment 2: Absolute Identification Paradigm

In this second experiment, the AIP is used to assess the feedback type's influence (only visual, only tactile and visual plus tactile) on the user's performance in identifying artery orientation (for more details about this method please refer to Chapter 3). Contrary to the first experiment, in this task the arteries were always located in the same place and had the same size. In the literature related to working memory there is great discrepancy about the maximum number of items subjects can correctly remember (Jones, 2002; Cowan, 2001). However, it has never been reported to be less than four items as Tan et al. (2007) proposed for sphere sizes. In order to avoid any influence of working memory limitations on the experiment we have therefore chosen four orientations (horizontal, vertical and the two diagonals) as illustrated in Fig. 5.17.

These orientations can be considered as four stimulus categories ($k = 2^{IT}$) that are rendered through three different feedback types in a random order.

Experimental Protocol and Subjects

In this second experiment, subjects were asked to identify the orientation of a hidden artery from a set of four different possibilities, see Fig. 5.17. When subjects were sure of the artery orientation they indicated it by pressing the corresponding key on the keyboard. Illustrations of the different orientations were added on the corresponding keys to facilitate the task. As in the previous experiment, a red sphere above the tissue indicates the pause time before the next trial was presented.

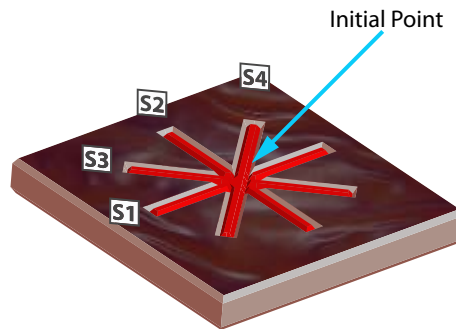


Figure 5.17: Virtual testbed to assess the effect of the feedback type on users' performance identifying the orientation of the hidden artery. The four different orientations represent the four stimuli (S_i) used in the calculation of the Information transfer. During the experiment the arteries were always invisible.

Subjects were asked to slide over tissue with constant pressure. During preliminary tests, it was observed that every subject has a preferred exploratory pattern and always starts exploring the tissue from the same point. To avoid a bias due to these individual exploratory patterns, subjects were instructed to always start from the center point (where all arteries cross), Fig. 5.18.

To avoid the influence of the learning curve on the results, the procedure started with a training phase until the subject obtains expert status. This was determined by comparing the task-completion times obtained with the ones obtained during preliminary tests. Subjects wear headphones and listen to white noise and a beep sound synchronized with the pulse signal to cover up auditory cues from the valve array.

Tan (1997), proposed that a total of $5 \cdot k^2$ trials should be performed to avoid over-correct results. We performed a total of 84 trials ($> 5 \cdot 4^2$) grouped in three sessions of 24, 24 and 36 trials respectively, in which the different combinations of feedback type and artery orientation were randomized.

This experiment was also performed with ten subjects who had no surgical experience (one woman and nine men) aged between 21-32 years. Three of them were left-handed and used the left-handed version of the setup. All participants gave written informed consent. The study protocol was performed in accordance with the ethical standards laid down in the Declaration of Helsinki.

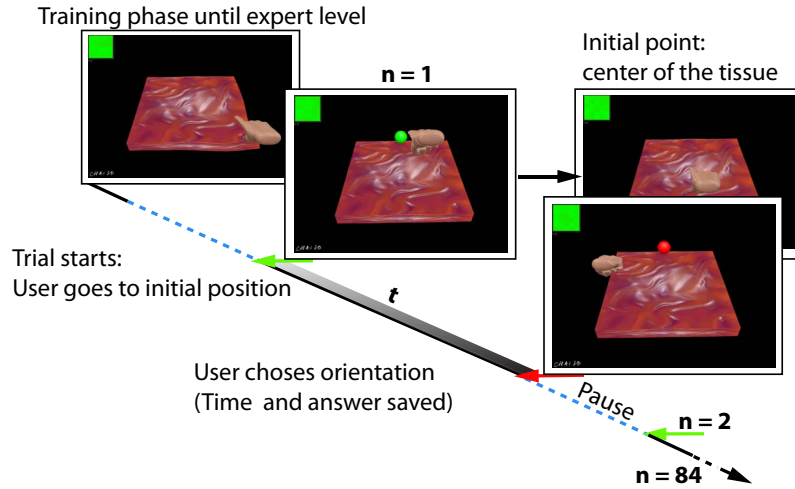


Figure 5.18: Experimental protocol for the second experiment. Subjects repeat the palpation task 84 times making a break between blocs of 24, 24 and 36 trials. A red sphere indicates that the answer has been saved. After 5 seconds of pause the sphere turns green to indicate the start of the next trial. The user starts palpating the center of the tissue. The feedback types and the orientations are presented in random order.

Results

The information transfer (IT) obtained are the following: $IT_V = 1.77$, $IT_T = 1.67$ and $IT_{VT} = 1.73$. There is no significant difference between the IT s obtained for each feedback type (note that differences are always lower than 0.1 bit). The Bonferroni post hoc test comparing the mean of correctness for different feedbacks did not find any significant difference. In addition, the repeated measures **ANOVA** performed with answer correctness shows that feedback type had no significant effect on this measurement (Table 5.4). On the other hand, the repeated measures **ANOVA** found influence of the feedback type on the overall task-completion time. Artery orientation was only significant for task-completion time. The Bonferroni post hoc test found that the vertical artery (S_2) was found significantly faster than the other three orientations independently of the type of feedback provided ($p_{S_1-S_2} = 0.019$, $p_{S_2-S_3} = 0.029$ and $p_{S_1-S_2} = 0.031$).

The mean values of task-completion times obtained during the identification task for each feedback type are shown in Fig. 5.19. The task-completion time is decreased with the types including tactile feedback. The Bonferroni post hoc test reveals a significant decrease when both visual and tactile feedbacks are available ($p_{V-VT} = 0.047$); however, there is no significant difference between tactile feedback alone and the combined feedback ($p_{T-VT} = 1.000$).

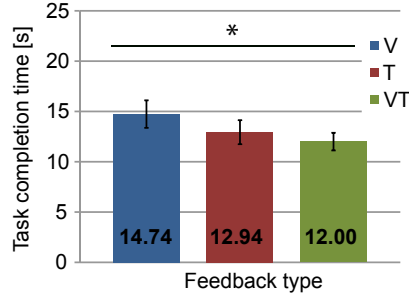


Figure 5.19: Average time that subjects spent on the identification task with each feedback type. Lines with stars above, connect average values that were found to be significantly different in the Bonferroni post hoc test (* for $p < 0.05$ and ** for $p < 0.001$). Note that task-completion times are lower when tactile feedback is available (T and VT). Error bars represent the standard error of the mean.

Discussion

The *IT*s obtained for each type of feedback are not significantly different. We realized that the users' attention can modify their performance. We tried to avoid a bias on the subjects' attention by randomizing the presented stimulus order. However, in the second experiment subjects had to start palpating from the crossing point of the different possible artery orientations thus, instantaneously noticing the feedback type presented in that trial. Therefore, from that moment on, the subject was able to pay more attention to that particular feedback type throughout the rest of the exploration task. This might be the reason why we could not find significant differences on the information transfer results for each feedback.

One hypothesis to explain why similar *IT* values were obtained could be that the task was relatively easy. However, if this was the case, a very high percentage of correct responses would result in *IT* values closer to 2 bit, which is the *IT* value corresponding to a perfect performance in this specific task.

The post hoc test showed that the artery with the orientation S_2 , which corresponds to the

Table 5.4: Identifying the orientation of the hidden artery: repeated measures ANOVA for correctness and task-completion time.

Measurement*	Feedback type*	Artery type*	Interaction*
Correctness	$F(1.77, 15.93) = 0.56$ $p_{corr} = 0.557$	$F(1.13, 10.22) = 1.73$ $p_{corr} = 0.220$	$F(2.26, 20.33) = 0.65$ $p_{corr} = 0.548$
Time	$F(1.69, 15.22) = 3.668$ $p_{corr} = \mathbf{0.055}$	$F(1.66, 15.22) = 4.850$ $p_{corr} = \mathbf{0.028}$	$F(2.28, 20.53) = 0.334$ $p_{corr} = 0.747$

* These factors did not pass the [Mauchly sphericity test](#), thus [Greenhouse Geisser sphericity correction](#) was performed.

artery parallel to the finger, was recognized significantly faster. Our hypothesis is that this orientation is easier because both the visual and the tactile displays have higher resolution in that direction.

5.2.4 Post-experiment Questionnaire

At end of the experiment every subject filled out the following questionnaire.

Questions

1. Age, gender and hand dominance.
2. Do you have previous experience with haptic devices? Yes, Some or None.
3. Do you have previous experience with tactile displays? Yes, Some or None.
4. How difficult did you consider the palpation task? Very difficult, Difficult, Medium, Easy or Very easy.
5. (Only for the 1st experiment) Were you aware of difficulty changes during the experiment? Always, Sometimes or Never.
6. What do you feel as the more natural feedback? Visual Feedback, Tactile feedback or Visual plus Tactile feedback.
7. Which feedback demands you more concentration? Visual Feedback, Tactile feedback or Visual plus Tactile feedback.
8. With which kind of feedback do you think that you performed the exploration faster? Visual Feedback, Tactile feedback or Visual plus Tactile feedback.
9. Do you think that you were paying more attention to any of these features? Virtual hand movement, Visual feedback window or Finger tactile sensation.
10. Comments

Results

Over the two experiments, most of the subjects affirmed to pay more attention to the virtual hand movement than to the visual or tactile feedback (Fig. 5.20). The 50% of the subjects affirmed that visual feedback demanded more concentration, 40% found tactile feedback more demanding and only 10% found visual plus tactile more difficult. Additionally, 80% of the subjects commented that they preferred the feedback type that included both visual and tactile feedback. Although the half of the subjects felt that tactile feedback alone was more natural, the combination of visual and tactile feedback allowed them to be more certain on their answer and thus, the 70% felt that they were performing faster with the combined feedback.

The five subjects that performed both experiments affirmed that the second experiment was easier because they already knew the location of the artery (only the orientation was unknown). Therefore, they just had to touch the middle of the tissue once to realize the feedback type that was active in that trial and could then concentrate on that feedback to perform the task. However, in the first experiment subjects did not know what type of feedback would be active on any particular trial and were more likely to pay more attention to the wrong one, which consequently caused in a total of 11 trials to overlook at first weak arteries and thus provoked longer task-completion times.

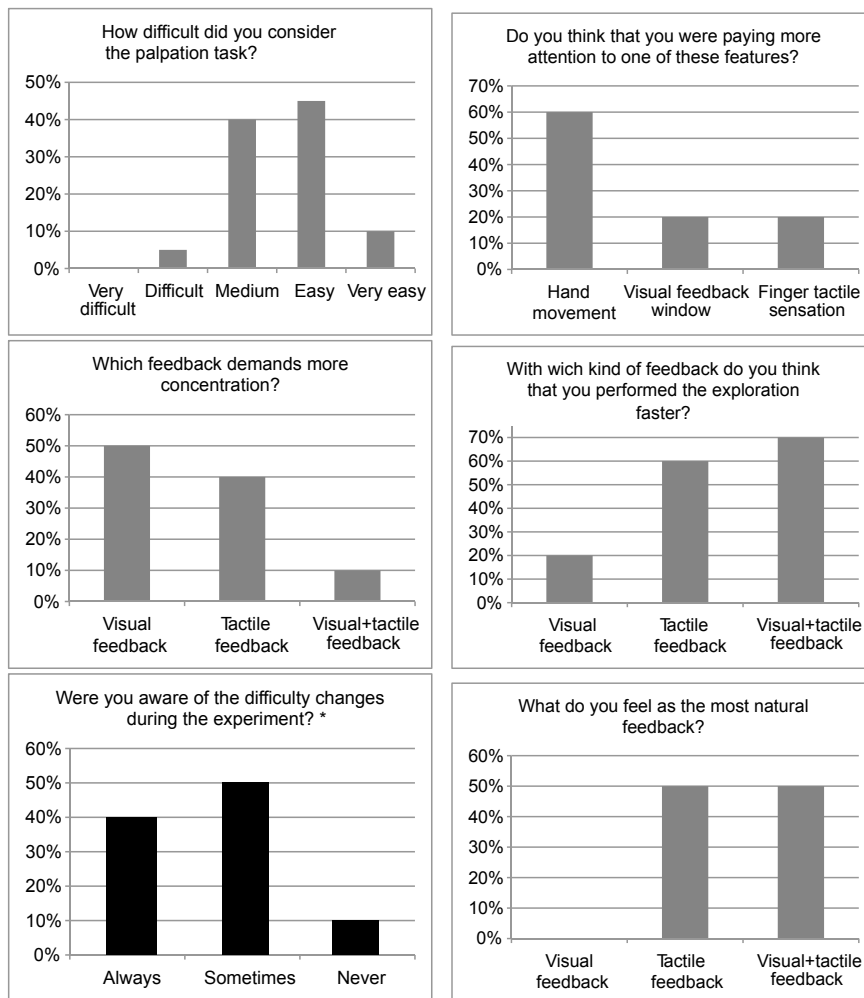


Figure 5.20: Bar plots with the questionnaire answers. Most of the subjects affirmed to pay more attention to the movement of the hand than to the visual or tactile feedback. The majority of the subjects felt that visual feedback alone was more demanding. The feedback types with tactile feedback were felt as more natural. The plot in black only applies to the first experiment in which several difficulty levels were used.

5.2.5 Discussion

The results of the two experiments presented in this paper show a significant decrease in task-completion time during a VR palpation task when tactile feedback is presented in addition to visual feedback. Nevertheless, this study also presents a number of limitations that must be discussed. VR-based testbeds are often criticized because it is difficult to determine to what extent the results can be generalized to a real teleoperated robotic system. In our case, the choice of a VR-based testbed was primarily motivated by the well-controlled and repeatable types that can be created. For instance, this solution permits to preserve the same types for all subjects (e.g. tissue properties, finger orientation). Furthermore, as it was discussed in Section 3.3.2, several studies have shown that in experiments performed through a teleoperated robotic system, the results are affected by the limitations of the slave robot (Feller et al., 2004; Talasaz et al., 2010; Trejos et al., 2009). The present study aimed to determine which channels of information are more convenient to improve the subject's performance. Therefore, the only parameter that should influence the rendered pulse's intensity should be the force and the movements that the subject applies. In addition, the VR-based testbed offers the possibility to mix feedback type and change artery position randomly during the experiment. Consequently, subjects cannot know what feedback and artery type will be displayed next, avoiding a bias in their attention.

In the first experiment, we found that for low difficulty levels the task-completion times were lower for tactile feedback than for visual feedback. We deduce that this is due to the difference in reaction times to tactile and visual stimuli. In the post-experiment questionnaire, 60% of the subjects affirmed to have paid more attention to the virtual hand movement than to the visual feedback, which might increase the reaction time to the visual feedback even more. It has already been shown that stimuli in the peripheral visual field provoked longer reaction times than the stimuli inside the visual field (Brebner and Welford, 1980). This presents a sort of limitation for this study as it implies that it might not be possible to generalize the results to every kind of visual feedback. Our implementation imitates a 2D color map, as it is the most commonly used in similar teletaction studies. The 2D color map is generally located in a corner of the screen or even displayed on a second monitor (Trejos et al., 2009; Gwilliam et al., 2010; Talasaz et al., 2010; Schostek et al., 2006). With this implementation, when the subject wants to monitor the motion of the virtual hand and the visual feedback his/her attention has to shift from one to another. Hence, another type of visual feedback overlying the virtual tissue, as the one used by Yamamoto et al. (2009), could increase the performance of the type with only visual feedback. The visual feedback used in this experiment tries to imitate the way that visual cues are currently presented in most of the systems. Therefore, besides its limitations, the results of this study show the potential benefits of adding tactile cues to those systems.

In the second experiment, we found that the information transfer for each type of feedback was similar but at the same time the task-completion time was significantly improved by the addition of tactile feedback. The 80% of the subjects asserted that they preferred visual plus tactile feedback because the redundant feedback served as confirmation when the difficulty level was high (i.e. when the arterial pulse was weak). This is coherent with the results of the

first experiment as we can clearly see that for the highest difficulty level, the task-completion time is significantly reduced when both types of feedbacks are present.

None of the participants in this study had previous surgical experience. The results with surgeons could be different as they develop perceptual skills to deal with the lack of feedback in MIS techniques and would probably pay more attention to the visual feedback. Our results indicate that this strategy could be avoided by providing tactile feedback.

Even though these results show the high potential of multimodal feedback in teleoperated robotic surgery, the main technological bottleneck that delays its clinical application is the integration of accurate and biocompatible tactile sensors in the robot. As it has been shown, multimodal feedback significantly benefits subjects without surgical experience. Therefore, a more immediate application could be its integration in surgical simulators to advance robotic surgery training and improve patient safety. To do so the effect on the surgeon's learning curve should be previously quantified by assessing the evolution of subjects' performance over the training period with different types of feedback.

5.3 Summary and Conclusions

This chapter addressed the importance of tactile feedback in several surgical gestures based on the tactile exploration of organs and tissues. The effect of different types of sensory feedback on the performance for a specific palpation task was analyzed through user studies. To achieve this, a new multimodal haptic display was developed by integrating a haptic device and a pneumatic tactile pulse display that simulates a pulsating artery. In addition, a virtual environment simulating the palpation task and with a small screen that can provide visually the tactile information of pulsating arteries were developed. A study comparing users' performance in a VR palpation task with tactile, visual or both types of feedback combined was carried out using this setup. Two different experiments were performed. Initially, task-completion times were analyzed in an experiment during which subjects had to localize a hidden artery by palpating a virtual tissue. Thereafter, the AIP was applied to an experiment where subjects had to distinguish the orientation of the hidden artery.

In the first palpation experiment, the feedback type combining both tactile and visual feedback got the best performance across different difficulty levels. Furthermore, this feedback type was preferred by most of subjects. Thanks to its intuitive nature and the fast reaction time to a tactile stimulus, the feedback types including tactile feedback significantly reduced task-completion times. In the second experiment, which entailed identifying artery orientation, the information transfer indices of the three types of feedback were very similar. However, the task-completion times were yet again reduced by adding tactile feedback especially when both visual and tactile feedbacks were together. These results show how the integration of kinesthetic, tactile and visual cues can significantly improve surgeons' performance during teleoperated palpation tasks. According to the subjects' answers, providing information simultaneously through several sensory channels permits the user to be more certain of his gestures, thereby increasing safety and potentially reducing cognitive load.

Part II

Towards an Ergonomic Surgeon's Console

Chapter 6

Survey on Surgical Instrument Handle Preferences: Ergonomics and Acceptance

The ergonomics in the OR have been progressively neglected in favor to more complex and less invasive surgical techniques. The surgeons are increasingly concerned about the ergonomic issues introduced by the new surgical instruments. A famous surgeon from the University of Wisconsin School of Medicine and Public Health has even affirmed in a public interview: “Ergonomics may be the most important issue facing surgeons today. [...] Our bodies have been abused and neglected” (Glickson, 2012).

Many studies have addressed the ergonomic issues that have raised with the use of different surgical instruments for various surgical techniques (Berguer, 1999; Berguer et al., 1998). These and other studies mainly investigated the surgeon’s posture (Nguyen et al., 2001; Lawson et al., 2007; Gofrit et al., 2008), the surgeon’s mental workload (Carswell et al., 2005; Zheng et al., 2010; Berguer et al., 2001) and the pressure distribution on the hand (Matern and Waller, 1999; Lawther et al., 2002).

The acceptance of a new surgical instrument within the medical community relies on many of factors that are not always impartial, and thus, it is challenging to assess them in a holistic way. One of the main goals of this thesis is to establish guidelines for future developments of surgical instruments and teleoperation handles. Therefore, a study based on a survey among surgeons was carried out.

This chapter presents an across-surgical techniques study that assesses the effects of various surgical approaches and instruments on the surgeons’ fatigue. Besides, an analysis of surgeons’ preferences with respect to instrument handles was performed to identify the main acceptance criteria. In all, 49 surgeons (24 with robotic surgery experience, 25 without) completed the survey. The results of this study showed that robotic surgery seems to alleviate physical discomfort during and after surgery; however, 28% of surgeons still complained about finger

and neck tension. Regarding the handle design surgeons generally preferred the handles that were controlled with a precision grasp. Comfort and precision have been found to be the most important aspects driving the surgeon's choice of an instrument handle.

The results of this survey have been published in [Santos-Carreras et al. \(2011\)](#). It should be noted that in the statistical analysis of this chapter a more conservative Bonferroni post hoc test has been performed differing from the published article, in which a Tukey post hoc test of Honestly Significant Difference was used. This has been changed for the sake of consistency in the methodology along the thesis, but the main results and conclusions coincide with those of the article.

6.1 Statistical Methods and Questionnaire Content

A total of 250 surgeons with experience in open, laparoscopic and robotic procedures were contacted for this study. Swiss public databases and Pubmed (US National library of Medicine) were used to gather contact information. Surgeons were contacted with an email explaining the aim of the study, including a link to the anonymous survey with instructions and a general password. The survey was conducted by means of a web-based form. The "Inform" platform of the [École Polytechnique Fédérale de Lausanne \(EPFL\)](#), Switzerland was used as the form support. Incomplete or incorrectly answered surveys were neglected. The valid answers were then statistically analyzed with STATISTICA (Stat Soft Inc.) and Matlab (The Mathworks, USA).

The survey contained 21 questions split into four parts: 1) demographic details, 2) discomfort and procedure duration, 3) the evaluation of seven different handles and 4) the choice of the preferred ones. The complete questionnaire is shown at the end of this chapter in Section 6.5.

Discomfort and Procedure Duration

The surgeons started the questionnaire by giving their demographic and background details. The second part of the questionnaire was related to the pain and discomfort experienced during or following surgical procedures. Surgeons reported in which body parts they experienced any kind of discomfort for each surgical technique. In order to compare the ergonomic issues associated with open, laparoscopic and robotic surgery, the percentage of surgeons that reported discomfort for each part of the body was calculated. The average duration of the surgical procedures was also enquired as it represents an important risk factor of work related injuries. The surgeons' percentage voting for each duration range was calculated for all the respondents first and then separately for two groups: with and without experience in robotic surgery.

Handle Evaluation

The third part of the survey consisted in the evaluation of various surgical instrument handles. Seven handles were presented (only as a picture) and the surgeons were asked about the ergonomics and usability of the open-close mechanism of each instrument.

The handles presented to the surgeons are controlled by various types of gripping movements (Fig. 6.1). According to the classification proposed by [Napier \(1956\)](#), three of the handles (H_1 , H_2 and H_6) are controlled by a precision grip (tool held between the tip of the thumb and the opposing digits). For the handle H_5 , the aperture can be controlled by a pure power grip (grip between all fingers and palm with the thumb adducted at both the metacarpophalangeal and carpophalangeal joints). For the H_4 the thumb is abducted to increase grip power. The handles H_3 and H_7 require a combined grip. For the H_3 the aperture is controlled by the thumb and index finger in a precision grip posture, while the remaining fingers are in a power grip. In the case of H_7 the handle is controlled by independent movement of the index and annular fingers; the thumb and the rest of the fingers hold the handle in a power grip.

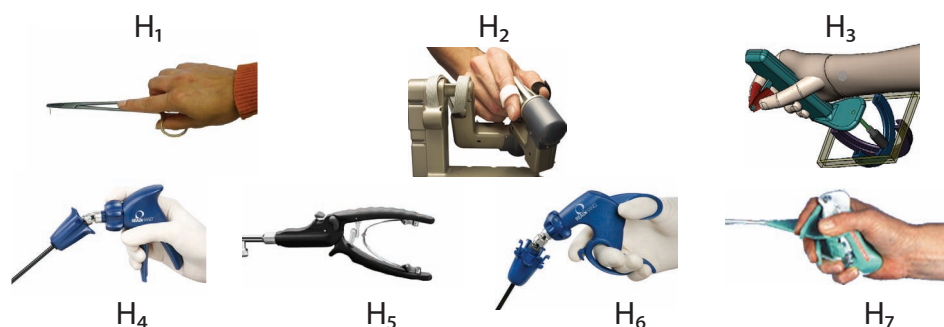


Figure 6.1: The evaluated handles are: H_1 conventional needle holder; H_2 from Intuitive Surgical systems ([Intuitive Surgical Inc., 2010](#)); H_3 joystick-like concept proposed by the authors; H_4 and H_6 from Novare Surgical Systems ([Novare, 2010](#)); H_5 from RWOLF ([RWOLF, 2010](#)) and H_7 from Mattern and Weller ([Mattern and Weller, 1996](#))

Having in mind the open-close action, surgeons had to score each handle according to four criteria: intuitiveness, comfort, precision and stability. The score ranged from 1 to 5 points (1 = bad, 5 = good). Repeated measures ANOVA of 4×7 (four criteria and seven handle types) was performed to determine which of the factors were significant and if there was interaction between handle type and criterion. In order to find the significant differences between handles for each of the four criteria, we performed a Bonferroni post hoc test for multiple comparisons ([Mauger and Kauffman Jr, 2001](#)). Thereafter, in order to detect cross influences between the different criteria, a correlation matrix was obtained by means of a Pearson correlation analysis with a critical value of $p = 0.05$.

A supplementary question, asked the surgeons their opinion about the addition of extra features and controls on the surgical instrument handle.

Handle Preference

In the fourth part of the survey, surgeons could choose their preferred instrument(s) and optionally explain the reasons for their choice. One of the goals of the present study is to determine which are the most influential aspects on the surgeons' preference regarding the surgical instruments. To do so, a model representing the degree of preference with respect to the different criteria had to be obtained. Therefore, an automatic stepwise multiple variable linear regression with a critical value of $p = 0.05$ was performed in Matlab. This method systematically adds or removes terms from a multilinear model basing the decision on the statistical significance of each term in a regression. The method begins with an initial model and then compares the results of adding or removing criteria. At each step, the p-value of an F-statistic is computed to test the model with and without a potential term. If there is sufficient evidence to reject the null hypothesis ($p < 0.05$), the new term is added to the model. On the other hand, if there is insufficient evidence to reject the null hypothesis ($p > 0.05$), the term is not included.

At the end of the form, surgeons had the opportunity to elaborate upon their response and give further comments and insights. The complete questionnaire is presented at the end of this chapter in Section 6.5.

6.2 Results

Respondents' Details

20.4% of all contacted surgeons completed the survey. A total of 51 surveys were collected, of which two were incomplete (4%) and thus, were removed from the analysis. Therefore, a total of 49 surveys were retained for the analysis. The majority of surgeons were male (88%) with a mean age of 43 ± 8 years. All were experienced in open surgery, most in laparoscopy and about 50% in robotic surgery (Table 6.1). The respondents mainly worked in Europe (73%) and the USA (17%), with predominance of surgeons from Switzerland (35%). The complete panel of surgeons is presented on Fig. 6.2.

Table 6.1: Surgeons' demographic and background characteristics

Gender	43 M & 6 F
Experience (n. of surgeons)	In open surgery: 49 In laparoscopic surgery: 45 In robotic surgery: 24
Mean age (years)	43 ± 8.36

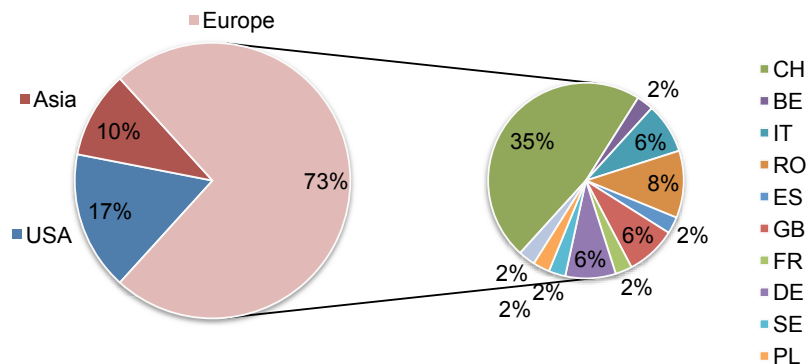


Figure 6.2: Surgeons' country of practice

Discomfort and Procedure Duration

During open surgery, surgeons claimed that the major discomfort is felt in the neck and the back (52.1% both) followed by the shoulders (20.8%). During laparoscopic surgery the main complaint was about the shoulders (41.9%), followed by the neck (37.2%), the back (34.9%), the fingers (30.2%) and the wrists (20.9%). Surgeons specialized in robotic surgery mostly complained about neck and wrist discomfort (28%), followed by the back (20%). None of the surgeons complained about fingers discomfort while performing robotic surgery, while 20.9% did for laparoscopic and 12.5% did for open surgery. For more details refer to Fig. 6.3.

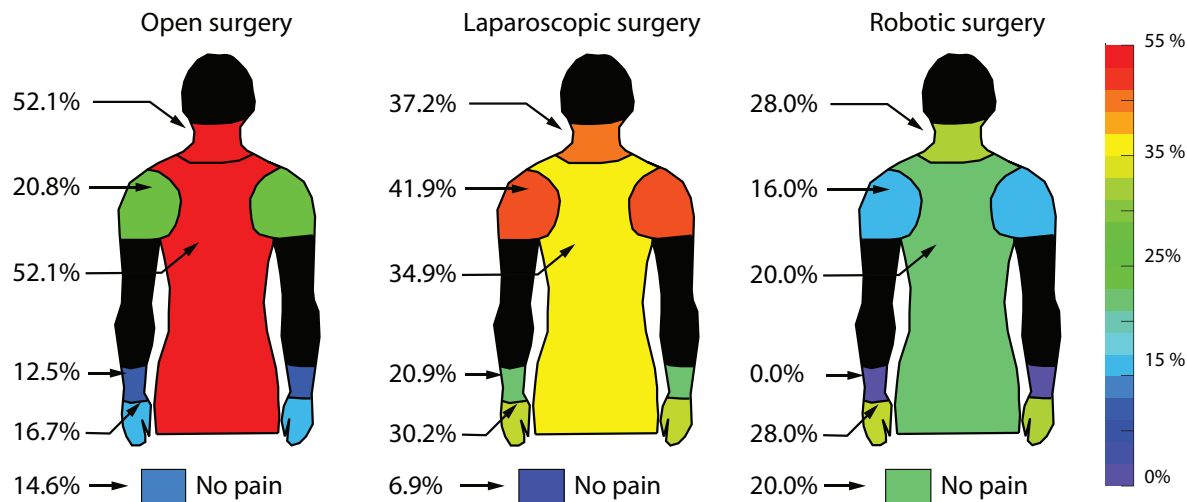


Figure 6.3: Body parts where the surgeons felt discomfort during or after surgery. The colors represent the percentage of surgeons suffering discomfort or pain in that body part.

The results concerning the duration of the surgical procedures are shown in Table 6.2.

Overall, across different surgical techniques, the majority of the surgeons (53%) stated that the average duration of the surgical procedure ranges from two to five hours. Most of the specialists in robotic surgery performed interventions with duration between two and five hours, the rest for more than five hours and only a few indicated that they perform surgeries lasting less than two hours. For non-robotic procedures the percentages were the same for both less than two hours and from two to five hours, and a minor percentage for operations above five hours (Table 6.2).

Table 6.2: Duration of the surgical procedure (percentage of surgeons)

Procedure length	< 2h	2 – 5h	> 5h
Robotic Surgery	6.1%	30.6%	12.2%
Conventional Surgery	22.4%	22.4%	6.1%
Total	28.57%	53.06%	18.37%

Handle Evaluation

We have performed repeated measures ANOVA in order to determine if there are significant differences on the ranking due to the handle-type or criteria (Table 6.3). All factors had a significant influence on the score. In Fig. 6.4 the average of all surgeons' scores for each handle is summarized.

Table 6.3: Repeated measures ANOVA 4×7 for handle-type and evaluation criteria

Effects	F-value	p-value
Handle-type	$F(6, 288) = 7.808$	< 0.001
Evaluation criteria	$F(3, 144) = 3.869$	0.01
Interaction H.type and criteria	$F(18, 864) = 2.985$	< 0.001

In terms of intuitiveness, the conventional needle holder for open surgery (H_1) and the da Vinci wrist (H_2) received 3.80 and 3.76 respectively. The scores of these handles were not significantly different ($p_{H_1-H_2} = 1.000$). However, they were significantly higher than the scores obtained by H_3 , H_4 and H_7 , which were found to be the least intuitive handles. No significant differences were found between them ($p_{H_3-H_4} = 1.000$, $p_{H_3-H_7} = 1.000$ and $p_{H_4-H_7} = 1.000$) (Table 6.4).

For the comfort criteria the results were as follows: H_3 received a score of 3.57, H_2 a score of 3.53 and H_1 a score of 3.47; differences between these three scores were not significant ($p_{H_1-H_2} = 1.000$, $p_{H_2-H_3} = 1.000$ and $p_{H_1-H_3} = 1.000$), but all of these scores were significantly higher than the pistol-like prototype of the Novare (H_4) and the axial handle of the RWOLF needle holder (H_5) with 2.88 and 2.90 respectively. The Bonferroni post hoc test results show that these handles were not significantly different between them ($p_{H_4-H_5} = 1.000$) (Table 6.5).

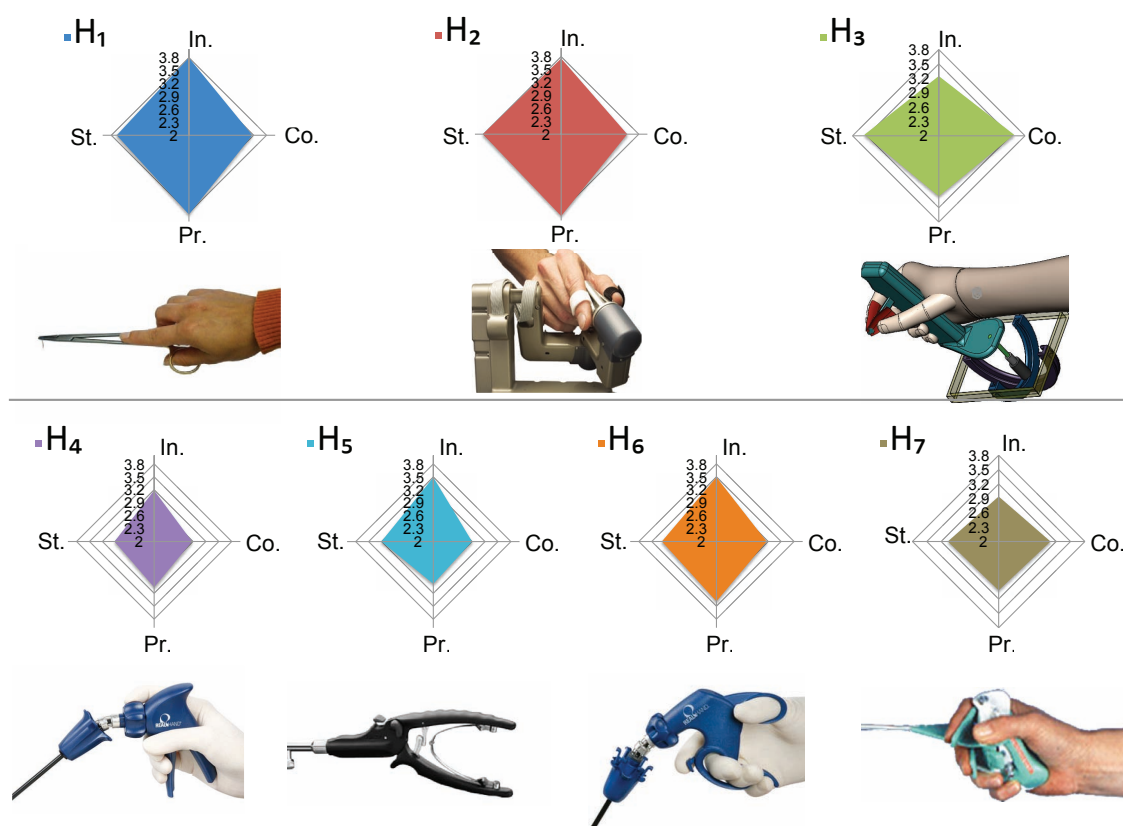


Figure 6.4: Score for each handle in terms of: Intuitiveness (In.), Comfort (Co.), Precision (Pr.) and Stability (St.). The evaluated handles are: H₁ conventional needle holder; H₂ from Intuitive Surgical systems (Intuitive Surgical Inc., 2010); H₃ joystick-like concept proposed by the authors; H₄ and H₆ from Novare Surgical Systems (Novare, 2010); H₅ from RWOLF (RWOLF, 2010) and H₇ from Mattern and Weller (Mattern and Weller, 1996)

Table 6.4: p-values resulting from the Bonferroni post hoc test for the intuitiveness scores.

Intuitiveness score	H ₁	H ₂	H ₃	H ₄	H ₅	H ₆
H ₁ (3.80)						
H ₂ (3.76)	1.000					
H ₃ (3.22)	0.023	0.016				
H ₄ (3.18)	0.006	0.004	1.000			
H ₅ (3.49)	1.000	0.969	1.000	1.000		
H ₆ (3.49)	1.000	0.969	1.000	1.000	1.000	
H ₇ (2.94)	< 0.001	< 0.001	1.000	1.000	0.012	1.000

The handles providing most precision while controlling the instrument aperture were found to be H₂ and H₁ with 3.90 and 3.84 respectively; differences between these scores were not

Table 6.5: p-values resulting from the Bonferroni post hoc test for the comfort scores.

Comfort score	H ₁	H ₂	H ₃	H ₄	H ₅	H ₆
H ₁ (3.47)						
H ₂ (3.53)	1.000					
H ₃ (3.57)	1.000	1.000				
H ₄ (2.88)	0.003	< 0.001	< 0.001			
H ₅ (2.90)	0.006	< 0.001	< 0.001	1.000		
H ₆ (3.16)	1.000	1.000	0.770	1.000	1.000	
H ₇ (3.08)	1.000	0.263	0.082	1.000	1.000	1.000

significant ($p_{H_1-H_2} = 1.000$). Significantly lower scores were obtained by H₅ (2.98) and H₇ (3.02). The Bonferroni post hoc test results show that H₅ and H₇ were not significantly different between them ($p_{H_5-H_7} = 1.000$) (Table 6.6).

Table 6.6: p-values resulting from the Bonferroni post hoc test for the precision scores.

Precision score	H ₁	H ₂	H ₃	H ₄	H ₅	H ₆
H ₁ (3.84)						
H ₂ (3.90)	1.000					
H ₃ (3.29)	0.012	0.001				
H ₄ (3.06)	< 0.001	< 0.001	1.000			
H ₅ (2.98)	< 0.001	< 0.001	1.000	1.000		
H ₆ (3.39)	0.263	0.044	1.000	1.000	0.770	
H ₇ (3.02)	< 0.001	< 0.001	1.000	1.000	1.000	1.000

On the stability aspect, H₂ (3.81), H₁ (3.67) and H₃ (3.55) were found to be the most stable handles; no significant differences were found between them ($p_{H_1-H_2} = 1.000$, $p_{H_1-H_3} = 1.000$ and $p_{H_2-H_3} = 1.000$). Significantly lower scores were obtained by H₄ (2.91) and H₇ (3.06). The Bonferroni post hoc test did not find any significant difference between them ($p_{H_4-H_7} = 1.000$) (Table 6.7).

The correlation matrix in Table 6.8 shows that there is a significant correlation between the scores given to comfort and stability (Pearson correlation coefficient = 0.92, $p = 0.0032$) and between intuitiveness and precision (Pearson correlation coefficient = 0.83, $p = 0.02$).

The 73.5% of the surgeons reported that they would not like additional features or controls on the surgical instrument handle. The rest of the surgeons (24.5%) reported that it could be useful to have the control of the ablation tool integrated into the handle (e.g. to activate the cauterization or to replace the pedals).

Table 6.7: p-values resulting from the Bonferroni post hoc test for the stability scores.

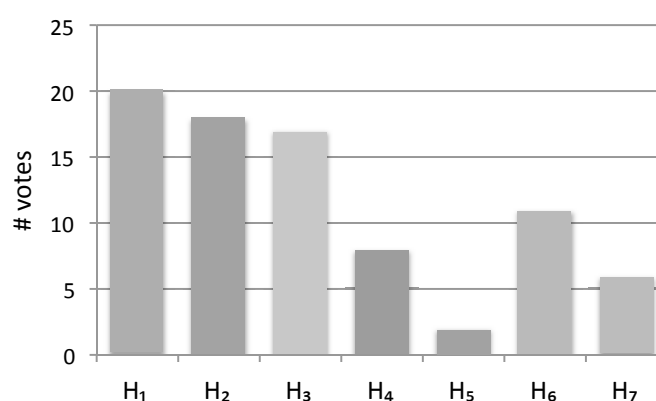
Stability score	H ₁	H ₂	H ₃	H ₄	H ₅	H ₆
H ₁ (3.67)						
H ₂ (3.81)	1.000					
H ₃ (3.55)	1.000	1.000				
H ₄ (2.91)	< 0.001	< 0.001	0.001			
H ₅ (3.20)	0.148	0.001	1.000	1.000		
H ₆ (3.26)	0.770	0.012	1.000	1.000	1.000	
H ₇ (3.06)	0.001	< 0.001	0.082	1.000	1.000	1.000

Table 6.8: Correlation matrix between the four evaluation criteria and the preference score

	Preference
Intuitiveness	0.554 (p = 0.192)
Confort	0.920 (p = 0.003)
Precision	0.878 (p = 0.008)
Stability	0.842 (p = 0.018)

Handle Preference

After completing the handle evaluation, surgeons voted for their preferred handle(s) to control the instrument aperture (note that multiple selections were allowed). The handles H₁, H₂ and H₃ were the preferred handles as they obtained a significantly higher number of votes (Fig. 6.5). Thereafter, a stepwise regression analysis was performed to obtain the model that best represent surgeons' choice pattern for surgical instrument handles.

**Figure 6.5:** Number of votes per handle. Note that multiple selections were allowed.

According to the correlation matrix between preference scores and the criteria shown in

Table 6.8, preference was not correlated with intuitiveness but presented a high correlation with the other three criteria (comfort, precision and stability). However, as reported in the previous section, there was a correlation between intuitiveness and precision as well as between comfort and stability. Therefore, the stepwise regression analysis showed that a model including the three aspects over-fitted the preference function and was therefore not valid. The model that best represented the handle preference pattern of the surgeons was found to be a function of comfort (c) and precision (p) ($R^2 = 0.911, p = 0.007$).

$$Hp(c, p) = -57.22 + 13.80 \cdot c + 7.27 \cdot p \quad (6.1)$$

The Fig. 6.6 illustrates the preference model as a plane related to comfort and precision. As it can be deduced from equation 6.1 and from the slope in Fig. 6.6, comfort (c) had more influence on handle preference than precision (p).

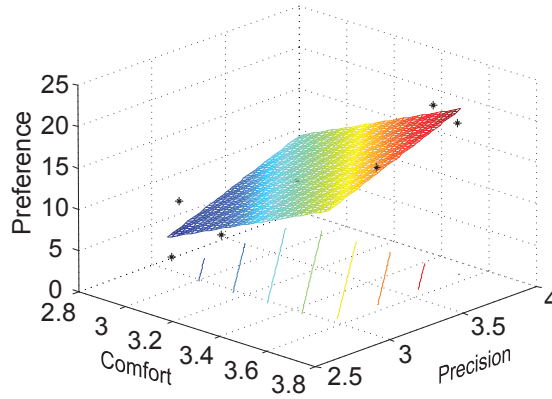


Figure 6.6: Regression model: handle preference as a function of comfort and precision

The Fig. 6.7 represents the percentage of surgeons that chose each specific handle. As it can be seen, considerable differences in preference were found for each background.

The highest score was given to the handles with which the surgeons were more familiar, for example the conventional needle holder (H_1) for surgeons used to conventional surgery and the da Vinci wrist for surgeons specialized in robotic surgery (H_2).

6.3 Discussion

MIS procedures, especially laparoscopy, require the surgeon to adapt non-neutral back postures and raised shoulder positions, resulting in higher muscular loading when compared to open surgery (Nguyen et al., 2001) and robotic surgery (Lawson et al., 2007; Gofrit et al., 2008). This fact is confirmed by the results of the present study regarding the body parts that suffered more discomfort and pain with each surgical approach. As it has been shown here, there is a clear decrease of pain aftereffects for robotic surgery. Nevertheless, we noted that a significant

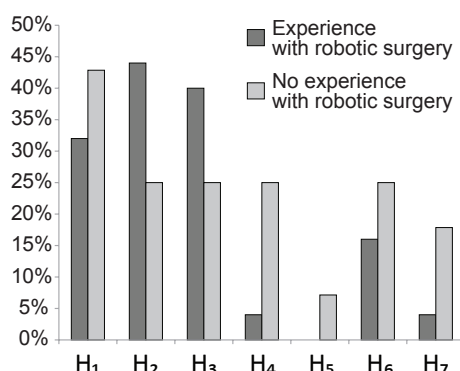


Figure 6.7: Percentage of surgeons who voted each handle separated by background: with and without experience on robotic surgery. Note that multiple selections were allowed.

number of surgeons complained about neck and finger pain during robotic surgery. Previous studies already reported surgeons' complains about neck pain due to the static posture that might be maintained to preserve the alignment of the eyes with the 3D monitor (Lux et al., 2010; Lawson et al., 2007). However, there has been no evidence to date of surgeons' discomfort related to the surgical console handle. The da Vinci handle (H₂) allows the surgeons to control the instrument with only two fingers. The hand posture adopted with this handle is the precision grasp, naturally performed by humans for fine manipulation. Even though it allows fine control, for manipulations requiring repetitive and large movements, the precision grasp might induce additional muscular tension. Nevertheless, the improvement felt by the surgeons with respect to wrist and shoulder pain is incontestable.

Task duration represents an important risk factor as it plays a significant role in the development and onset of musculoskeletal injuries. Longer procedure duration will definitely increase the risk of adverse effects produced by a poor ergonomic design. Judging from surgeons' answers it seems that the majority of the procedures performed with a surgical robotic platform last more than two hours (42.8%) whereas with the other surgical techniques the same percentage was obtained for a duration of less than two hours and from two to five hours (22.4% for each duration). Similar results were found in other studies comparing operative times for a common cholecystectomy performed laparoscopically and with a da Vinci robot. These studies showed longer procedure times with the robot due either to the required setup of the sterile draping (Ruurda et al., 2003) or to the slow motion of the robot arms (Nio et al., 2004). However, in the study of Lawson et al. (2007), the operative times to perform a Roux-Y gastric bypass laparoscopically took longer than when it was performed with a surgical robot. The variation of the reported results suggests that the difference of the operation time significantly depends on the surgical procedure. It might be advantageous in terms of operation time to use the robot in complicated procedures, which are typically long, whereas for simple procedures, the extra time to set up the device dominates the duration of the surgical procedure. Nevertheless, it should be highlighted that even though in average robotic cases last longer, the reported discomfort suffered by the surgeons was significantly lower.

The results of the handle evaluation showed a strong correlation between the scores given for comfort and stability aspects, as well for intuitiveness and precision. We noticed that the handles requiring the surgeon to employ a power-grip to control surgical instrument aperture (H_4 and H_5) received low precision scores. The handles in which the instrument aperture was controlled by a precision grip that only employed index and thumb fingers (H_1 , H_2 and H_3) obtained the highest scores for both comfort and stability. It seems that the pistol-shape or a joystick-shape that should be grasped with the whole hand (H_4 , H_3 and H_7) were found to be less intuitive.

With the intention of determining the most important underlying aspects that support the surgeons' preference criteria, a correlation analysis was performed between the handle preference rank and the criteria. This research suggests that surgeons chose the handle mainly based on the comfort aspect and on a lower extent because of the precision they provide. We appreciate the argument that the aspects that surgeons scored in this survey are subjective and multidimensional in nature and therefore several other variables might be necessary to adequately represent this theoretical preference model. However, the objective of this research is not to test theoretical models, but to understand the choice behavior of surgeons. This information can help the engineers to design the devices that better meet the surgeons' needs.

The background of the surgeon was found to be a very influential factor in the handle preference. For both groups, with or without experience with surgical robots, the preferred choice was the handle with which they are more familiar. Generally, the surgeons with robotic experience preferred the da Vinci handle, whereas those with no experience in robotic surgery preferred the conventional needle holder used for open surgery. This hypothesis is supported as well by the additional comments given by several respondents who suggested that their choice was based on their previous experience (e.g.: "because I'm used to", "experienced with these devices", "habits", etc.). Therefore, the design of new instruments should take into account the instruments already used for that specific field or in daily life. Totally unknown instruments whose control must be relearned will alter a surgeon's clinical practice.

This study presents a number of limitations that must be discussed: In our opinion, the major factors that have to be taken into consideration when interpreting the survey results are the Internet-related aspects of the survey and the high proportion of responding surgeons experienced in robotic surgery. In order to compare surgeons' preferences with respect to their background, we had sought to have a similar number of surgeons performing robotic surgery and surgeons who never performed it. However, nowadays the number of surgeons performing robotic surgery does not represent 50 % of the total (only 3450 surgeons are officially registered in the database of [Intuitive Surgical Inc. \(2010\)](#)). Furthermore, the respondents average age is 43 years, reflecting the fact that younger surgeons tend to use computers and Internet on a daily basis and are probably more familiar with this type of media than older generations. We therefore acknowledge an age-selection bias, the consequence of which is that our results concern mostly a younger population of surgeons roughly 30 to 55 years of age and thus more acquainted with new surgical trends and instruments. Although a more extensive study should evaluate our results in the remaining population of surgeons, we consider these results as a first appreciation of a population who will certainly have, due to their background, a

high degree of concern about new surgical technologies and thus well represent the preferences of potential users. Another limitation that should be considered is that surgeons evaluated the handles purely based on the provided pictures, and thus had more information about the handles if they had previously used them. This issue might have influenced the result that relates handle preference to surgeons' experience. A survey allowing surgeons to try the real instruments would give more detailed insights on this point.

6.4 Conclusions

The current study strongly supports the hypothesis that there are significant ergonomic problems in surgical techniques and instruments that result in frequent physical discomfort for a substantial number of practicing surgeons. According to the surgeons' answers, the arm support brought by the master console of robotic surgery systems significantly alleviates wrist and shoulder pain typically found in traditional surgery. Nevertheless, further improvements in the surgeon's posture while seated at the master console and the handle of the robotic surgery instruments should be made to decrease the likelihood of work-related physical injuries.

The results of handle comparison suggest that surgeons' choice is mainly driven by two factors: comfort and precision. Handles that control the instrument aperture with a power grip posture were associated with low precision. Handles in which the control is performed with only two fingers (precision grip) were preferred in terms of comfort. In addition, it was found that handle preference is strongly correlated with the surgeons' background. Therefore, surgical instrument designers should first study the instruments already used in the surgical practice or general tools used in common life to ensure the acceptance of new instruments.

6.5 Survey Form

Here is the questionnaire as it was presented to the participants to fill out online.

Demographic and Background Data:

- Field of expertise (text box), institution (text box), age (number box), gender (M, F), country (drop-down list).
- Years of experience:
 - Open surgery: < 3, 3 to 5, 5 to 10 and > 10.
 - Laparoscopic surgery: < 3, 3 to 5, 5 to 10 and > 10.
 - Robotic surgery: < 3, 3 to 5, 5 to 10 and > 10.

Discomfort and Procedure Duration:

- Average number of hours that surgical procedures last: < 2, 2 to 5, > 5.
- Have you ever experienced abnormal amount of pain or discomfort in the following areas?

Check the box if yes.

- While performing open surgery: neck, shoulders, back, wrists, and fingers
- While performing laparoscopic surgery: neck, shoulders, back, wrists, and fingers
- While performing robotic surgery: neck, shoulders, back, wrists, and fingers

Handle Evaluation:

- Please look at the pictures of the following handles and imagine how you will open and close the surgical instrument with it. Give a score from 1 to 5 to each aspect.
 1. Scissors-like handle (H_1 in Fig. 6.4: Common needle holder for open surgery): Intuitiveness (1 to 5), Comfort (1 to 5), Precision (1 to 5) and Stability (1 to 5)
 2. Index-Thumb control (H_2 in Fig. 6.4: da Vinci master gripper from Intuitive Surgical SystemsTM): Intuitiveness (1 to 5), Comfort (1 to 5), Precision (1 to 5) and Stability (1 to 5)
 3. Joystick plus index-thumb control (H_3 in Fig. 6.4: 3D model proposed by the authors): Intuitiveness (1 to 5), Comfort (1 to 5), Precision (1 to 5) and Stability (1 to 5)
 4. Pistol-like handle (H_4 in Fig. 6.4: Real Hand prototype gripper from Novare Surgical Systems (Novare, 2010)): Intuitiveness (1 to 5), Comfort (1 to 5), Precision (1 to 5) and Stability (1 to 5)
 5. Grip between all finger's and the palm (H_5 in Fig. 6.4: Axial handle of a RWOLF needle holder (RWOLF, 2010): Intuitiveness (1 to 5), Comfort (1 to 5), Precision (1 to 5) and Stability (1 to 5)
 6. Scissors-like handle: grip between all fingers and thumb (H_6 in Fig. 6.4: Real Hand commercially available gripper from Novare Surgical Systems (Novare, 2010)): Intuitiveness (1 to 5), Comfort (1 to 5), Precision (1 to 5) and Stability (1 to 5)
 7. Pistol-like with different finger support and index-thumb control (H_7 in Fig. 6.4: Ergonomic prototype from Mattern and Waller (Mattern and Weller, 1996)): Intuitiveness (1 to 5), Comfort (1 to 5), Precision (1 to 5) and Stability (1 to 5)
- Would you like to have additional commands and buttons in the instrument handle? (yes-no)

Handle Preference:

- Please select the instrument handles that you prefer: (multiple selection list)
- Could you briefly explain why do you prefer those instrument handles? (text box)
- Additional comments (text box)

Chapter 7

Ergonomic Guidelines for the Design of a Surgeons' Console

In a teleoperated robotic system, the human-robot interfaces are located in a workstation, in this case the surgeon's console, from where the surgeon will actually perform the surgery. Surgeon's performance may be influenced by design characteristics that can affect sensorimotor performance, vision, and comfort. In order to design an ergonomic surgeon's console the following points need careful consideration:

- console height;
- clearances for legs and feet;
- location and type of screens and displays (i.e., position of frequently and infrequently monitored display devices, orientation relative to the surgeon's line of sight, viewing distance, 2D or 3D visualization, etc.);
- location and mechanical properties of buttons and joysticks (i.e., placement the controls and distance from front edge of table); and
- lateral spread of control and display devices.

The aim of this chapter is to provide ergonomic guidelines related to workstation layouts and instrument handles. The majority of these guidelines have been proposed by well-known governmental commissions or agencies such as the [US National Aeronautics and Space Administration \(NASA\)](#) and the [US Nuclear Regulatory Commission \(NUREG\)](#), or ergonomic books ([Pheasant and Haslegrave, 2006](#); [O'Hara et al., 2002](#); [NASA, 1995](#)). These guidelines were initially developed for industrial or aerospace applications and thus, only the guidelines applicable to a surgeons' console have been included in this chapter. Additional guidelines extracted from the conclusions of the survey presented in Chapter 6 have also been considered.

7.1 Seat and Table Clearances

According to NUREG guidelines, the clearances must accommodate or allow passage of the body or body parts for the 95th %_{ile} (large) men data. However, when designing the reach distances, control movements, display and control locations that restrict or are limited by body or body part size, the design should be based upon the 5th %_{ile} (small) women data for the applicable body dimensions (US Department of Defense, 2000).

If the equipment dimensions need to be adjusted for the comfort or performance of the surgeon it should be adjustable over the range of the 5th to 95th %_{ile}.

The seat and backrest should be cushioned with at least 2 cm of compressible material, enough so that some resilience remains when the user occupies the chair. If the user is supposed to remain seated for relatively long periods, chairs with arm support should be provided. Armrest should be added also for the sake of accuracy. Safwat et al. (2009) showed that when armrest was provided, the hand tremor was significantly reduced. Height-adjustable or retractable arm support may be necessary to allow the elbows to rest in a natural position. Besides, in the results of the survey shown in Chapter 6, the arm support was found to be a key feature in a surgeon's console as it significantly alleviates the wrist and shoulder discomfort typically suffered during traditional surgery.

7.2 Display Arrangement

The main factors that can affect the readability of displays and visual indicators are the following:

1. the display height and orientation relative to the user's line of sight when standing directly in front of the display;
2. the display distance and orientation relative to the user's line of sight when the user must read the display from outside the console; and
3. the size of display indicators relative to the distance at which the display must be read.

All displays, including alarm indicators, should be within the upper limit of the visual field (75° above the horizontal line of sight) of the 5th %_{ile} of women, and should be installed so that the inner angle between the line of sight and the display face is more than 45°. In Fig. 7.1 an example of a display designed to accommodate from the 5th %_{ile} of women to the 95th %_{ile} of men is presented. The upper limit of the displays is established taking into account the 5th %_{ile} of women. Practically, there is no lower limit when designing sit-down consoles (O'Hara et al., 2002).

In stand-up consoles, the screens that require continuous monitoring or that may display important information such as alarms or vital signals, should be located at no more than 35° to the left or right of the user's line of sight, and at no more than 35° above and 25° below the user's horizontal line of sight. In case of a sit-down console, the vertical range changes to

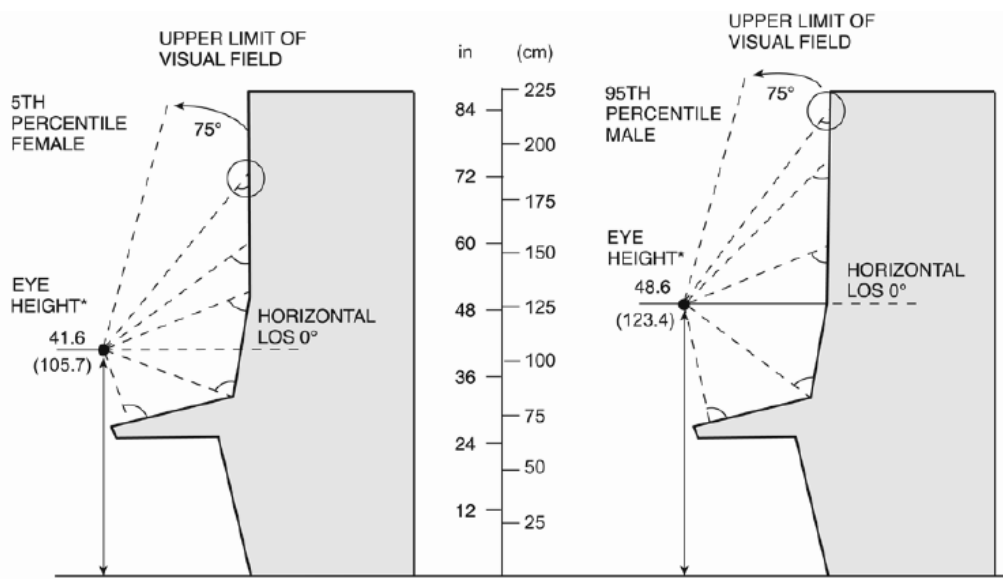


Figure 7.1: Vertical arrangement of the displays to allocate from the 5th %_{ile} to the 95th %_{ile} of the population (O'Hara et al., 2002). The circle mark indicates the angles with the user's line of sight that are too small to allow reading the screen. To increase the readability of that part, the display should be tilted forward.

20° above and to 40° below the user's horizontal line of sight.

The location of infrequently monitored displays is the same for both types of consoles and should be located not more than 95° to the left or right of the user's line of sight.

The exponential growth in the number of physiological variables that are generally conveyed through the visual and auditory displays of the OR, increase the cognitive load on the clinicians. This audio-visual overload motivates providing this information over other modalities for instance through tactile or haptic interfaces (Ng et al., 2005; Hansen Medical Inc., 2011).

Display Type

Recent studies support that stereoscopic vision increases the surgeons' performance and accuracy during robotic surgery (Munz et al., 2004; Jourdan et al., 2004). For instance the following spatial concepts are difficult and some times impossible to convey with a 2D displays: object shape, object position and orientation, relative location/orientation of objects, object contact/interference, intersection of contours and volumes, projections onto viewing/cut planes and surface properties such as convexity and curvature. Therefore, it might be necessary to provide a stereoscopic view of the operating field and a secondary screen with a 2D view with the rest of the vital signals that must be monitored with less frequency.

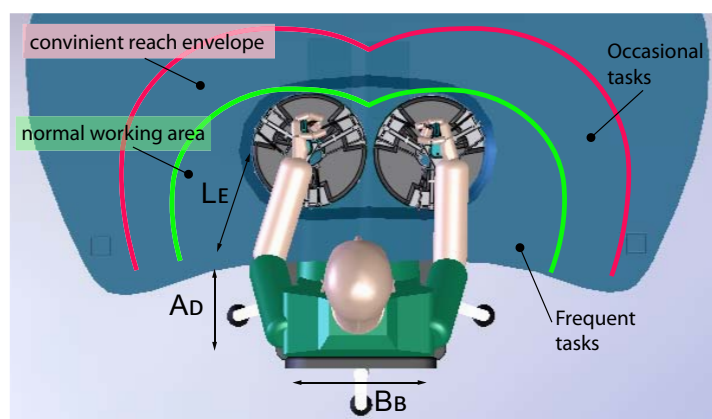


Figure 7.2: Convenient Reach Envelope (CRE), Normal Working Area (NWA) and the human's dimensions that determine the size of those regions: biacromial breadth (B_B), abdominal depth (A_D) and elbow to grip length (L_E).

7.3 Reach and Work Envelopes

The definition of reach and work envelopes allows one to optimize the location of the buttons and manipulators that will be maneuvered by the surgeon. To calculate reach distances during the design of a workstation, the recommended approach involves identifying the user tasks and positions and establishing reference points and envelopes for those tasks. The effects of clothing or carried equipment are then used to expand these calculated spaces. All users' tasks should be taken into account. Therefore, those performed during normal operation are not enough and the movements and operations performed during cases of emergency or maintenance should also be studied: i.e. if the surgeon should move to the patient's bed he/she should be able to leave the console easily (NASA, 1995).

The so-called Convenient Reach Envelope (CRE) has been defined in Pheasant's ergonomics book (Pheasant and Haslegrave, 2006) as the area within which manual tasks can be performed easily. It defines the boundary of the area that can be easily reached for all occasional actions to be performed. Within the limits of the CRE, a more reduced area called Normal Working Area (NWA) is defined as the area within which the most frequent tasks should be performed, and therefore where the surgeon's manipulators should be installed. All buttons and control panels for the surgeons should be located with respect to the CRE and the NWA and take into account the frequency of the task, as shown in Fig. 7.2. The surgeon is not expected to reach any area outside the zone of convenient reach for any regular work. This rule is not only based on comfort reasons; a study of Sengupta and Das (2004) confirms that this can lead to physiological cost and muscular fatigue. When repetitive tasks are performed: back muscle activity, oxygen uptake and heart rate increase from one region to the next and especially beyond the boundaries CRE.

The NWA is defined when the user performs a comfortable sweeping movement of the upper limb about the shoulder with the elbow flexed approximately 90° , see Fig. 7.3 (top left).

Moving from the center point (H_1), the right hand can sweep an arc out to the side as the humerus is rotated around the shoulder about its own axis. When the elbow is flexed at 90° , the comfortable limit of arm rotation is about 25° . However, the elbow can swing out naturally as well, and this extends the working area further. As a result, the path of the hand drawing the outer limit of the **NWA** is a prolate epicycloid formed by two simultaneous rotations: the forearm rotates through $\Theta + 25^\circ$, while the elbow itself moves outwards and backwards through a 90° arc (from E_i to E_f).

In order to achieve the best possible match for the majority of users, the **NWA** has been defined using different anthropometric data including the 5th %ile. It therefore applies to men and women of less-than-average height (O'Hara et al., 2002). As shown in Fig. 7.3 (top left), biacromial breadth (B_B), abdominal depth (A_D) and elbow to grip length (L_E) are those parameters that affect the dimensions of the **NWA** boundary. A parametric analysis was performed by implementing the equations that describe this sweeping movement in Matlab to quantify the effect of the above-mentioned parameters on the boundaries. Results for the different anthropometric variations are shown in Fig. 7.3 (top right), (bottom left) and (bottom right).

In Fig. 7.3 the red lines represent the movement of the surgeon's hand in a grip position and the black lines represent the sweeping movement of the elbow. Boundaries have been built up separately for each arm and overlap in the middle where both hands can reach. This is the area where two-handed work can be done. It should be noted that for a surgical platform in which the surgeon will control the robot through haptic devices the area where bimanual tasks are performed should not be used in order to avoid collisions between the two devices.

The reach distances, which are limited by the size of a body part, should be based on the 5th %ile of women data because they represent the population with the smallest size. Accordingly, what we take into account for the design are the smallest limits of the resulting plots. In the Fig. 7.3 the sweeping movement of the elbow has been plotted (black lines) to visualize the clearance that we should respect to allow the elbow to move freely. It is known that abdominal depth is poorly correlated with limb lengths and as we can see in Fig. 7.3 (bottom left), there is no significant change in the boundaries of the **NWA** when this dimension is changed. Therefore, for further studies this dimension can be based on the 50th %ile. In addition to these boundaries, very close reach, close to the table edge, is not efficient or comfortable because it involves moving the upper limb backwards while raising the elbow. We have identified this as an inner boundary to the **NWA**: no task should be performed within approximately 10 cm to the table edge.

The study of the vertical workspace is more straightforward. According to the available anthropometric data, for the 5th %ile of women the vertical workspace should not exceed 40 cm, a dimension that matches the results obtained by Takahashi et al. (2008) when they calculated the vertical workspace of the human arm for the design of a master console. Certainly, if there is a repetitive or a long duration task taking place several centimeters over the desk, an armrest must be provided, for both comfort and for stability. In addition, forearm support is associated with decreased shoulder and neck muscular activity and therefore, less reported discomfort (Pheasant and Haslegrave, 2006).

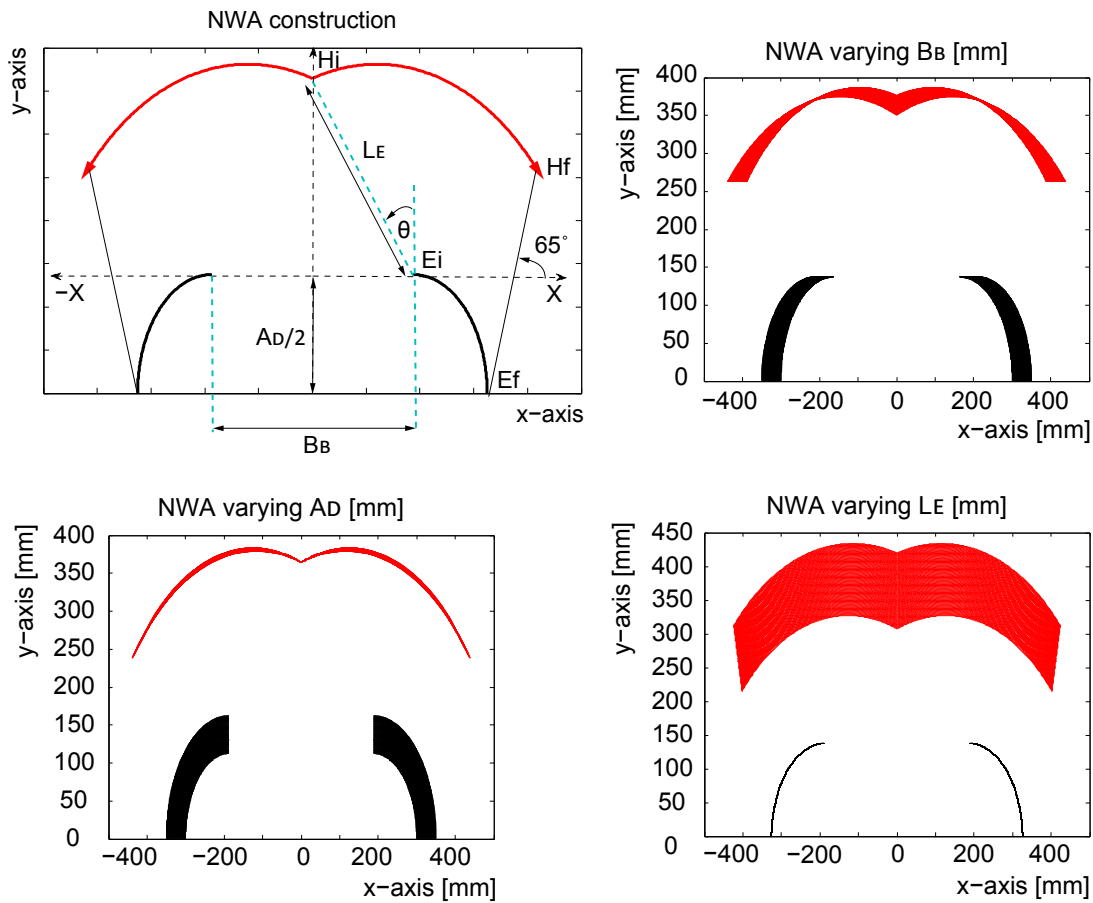


Figure 7.3: (top left) general NWA construction, (top right) NWA varying the biacromial breadth (B_B), (bottom left) NWA varying the abdominal depth (A_D) and (bottom right) NWA varying the elbow to grip length (L_E). The red lines represent the movement of the surgeon's hand in a grip position and the black lines represent the sweeping movement of the elbow.

The console should look simple to unload the visual system as much as possible. Speech recognition systems or eye tracking can substitute several buttons and commands. In addition, these types of systems allow using or reading equipment without needing physical contact and thus assuring sterility. Eye tracking systems can be used to select a secondary window to appear in the center for a while to see in detail a specific vital sign. Voice input can facilitate discrete command-based tasks, but it is more difficult to translate direct manipulation tasks which require motor/visual coordination to a voice interface, for instance tilting the in a continuous way the distal camera.

The dimensions of the [NWA](#) and the aforementioned guidelines have been used by our collaborators of the Imperial College of London to design a master console, see Fig. 7.4. The height of this master console can be adjusted and thus, it is adapted to any person between

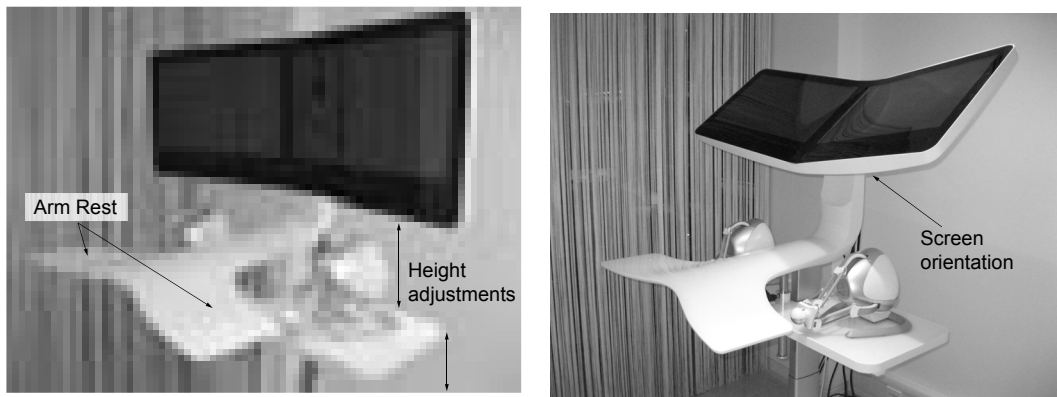


Figure 7.4: The surgeon's console designed by our collaborators from Imperial College London following the guidelines proposed in this thesis.

the 5th of women and 95th %ile of men. In addition, it can be used in a standing position or while seated. Armrest is provided and its height can be also modified. The stereoscopic screen can be tilted to adjust its orientation for the standing and seated configurations. This group is working in the integration of an eye tracking system to select and amplify different regions of the screen.

7.4 Handle Specifications

7.4.1 Wrist Posture and Mobility

It has been shown that the forces applied by the fingers while grasping an object are correlated with the wrist position and generally decrease as the wrist deviates from the neutral posture. [Imrhan \(1991\)](#) measured the grasping strength under different wrist deviations to quantify the influence of the wrist posture. Their results demonstrated that palmar flexion represented the worst posture degrading the grasping strength by up to 43%. In a more recent study, [Yuh-Chuan Shih \(2005\)](#) found similar results; the maximum force was applied with the wrist in neutral position and weakest force when the wrist was totally flexed. This is due to the fact that finger flexors are shortened, which reduces their strength. Contrarily, deviations in the pronosupination [DOF](#) of the wrist do not have any significant effect on the pinching strength ([Jansen et al., 2003](#)). Based on these facts, one of the specifications is to keep the user's wrist close to the neutral posture but allowing an ample movement in the pronosupination [DOF](#).

Additional factors that influence grasping strength such as gripping width and hand-object contact area should also be taken into account. [Yuh-Chuan Shih \(2005\)](#) found that the maximum force applied generally increased with the grasping span but only up to 6 cm; after that value the strength was degraded for some of the postures. In order to optimize force control and comfort, a large contact area with the hand is desired and the grasping width should not be smaller than 30 mm ([Shivers et al., 2002](#)).

For the sake of **transparency**, the device should allow ample range of angles in each orientation **DOF** to match the device and the surgeon's workspaces. However, extreme angles in ulnar and radial deviation should be avoided, especially when coupled with flexion or extension **DOF**. When extreme ulnar or flexion deviation occurs, finger tendons passing thorough the carpal tunnel are bent. If this movement is performed frequently, it can lead to tenosynovitis and carpal tunnel syndrome (disorder caused by an injury of the median nerve). This syndrome produces finger numbness, reduced tactile feeling and grip strength, which can considerably reduce surgeon's performance (Sanders et al., 1993).

In Fig. 7.5, the mobility ranges of the wrist and the recommended maximum angular ranges are summarized. Note that the dexterity necessary to perform sutures with a circular needle imposes to extend the mobility of the pronosupination **DOF** of the wrist with additional elbow movement. This gesture is frequently repeated during surgical procedures.

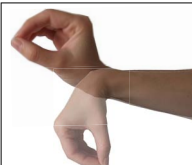



	<p>Flexion-extension DOF Joint mobility range: flexion (0°, 90°) and extension (0°, 99°). Recommended working range: (0°, 45°) and (0°, 80°)</p>
	<p>Pronosupination DOF Joint mobility range: pronation (0°, 77°) and supination (0°, 113°) Extended range swapping the elbow: (0°, 90°) and (0°, 180°) Recommended working range: (0°, 90°) and (0°, 170°)</p>
	<p>Ulnar-radial (adduction-abduction) DOF Joint mobility range: adduction (0°, 47°) and abduction (0°, 27°) Recommended working range: (0°, 30°) and (0°, 27°)</p>
	<p>Grasping (thumb open-close) DOF The thumb axis forms an angle of 110° with the forearm</p>

Figure 7.5: Wrist mobility ranges for the 50th *percile* (Pheasant and Haslegrave, 2006). The recommended working ranges prevent the wrist to reach extreme postures while providing enough dexterity for common surgical gestures such as suturing or tissue dissection. The orientation (0°, 0°, 0°) corresponds to the neutral posture of the wrist.

An additional factor to consider is the way to control the open-close **DOF** of the slave robot through the surgeon's handle. As reported in Chapter 6, the handles in which the grasping **DOF** was controlled by a combined power and precision grip were preferred in terms of comfort and had good scores in terms of intuitiveness.

7.4.2 Grasping Strength

It is difficult to find an exact range of grasping strength in the literature because of the great variety between samples and the measurement methods used for each study. For instance, the lateral pinch using traditional clinical methods of measurement ranges between 60 N

(Swanson et al., 1970) and 114 N (Mathiowetz et al., 1985) in males. The majority of these studies, however, show a range of 80 to 100 N for men and from 60 to 80 N for women. These values represent the maximum force that the user can apply during a short period. However, an ergonomic rule extensively used is to consider that when a force has to be exerted continuously during a long period of time, it should not exceed the 10% of the maximum strength. Furthermore, if a task is carried out frequently or during short periods of time, it should not exceed 25 – 30% of the maximum strength (Wiker et al., 1989). And finally if the force is just exerted occasionally and for a brief moment it should not exceed 60% of the maximum strength (Pheasant and Haslegrave, 2006).

7.5 Summary and Conclusions

This chapter provides guidelines for the ergonomic design of a surgeon's console. However, these guidelines are not enough to guarantee a perfectly ergonomic development. The design of a surgeon's console is a complex process which is user-centered and has to further consider a lot of aspects regarding safety and OR compatibility. Therefore, an iterative methodology should be followed, in which a research phase is followed by a design phase and then by a prototype that can be evaluated. In all these iterations the final users, which are in our case the surgeons, must be enrolled as active participants. The multiple iterations help the designer to understand the links between the different design aspects and allow a stepwise approach to an optimum design.

The following list provides a brief summary of the most important ergonomic specifications that were discussed in this chapter.

- When locating controls and surgeon's manipulators:
 - the reach distances should be based upon the 5th %_{ile} (small) women data, and
 - clearances should be based on the 95th %_{ile} (large) men data.
- Armrest should be added for the sake of accuracy and to reduce fatigue.
- The disposition of a visual indicators should take into account the frequency at which it should be monitored and its importance.
- The definition of CRE and NWA areas provide the boundaries in which occasional and frequent tasks can be performed.
- The surgeon should not perform any regular work outside the zone of convenient reach.
- It has been shown that wrist position, gripping width and hand-object contact area affect the grasping strength of the surgeon.
- The console should be kept visually simple and unloaded whenever possible, e.g., through speech recognition and eye tracking systems.

Chapter 8

Design and Evaluation of an Ergonomic Handle

Dr. Berguer, chief of surgery at Costa Rica Regional Medical Center in Martinez, California declared in a recent interview that “Surgeons depend on tools to conduct their trade”, stressing out the importance of ergonomic issues in the OR (Glickson, 2012). He additionally commented: “How we work with these tools affects not only the length of the procedure and the overall morbidity of our patients but also how comfortably we can use our limbs and muscles when we leave the OR”. In that article, the surgeons affirmed that the ergonomic issues are not only caused by the new surgical techniques but also by the design of the instruments, which is not appropriate. In Chapter 6, we already saw that robotic surgery significantly improved the ergonomics of MIS techniques but there are still some issues that cause fatigue in the surgeons’ back, neck, shoulders and fingers. Specifically, the surgeon’s handle of the da Vinci robotic system induces some tension on the surgeon’s fingers, a problem that - if proper care is not taken - could be aggravated by the addition of force feedback. Current haptic displays providing six (active or passive) DOF plus active grasping feedback are not specifically designed for surgical tasks and thus have a limited grasping movement constraining the user to work always using a precision grasp or a power grasp.

In this chapter, we propose a novel handle based on a Remote Center of Motion (RCM) double-parallelogram mechanism that provides a wide range of motion for the pronosupination DOF of the wrist while controlling the range of ulnar-radial deviation. The grasping feedback module is designed to combine both power and precision grip, thus providing strength and accuracy. The prototype integrates additional safety features such as brakes and hand presence detection. This chapter starts with the prototype description followed by the technical evaluation of its different components. The second part of this chapter presents a psychophysical and ergonomic experiment to evaluate the usability of the device and compare its performance with that of a standard omega.7 haptic device. The results show that the proposed design can help users to be faster in an assembly task and that it can potentially decrease the fatigue of the muscles involved in the grasping gesture.

8.1 State of the Art

As this thesis aims at introducing haptics manipulators in a surgical workstation, the ergonomics of several haptic devices designed for general purposes were reviewed with respect to the guidelines presented in Chapter 7. This comparison focuses on how those devices control the orientation of the wrist and the opening and closing movement of the tool.

Many thimbles and haptic handles have been developed so far for various applications. It is well known that having the center of rotation inside the user's hand facilitates the control of the device; therefore, it has been adopted as a key design rule. The spherical mechanisms used for most of devices are generally based on three revolute joints in series with the axis intersecting in the middle of the hand and allowing the same angular range for the three DOF (Madhani et al., 1998; Tobergte et al., 2011). However, some of these orientations may lead to cumulative trauma and are typically not needed during surgical gestures, for instance extreme ulnar or radial deviations combined with the flexion of the wrist can induce carpal tunnel syndrome.

The first haptic devices used a stylus-shaped handle without active grasping feedback capabilities (Tadano and Kawashima, 2007; Massie and Salisbury, 1994; Takahashi et al., 2008). As various manipulation tasks demand grasping feedback, new commercially available devices appeared integrating this feature. Usually, the handle is controlled either by a precision grip or a power grip. Examples of handles controlled by a precision grip are the devices with a scissors-like tool held between the tip of the thumb and opposing digits like the Freedom 7 haptic device (Hayward et al., 1998) or the Phantom 7-DOF with the scissors end-effector (Sensable Technologies, 2011). Another example using precision grip is the omega.7 device, in which the user grasps a cylinder between the index and the thumb (Force Dimension, 2011). On the other hand, the Phantom 7-DOF with the thumb-pad end effector provides a pure power grip between all fingers and palm against the thumb adducted at both the metacarpophalangeal and carpophalangeal joints (Sensable Technologies, 2011). All these handles are advantageous to enhance either precision or strength.

8.2 Design Requirements

The design of the surgeon's manipulator should fulfill several technical and functional requirements. As shown in Chapter 2, there are many available haptic devices that convey force feedback in 3-translational-DOF. Since this technology is well established it was decided to use a commercially available force feedback device as a kinesthetic base for the surgeon's manipulator. From this point, the surgeon's handle was customized in order to achieve the ergonomic specifications. The base of the omega.7 device was chosen for its high performance and structure stiffness. An additional advantage of this device is the accessibility and flexibility of its control hardware. It can control up to four actuators and seven encoders and can be reconfigured to adapt it to the customized handle. The additional actuators could be then fully integrated in the device and controlled through a single USB port. The fact that a

version of the omega.3 has been FDA approved and already employed in a medical application - the Sense robotic catheter (Hansen Medical Inc., 2011) - proves the reliability of this device and was an important point in the choice.

As the ergonomic handle is intended to be integrated in an omega.7 to guarantee its performance the added inertia should be minimized. This means that a very important design factor consist in reducing the device weight as much as possible.

To provide a natural control of the instrument orientation the center of rotation must be located at the center of the surgeon's hand. Three DOF of orientation: yaw, pitch and roll, that coincide with the flexion-extension, ulnar-radial deviation and pronosupination DOF of the human's wrist are necessary to allow enough dexterity. The spherical mechanism that controls the orientation of the device must be designed so that the user mainly controls the device with postures that slightly deviate from the neutral position of the wrist. This implies that the stroke of some of the DOF, especially the pitch DOF should be limited to avoid problematic postures.

Napier (1956) identified two main kinds of prehensile movements: power grasp and precision grasp. In the power grasp, the palm holds the object and the force is applied with the thumb opposed to the other fingers. In this type of grasp, muscular force is dominant and thus allows good generation of high forces, but not necessarily good control over these. In a precision grasp, the object is held between the flexor aspects of the fingers and the opposing thumb, and whereas the muscular force application is reduced, the dexterity is increased, allowing a much finer control over grip forces. During surgical procedures both types of grasp are necessary, therefore the handle should be controlled with a hybrid prehensile movement that allows the surgeon to be precise while receiving comfortably the rendered grasping feedback.

According to the guidelines and human factors discussed in Chapter 7, the specifications of the grasping feedback are set as follows: the manual operations that the surgeon is going to perform should not require forces near their maximum. For this reason, and to be on the safe side, we have set as design specification a force peak of 30 N (30% of 100 N) and constant values that do not exceed 10 N (10% of 100 N).

In Chapter 4 it was shown that, unlike force feedback, torque feedback did not significantly improve surgeons' performance in a suturing task. It was concluded that the addition of torque feedback in this handle, which would lead to significant complication of the system (added inertias, space constraints, etc.), could be left out. However, leaving the orientations totally passive could introduce safety issues. If any problem arises and the orientations cannot be constrained the surgeon could damage delicate tissues. Therefore, for safety reasons and while keeping the design simple the new handle should integrate a brake for each orientation-DOF. Furthermore, if some of the orientations can be blocked, the surgeon's movement can be constrained to a subset of DOF. This feature can be useful to actively guide the surgeon along a certain path by providing passive haptic cues.

In telerobotic surgery the "clutch" option is often used to disengage the master manipulators from the slave robot, in order to reposition them into a more comfortable configuration without disturbing the remote instruments. After using this option, the kinematic control uses

the positions relative to the location of the surgeon's hands before pressing the "clutch". The relative kinematics also applies to the orientations. This means that if the surgeon's hands change orientation while pressing the clutch there would be an offset between the surgeon's hand orientations and the slave robot end-effectors. This considerably affects the intuitiveness of the system, and due to its additive nature, the offset will increase along the surgical procedure aggravating the problem. The actual da Vinci system solves this issue by fixing the orientation of the master manipulator when the "clutch" is pressed. Furthermore, the handle of the da Vinci are actuated and can actively centered the handles. Therefore, to be able to use the "clutch" option, a braking system blocking the three orientation **DOF** is necessary. In order to maintain the performance of the kinesthetic base the brake system should be lightweight and small, thus minimizing the added inertia. A mass lower than 40 g was fixed as a design guideline. In addition, the brake system should not introduce any friction to the orientation mechanism when disengaged, be able to provide a high braking torque (> 0.2 Nm) and a good responsiveness.

In the current da Vinci surgical system the surgeon looks at the surgical scene by placing his/her head on the padded viewer, which contains sensors that detect the surgeon's head contact. For safety reasons these sensors are used to detect the surgeon's presence and thus the slave robot arms are only activated when the surgeon is in the viewing position. As it was shown in Fig. 7.4, the surgical robotic system in which this haptic manipulator should be integrated uses an open surgical console. Therefore, the detection of the surgeon's presence has to be performed by other means. The ergonomic handle must incorporate then a detection system to recognize when the handle is not properly grasped in order to activate the brakes and disengage the slave robot control.

8.3 Prototype

In order to meet the ergonomic and safety requirements given in the previous section, a haptic handle was designed, which consists of three main parts: 1) a spherical mechanism for an ergonomic workspace, 2) a grasping force feedback module, and 3) safety features.

8.3.1 Spherical Mechanism

Numerous combinations of revolute joints, parallelograms, synchronous transmission or instantaneous **RCM** can be used to design a three-**DOF RCM** (Xu et al., 2007). In the present case, a combination of two revolute joints and a double-parallelogram has been chosen in order to control the stroke of each **DOF** of the surgeon's wrist. A parallelogram (Fig. 8.1, left) can be used to displace the pointing motion in parallel to the actuated link. Each point of the bottom link of the parallelogram performs a circular displacement, however the link remains aligned parallel to the top link. The rotation is thus created by a one-**DOF** displacement around a circular trajectory. The relative displacement between two platforms parallel to each other (Fig. 8.1, right) can be used as well for circular motion generation. In this case a virtual pivot

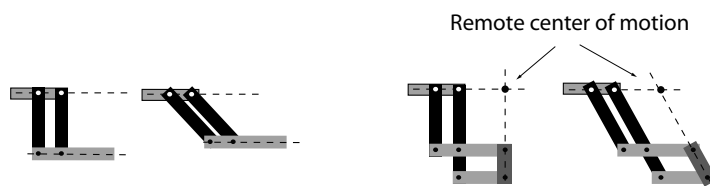


Figure 8.1: (left) Single-parallelgram mechanism and (right) double-parallelgram mechanism with RCM

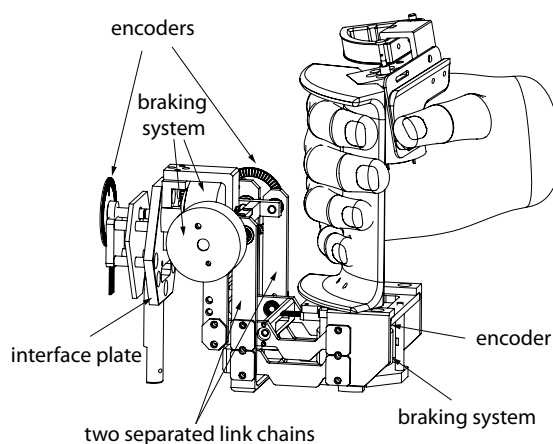


Figure 8.2: CAD model of the ergonomic haptic handle. The design is composed of a spherical mechanism providing hand orientation with brakes, and an active grasping module. The interface plate ensures the mechanical and electronic connection with the omega.7 haptic device.

point or **RCM** is obtained, as the rotation is performed around a point, which is not part of the linkage.

In the mechanism proposed in this work (Fig. 8.2), the **RCM** is located inside the user's grip providing a natural control of the orientation. This mechanism provides three **DOF** of orientation: flexion-extension, ulnar-radial deviation and pronosupination **DOF** (Fig. 8.3). The stroke of the pitch **DOF** is limited to avoid problematic postures. As it can be seen in Fig. 8.3 (2), to constrain the movement of the double-parallelgram, the profiles of the adjacent links make contact at the limit of the angle range.

To reduce backlash and friction, each pivot joint features two preloaded bearings. To increase stiffness of the overall handle, the double parallelgram is split into two parts forming two parallel link chains. The axes are also split into two parts and each of them features a bearing. This provides free space between the two double parallelgrams for the yaw **DOF** (Fig. 8.2).

Using a parallel structure the mass of the mechanism can be then distributed in two chains

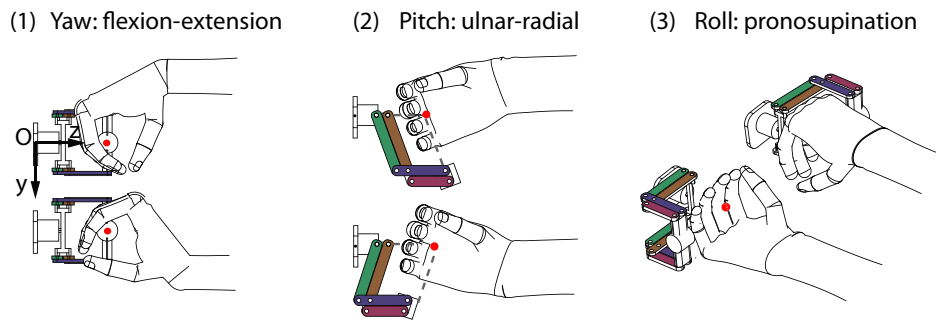


Figure 8.3: Simplified model of the spherical mechanism representing the mobility of the mechanism with respect to the user's wrist. The red dot at the center of the hand represents the RCM. Note that to increase stiffness the double-parallelogram is formed by two parallel chains of links.

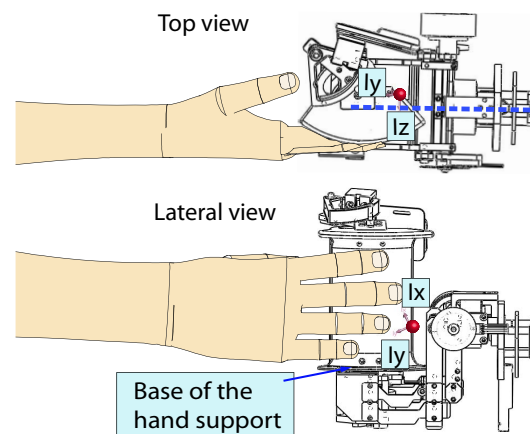


Figure 8.4: Top and lateral view of the mechanism and its center of mass (red sphere). The center of mass is close to the RCM but slightly deviated from the symmetry axis of the mechanism (blue dashed line in the top view) and to the side opposite to the user's hand. When user holds the device, thanks to the weight of the hand the center of mass moves towards the RCM.

to passively equilibrate the weight. As shown in Fig. 8.4, the brake in the pitch **DOF** has been located in the side opposite to the user's hand. Since the brake is heavier than the encoder the center of mass is close to the **RCM** but slightly deviated from symmetry axis of the mechanism to the opposite side of the user's hand (Fig. 8.4). When the user is holding the device, the weight of the hand naturally compensates for the mass of the brake and the center of mass moves towards the **RCM**.

Each **DOF** is equipped with a magnetic incremental encoder (0.09° of resolution) to measure the angles and thus determine the orientation of the surgeon's hand by solving the handle forward kinematics.

8.3.2 Grasping Force Feedback

The solution proposed for the grasping feedback module combines precision and power grasp. The manipulation is performed between the thumb and the opposing digits as in a precision grasp. In order to increase the power and stability of the user's grip, the handle surface is in contact with part of the palm and opposing fingers and has a rounded shape. This introduces features that are more characteristic of a power grasp.

Our initial hypothesis is that with this type of handle the user will be more stable if a sudden change of forces happens than with the standard handle while keeping the dexterity of the precision grip already provided by the standard omega.7 handle.

As shown in Fig. 8.5, the axis of the pulley is oriented towards the axis of the human's thumb. Furthermore, the motor is attached to the fixed part of the grasping mechanism through a slanted plane replicating the deviated axis of the human's thumb. This ergonomic configuration allows the user to move the thumb naturally without forcing it to stay in a horizontal plane. The stroke of the grasping mechanism is 80° . A pin located in the motor fixation limits the stroke of the moving pulley for safety reasons.

A DC motor (018SR, Faulhaber, Schönaich, Germany) capable of generating a peak torque of 47.7 mN.m and a Nominal torque of 10 mN.m was selected. To increase the torque of the motor, a reduction was required. Therefore, in order to avoid backlash, a cable driven solution was found to be the most suitable for this application. Due to the high reduction a tungsten cable of 0.4 mm in diameter was chosen. The standard handle of the omega.7 device integrates an 118746 Maxon motor with a nominal torque of 28.8 mN.m and a mass of 130 g. The characteristics of this motor were used as a reference to find a tradeoff between using a large motor or a motor plus a reduction.

The characteristics of the chosen actuator, before and after the reduction, are shown in Table 8.1. Since the distance between the thumb pad and the pulley center is 40 mm, working at the nominal torque, the device can render 7.5 N and for brief peaks of force, closer to the stall torque of the motor, forces up to 30 N should be achieved. Note that with the selected motor and this reduction we get a larger nominal torque and a slightly lower weight than with the motor already employed in the standard handle of the omega.7.

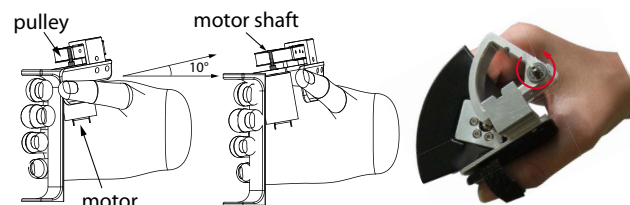


Figure 8.5: Detailed view of the grasping force-feedback module. The axis of the pulley is oriented towards the thumb and inclined to allow a more natural grasping movement.

Table 8.1: Motor and encoder characteristics before and after the reduction

Characteristic	Motor shaft	After 1:30 reduction
Stall torque	47.6 mN.m	1.43 Nm
Nominal torque	10 mN.m	300 mN.m
Encoder resolution	0.175°	0.0058°
Total weight	62 g	100 g

8.3.3 Safety Features

Brakes

As it was specified in Section 8.2 the ergonomic handle should integrate brakes for three DOF in orientation. A pneumatic solution has been chosen due to its high power to weight ratio. The main component of the braking system is a pneumatic ring, which consists of a cylindrical piece with a ring-shape air chamber connected to an air input (Fig. 8.6). This pneumatic ring is attached to the grounded base of the DOF by two anti-rotational pins. A moving shaft passes through the hole at the center of the pneumatic ring without making contact with it and is attached to an external drum. When the brake is switched off the drum moves freely around the pneumatic ring concentrically. Therefore, the relative movement between the two links is allowed. When the brake is activated the air inflates the air chamber of the pneumatic ring and thus, it makes contact with the external drum. Consequently, the fixed part and the moving shaft are mechanically connected preventing relative movement between them.

A proportional pneumatic valve actuates these brakes. The proportional operation is achieved by filling the brake with air pressure pulses. The number of pressure pulses and accordingly the braking force depends on the preprogrammed position. The direction, the range and the first break pressure can be programmed into the valve during calibration. As the valve is deactivated after each pulse, the consumption is minimal and never reaches values over 200 mA.

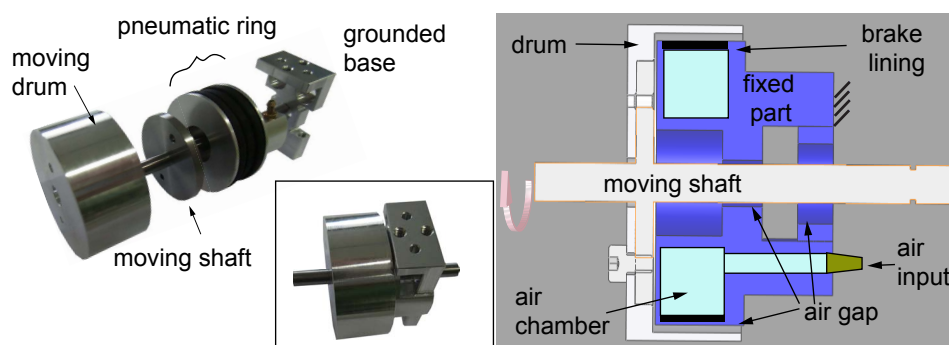


Figure 8.6: Exploded view and assembly of the brake system. The pneumatic ring is static while the drum moves concentrically to it. When the pneumatic ring insufflates, the brake lining makes contact with the drum producing friction and thus, braking torque.

Hand Presence Detection

A capacitive sensor integrated in the ergonomic handle is used to detect the presence of the surgeon's hand (Fig. 8.7). Capacitive technology has been preferred because the sensor is still sensitive to the hand when the surgeon is wearing gloves and is not sensitive to humidity. The sensor is composed of a PCB touch pad that includes individual power management and an ATMEL chip QT1011 controlling the sensor. The internal drift algorithm of the QT1011 compensates for long-term shifts in the power supply but spikes can be problematic. A dedicated low dropout voltage regulator has been used to avoid this problem. To increase the electromagnetic compatibility, all the passive components associated with the capacitive sensor (such as the reference capacitor and the associated resistors) have been placed physically close to the QT1011, in the handle. The PCB manufactured in glass-reinforced epoxy laminate (FR4) with a dielectric constant of $\epsilon = 5.2$ and a 0.8-mm thickness works as a touch panel.

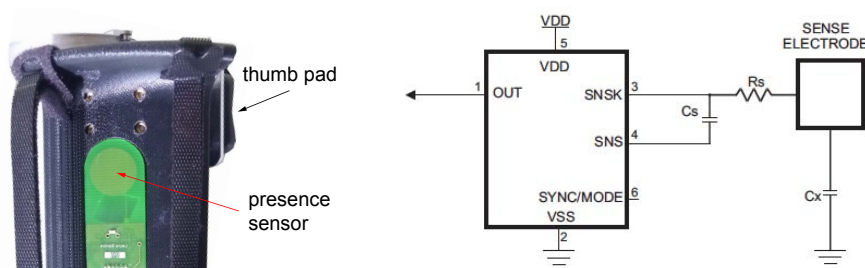


Figure 8.7: (left) Detailed view of the capacitive sensor to detect the presence of the surgeon's hand and (right) basic circuit configuration of the QT1011 chip from ATMEL.

8.4 Technical Evaluation

8.4.1 Workspace

Workspace is one of the most important issues when designing a haptic device since it determines the dexterity limits of the operator when controlling the slave robot. The workspace in orientation provided by the ergonomic handle was geometrically calculated and plotted with Matlab (The MathWorks, Inc). The double-parallelogram mechanism does not allow the alignment of two DOF and thus, the resulting workspace is free of singularities (Fig. 8.8). The mobility range allowed for each DOF is shown in Table 8.2.

The workspace envelope shows that the mechanism allows a wide range of orientations

Table 8.2: Mobility ranges of the mechanism

Pronation and supination	85°	85°
Flexion and extension	45°	80°
Adduction and abduction	30°	30°

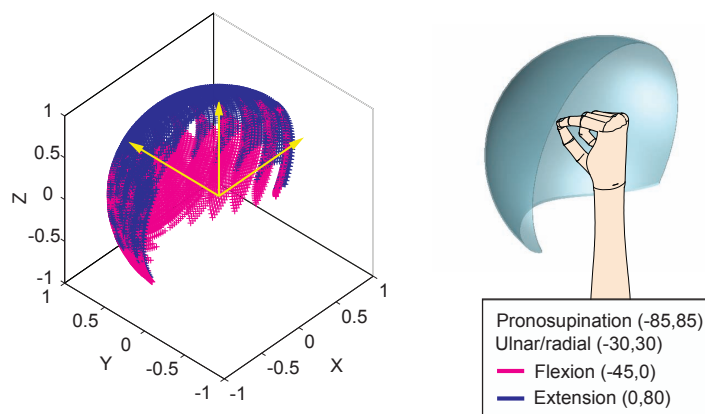


Figure 8.8: (left) Singularity free workspace of the spherical mechanism. The pink points correspond to the orientations on the flexion range and the blue purple points correspond to the extension range. (right) Surface representing the workspace envelope with respect to the user's hand.

providing high dexterity to the surgeons. Note that the boundaries at the bottom of the workspace limit the orientations in which the surgeon would point towards his/her own arm, which is a posture out of the wrist mobility limits. The boundaries of the top of the workspace correspond to pointing the hand outwards (with a very exaggerated extension of the wrist or with a pronation higher than 90°). This posture is also unnatural and not practical taking into account that to perform bimanual tasks the hands should be oriented inwards (facing each other).

The ergonomic handle is kinematically decoupled from the rest of the haptic device to which it is attached (Fig. 8.9). This means that the surgeon could use different hand orientations to approach the same point within the workspace.

8.4.2 Grasping Feedback

The evaluation of the grasping feedback module is made through several measurements: maximum continuous force, Z-width and maximum stiffness. The first measurement assesses the interaction force between the grasping feedback module and the user's finger to determine the force limit of the mechanism and the amplifiers. The force sensor used is a CentoNewton 100 piezo-resistive force sensor with a range from 0 to 100 N (Maeder et al., 2005). As shown in Fig. 8.10 the sensor is directly placed in the thumb pad. The data acquisition card used is a Phidget interface kit 8/8/8 (Phidgets Inc., Canada).

In order to measure the maximum continuous force of the grasping module, the force command was increased in small steps while the interaction force and grasping aperture were measured. The grasping device pushed against a rigid body that was fixed to the ground.

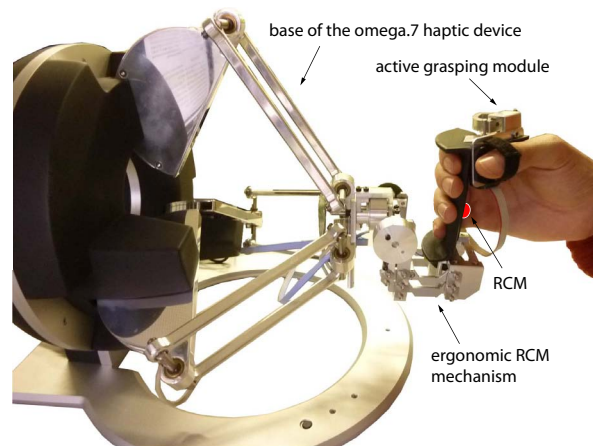


Figure 8.9: Ergonomic handle with remote-center-of-motion (RCM) attached to an omega.7 haptic device (Force Dimension, 2011).

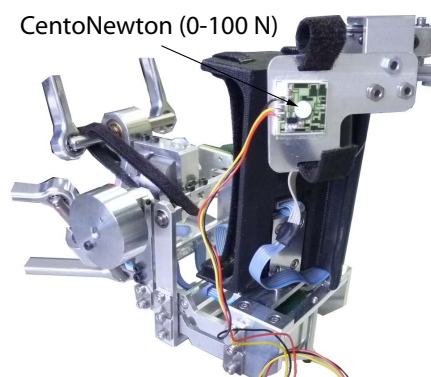


Figure 8.10: Setup to measure the performance of the grasping module. A piezo-resistive force sensor CentoNewton-100 is used to measure the force applied by the device against a rigid body.

The resulting maximum continuous force that can be applied by the motor was around 8.5 N, which is more than the 7.5 N calculated from the motor characteristics (Fig. 8.11).

The impedance range or Z-width defines the ability of a device to render a wide range of haptic stimuli and therefore, it is a good way to assess the haptic device performance (Colgate and Brown, 1994). A force sensor sensitive to both tension and compression forces was necessary for this measurement. A XFTC320 load cell with a range of ± 50 N from the company Measurement SpecialtiesTM was selected. An accelerometer was attached to the end-effector in order to measure its acceleration and then estimate the velocity (Fig. 8.12). The same acquisition card as for the previous measurement was used.

To obtain the minimum impedance, the user jiggled the end effector while the VR was rendering zero impedance. The measurement is limited to the different frequency levels that can be achieved by voluntary human motion (0 to 10 Hz). Resulting velocities and forces at

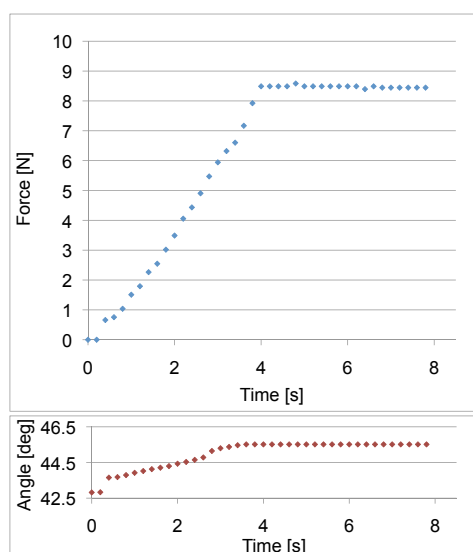


Figure 8.11: (top) Maximum continuous force of the grasping module. (bottom) Small variations in the angle of the device during the measurement by the compliance of the fixations.

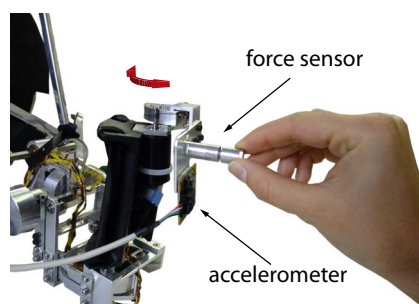


Figure 8.12: Setup for the Z-width and maximum stiffness measurements. A 3-axis accelerometer ($\pm 30 \text{ m/s}^2$) and a 1-DOF-force sensor ($\pm 50 \text{ N}$) were assembled to the thumb pad. The user had to move the thumb pad by directly pushing or pulling the force sensor.

the end effector were measured. Thereafter, a [Fast Fourier Transform \(FFT\)](#) was performed on the measured data and the minimum impedance was calculated as the force divided by the velocity.

The maximum impedance was obtained by tapping a stiff [VR-wall](#) at different frequencies. Measured contact forces and velocities were once again analyzed using the [FFT](#) and the impedance was calculated as the output force divided by the end-effector's velocity. The obtained Z-width is given in [Fig. 8.13](#). The minimum impedance value at a very low frequency is due to the static friction of the device produced by an assembly tolerance in the alignment of the motor axis. In average the Z-width is around 20 dB.

With the same setup a measurement of the maximum stiffness was performed. A trial with a [VR-wall](#) is shown in [Fig. 8.14](#). In the free space there was a virtual damping of $B =$

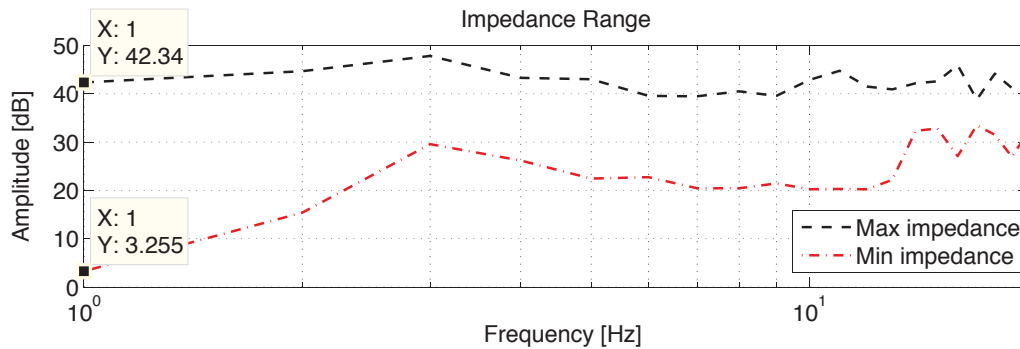


Figure 8.13: Z-width of the grasping module. In average, along the different frequencies the Z-width is around 20 dB.

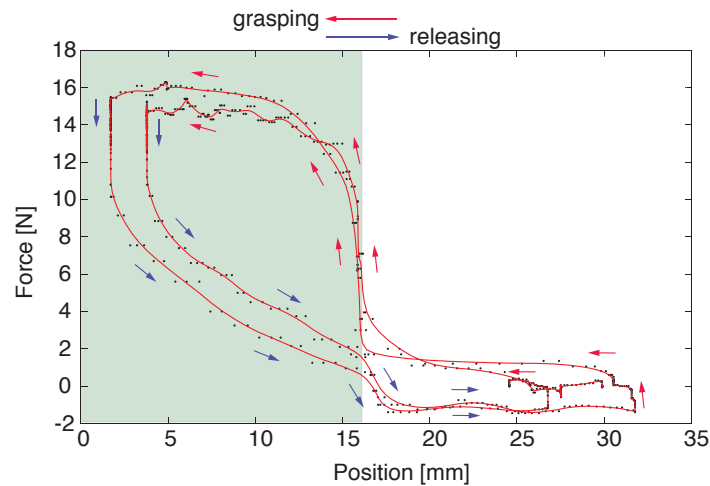


Figure 8.14: Force measurement versus position when a virtual wall is simulated at 16 mm of aperture. The maximum stable stiffness is around 11 N/mm. In the free space there was a virtual damping of $B = 0.02$ Ns/rad.

0.02 Ns/rad. The maximum stable stiffness is around 11 N/mm; after this value the force can increase up to 16 N but the stiffness considerably decreases. Note that taking into account the stall torque of the motor the device should render peaks of force up to 30 N however the continuous force that can be maintained during long periods is only 8.5 N.

8.4.3 Brake Performance

The setup used for the assessment of the brake is shown in Fig. 8.15. For this experiment the pressure input of the brake was incremented in steps of 0.2 bar. The shaft was pulled perpendicular to the shaft with a dynamometer until the shaft started moving and the maximum

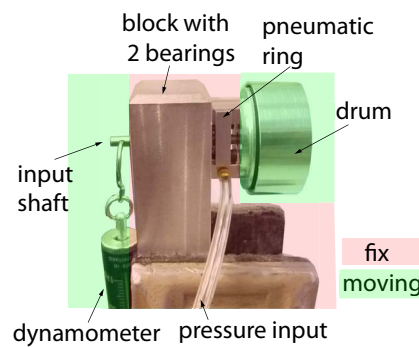


Figure 8.15: Setup to measure the brake behavior. The dynamometer is pulled perpendicular to the shaft until the shaft starts moving. The maximum force value is registered to calculate the braking torque at each pressure.

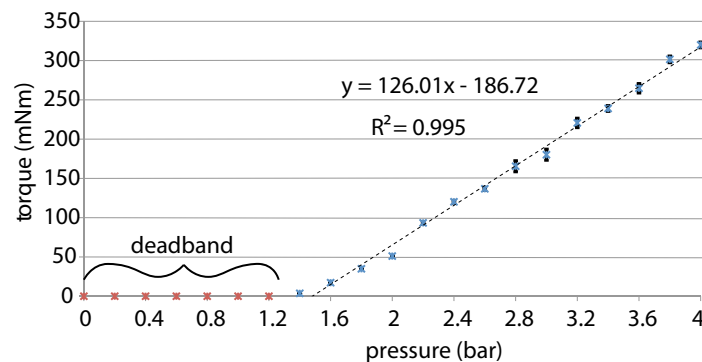


Figure 8.16: Brake torque in function of input pressure. There is a deadband up to 1.4 bar. With pressures ranging from 1.4 to 4 bar the output torque is proportional to the input pressure. Note that from 2.8 to 4 bar a bigger dynamometer with lower resolution was used, this is the reason why there a higher measurement variance appears for those pressures.

force achieved at that pressure was recorded. This procedure was performed four times for each pressure level.

The dynamometer was attached to the shaft through a hook and thus the force was applied at 15 mm from the shaft. This distance was taken into account when calculating the torque from the measured force. As shown in Fig. 8.16, the relationship between the braking torque and the input pressure can be linearized within the range 1.4 to 4 bar ($R^2 = 0.995$). The offset between 0 to 1.4 bar is due to the gap between the pneumatic ring and the drum. We expect a saturation for higher pressures; however, the manufacturer of the valves does not recommend to overcome 5 bar and the 0.2 Nm braking torque fixed in the specifications is already achieved at 3.2 bar.

In order to allow for a free-of-friction movement, it is necessary to leave a small gap between the pneumatic ring and the drum which means that a minimum of deadband is

needed. However, the valves can be calibrated to release the brake with a pressure of 1.2 bar, therefore reducing the rise time of the actuator. With the actual calibration (valve range from 0 to 3 bar) the total activation time of the brake is 15 ms (5 ms of delay plus 10 ms of rise time). The disengagement time of the brake highly depends on the input tank pressure; the fall time is smaller for a higher input pressure. With an input pressure of 3 bar the fall time was 20 ms (5 ms of delay plus 15 ms of fall time).

8.4.4 Discussion and Conclusions

In this section, a novel ergonomic haptic module with active grasping capabilities for a surgical application has been described and evaluated. The human-task based requirements, the spherical mechanism, the active grasping module and the lightweight brake system have been described in detail. The use of a spherical mechanism based on a double parallelogram allowed placing the remote-center-of-motion at the center of the users hand and helped to passively equilibrate the weight of the device. One of the main advantages of the proposed design is that it provides a large range of motion for the pronosupination **DOF** of the wrist while limiting the range of ulnar-radial deviation and extreme flexion to avoid dangerous wrist postures. The mechanism results in a very stiff structure, with low friction and backlash, and a workspace without singularities. The workspace analysis shows that, although certain orientations are excluded for ergonomic reasons, the handle still provides the dexterity necessary to conduct representative surgical tasks. There is still room for improvement which concern the integration of the electrical cables along the mechanism.

The assessment of the grasping feedback shows that the continuous force that can be applied by the device is slightly higher than the one expected with this motor (8.5 N). The maximum stable stiffness is 11 N/mm making it possible to render the sensation of grasping stiff objects. And the impedance range is about 20 dB. The grasping feedback module presents more static friction than expected due to a tolerance problem in the alignment of the axis that should be improved.

A key new feature is the brake system, which provides a high power to weight ratio (0.2 Nm for 0.03 kg) and a linear behavior. Thus, it can be used as a safety brake, to fix the orientations while using the clutch or to provide passive torque feedback. The presence sensor is currently used to brake and fix the handle orientations automatically if the surgeon suddenly releases the device.

8.5 Psychophysical Evaluation

A peg-in-hole test was implemented to evaluate the usability of the ergonomic handle and to compare it to a commercially available haptic device. This type of test represents a simplified assembly task in which the difficulty level can be controlled similarly to the Fitts law. This task has been widely used as an evaluation technique. [Harders et al. \(2006\)](#) performed 3D peg-in-hole tests to compare three different haptic devices. [Hannaford et al. \(1991\)](#) used the

peg-in-hole task to assess the performance of a 6-DOF telemanipulator. Samur et al. (2007b) proposed this setup to specifically evaluate the selection and manipulation capabilities of three different haptic devices. The work of Unger et al. (2001) revealed that with a VR-based peg-in-hole task with force feedback, the subjects used similar strategies than during a real peg-in-hole task.

In this work the peg-in-hole task was performed with two haptic devices: (1) the omega.7 with its standard handle and (2) the omega.7 with the ergonomic handle previously presented (Fig. 8.17).



Figure 8.17: (left) standard handle of the omega.7 and (right) the ergonomic handle presented in the previous section.

8.5.1 Methods

Peg-in-hole Task

This VR-based testbed is similar to the one proposed by Samur et al. (2007b), in which the user was asked to select the yellow peg located at the center of the group of pegs and introduce it in the target hole (Fig. 8.18).

According to Fitts law the different indices of difficulty for the peg-in-hole task were calculated as indicated by Eqn. 3.4. In this case, W represents the insertion clearance between the peg (p) and the target hole (h). In order to obtain an information range ID from 3 to 8 bit, six combinations of distance and insertion clearances were implemented as presented in Table 8.3.

The cubic objects in Fig. 8.18 including the hole were modeled as rigid dynamic bodies in Chai3D. The hole and the yellow peg were located on a straight line parallel to the screen. This constraint was imposed to avoid violation of the one dimensional nature of Fitts law given in Eqn. 3.3. When the user moved without the peg, the collision detection considered the tip of the haptic device as a small sphere. However, when the peg was grasped, the collision detection changed to detect the interactions between the cubic peg and the rest of the environment.

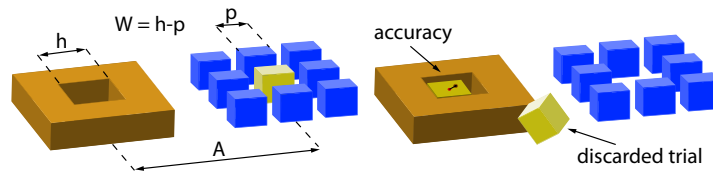


Figure 8.18: Sketch of the peg-in-hole task. The different indices of difficulty (ID) were achieved by varying the distance (A) and the insertion clearance (W) between the peg and the target hole.

Two different tasks were developed: 1) the peg orientation was kept invariant and 2) the subject had to properly orient the peg before its insertion. During the task involving orientations when the cube was not properly oriented its corner or edges could collide with the hole walls and consequently the user would be pushed away from the wall. To make the task more complex incongruent forces would appear if the peg was not properly oriented. Since both devices, the omega.7 with the standard handle and the omega.7 with the ergonomic handle, present a sensor/actuator asymmetry this task was a good example in which, in absence of torque, incongruent forces could emerge.

The pegs have a 10 mm edge a stiffness of $K = 1.6$ N/mm and weight 50 g when the peg was grasped a continuous force of 1.5 N was rendered as grasping feedback. When subjects separated their fingers more than 15 mm the peg was released. The blue pegs and the hole were attached to the floor of the workspace; only the yellow peg could be freely moved by the subject. Shadows and reflexions were added to help the subject with the depth perception of the environment.

Experimental Setup

The VR-based testbed of the peg-in-hole task ran on a Mac Book 5.1 laptop with an Intel Core 2 Duo 2.4 GHz CPU. The computer graphic card was an NVIDIA GeForce 9400M 256M GPU. The haptic and graphic loops were updated at 1 kHz and 30 Hz respectively. Two haptic devices were used: the omega.7 with the standard handle and the omega.7 with the ergonomic handle. The complete experimental setup is shown in Fig. 8.19.

Table 8.3: Index of difficulty of the peg-in-hole task

Clearance (W)	Distance (A)	Index of difficulty (ID)
4	32	3.17
2	32	4.08
1	32	5.04
2	128	6.02
1	128	7.01
0.5	128	8.01

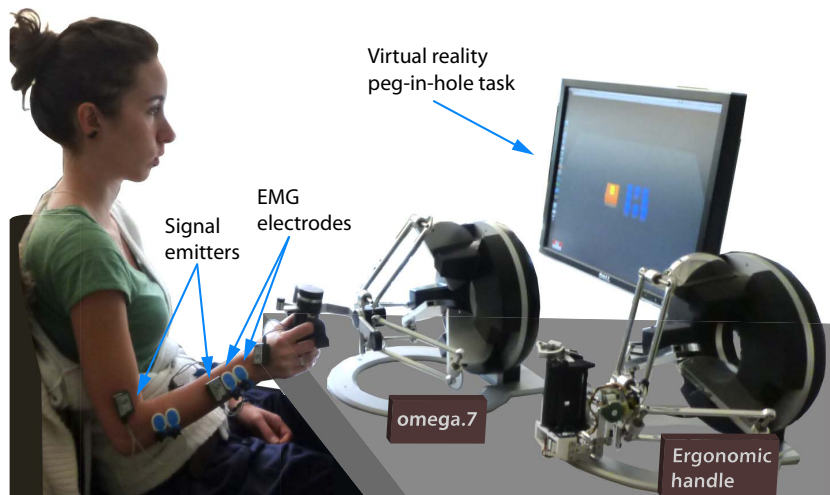


Figure 8.19: Setup for the peg-in-hole experiment. The subjects performed two peg-in-hole experiments (with and without orientations) with both haptic devices. The order of the experiment and device was randomly assigned to each subject.

Experimental Protocol

The experimental protocol followed a full factorial design with the following factors and levels:

1. Haptic device (two levels);
 - (a) omega.7 with the standard handle; or
 - (b) omega.7 with the ergonomic handle.
2. Peg-in-hole task (two levels);
 - (a) task without orientations; or
 - (b) task in which the peg has to be re-oriented before being inserted.

Before the experiments, subjects performed a training phase to get familiar with the test: (1) subjects were asked to explore the VR environment and manipulate the peg during an unlimited time, and (2) a training phase with the same protocol of the experiment was carried out. The aim of this part of the training was to familiarize subjects with the task so that there would be no further learning effect during the experiment. When the accuracy and the task-completion time had the same order of magnitude than those obtained during preliminary experiments the subject could start the actual experiment.

Subjects were asked to grasp the peg and introduce it in the indicated location. They were aware that time was measured; however, they were instructed to perform the task as accurately as possible. A visual cue appeared over the virtual table when the peg was released into the hole or dropped to indicate that the trial was completed. Subjects were instructed to lift the haptic devices pointer towards this visual sign to make a pause. After three seconds the

visual cue turned green and then disappeared. During this time, the VR changed to the new ID (Fig. 8.20). The order of the peg-in-hole experiments (with and without orientations) and the device (standard or ergonomic handle) was randomly assigned to each subject. For each experiment all the difficulty levels were repeated 7 times resulting in a total of 42 trials per task. In total with the two different tasks and the two haptic devices each subject performed 168 trials plus the training.

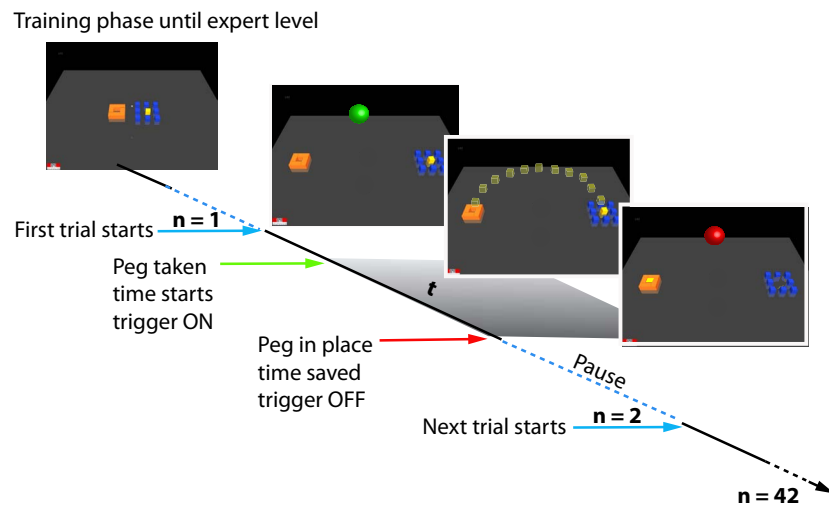


Figure 8.20: Experimental protocol followed during the peg-in-hole experiment. Subjects repeated the peg in hole task 42 times for each experiment making a break of around 5 minutes between experiments. A red sphere indicated the 3-second pause between trials. The sphere turned green to indicate the start of the next trial. The indices of difficulty were presented randomly within each experiment. The order of the device to be used and the task (with or without orientations) was randomly assigned to each subject.

During this experiment the following measurements have been recorded:

1. the time between grasping the peg and inserting the peg in the hole;
2. the insertion accuracy;
3. the maximum force while interacting with the environment; and
4. the maximum velocity during the movement.

Subjects

The experiment was conducted with 13 subjects each, aged 21-28, all right-handed. The subject group was composed of 10 men and 3 women. All participants gave written informed consent. The study protocol was performed in accordance with the ethical standards laid down in the Declaration of Helsinki.

8.5.2 Results

The trials with an error larger than 20 mm were discarded because they meant that the peg was dropped during the movement. One of the subjects performed the experiment too fast and dropped the peg too many times. Therefore, only the data of the other 12 subjects was considered for further analysis. Repeated measures ANOVA was performed with the aforementioned factors: task type (with or without orientations), haptic device (standard or ergonomic) and ID (6 levels). The results for each of the measurements are summarized in Table 8.4.

The task type had a highly significant effect on maximum force ($p = 0.002$), maximum velocity ($p = 0.001$) and time ($p < 0.001$). The ID was significant for all the measurements ($p < 0.001$ for all). The device factor alone was not a significant for any of the measurements; however, the interaction between device and task type was significant for time ($p = 0.014$). The interaction between task type and ID was found to be significant for both maximum velocity and time ($p = 0.002$ for both).

The IP of each device and the intercept (a) were determined by a linear regression and by using Eqn. 3.3 and Eqn. 3.5. As shown in Fig. 8.21, the results of this experiment showed that the performance in a manipulation and selection task is similar for the two interfaces. For the task that did not involve orientations the result was slightly better for the standard device (IP = 3.90 and intercept $a = 1.05$) than for the ergonomic handle (IP = 3.07 and intercept $a = 0.79$). In the task with orientations the ergonomic handle (IP = 2.43 and intercept $a = 0.79$) reduced the task-completion time along all difficulty levels and obtained a slightly

Table 8.4: Results of the repeated measures ANOVA for the peg-in-hole test

	Accuracy	Max. force*	Max. velocity*	Time*
Task type (T)	$F(1, 11) = 0.314$ $p = 0.568$	$F(1, 11) = 15.511$ $p = \mathbf{0.002}$	$F(1, 11) = 18.578$ $p = \mathbf{0.001}$	$F(1, 11) = 45.897$ $p < \mathbf{0.001}$
Device (D)	$F(1, 11) = 0.226$ $p = 0.643$	$F(1, 11) = 3.066$ $p = 0.107$	$F(1, 11) = 0.615$ $p = 0.449$	$F(1, 11) = 0.838$ $p = 0.379$
Index of Difficulty (ID)	$F(5, 55) = 7.021$ $p < \mathbf{0.001}$	$F(2.7, 30.0)^* = 3.066$ $p^* < \mathbf{0.001}$	$F(1.1, 12.6)^* = 188.4$ $p^* < \mathbf{0.001}$	$F(1.4, 15.2)^* = 103.5$ $p^* < \mathbf{0.001}$
Interaction (T,D)	$F(1, 11) = 0.002$ $p = 0.962$	$F(1, 11) = 3.737$ $p = 0.079$	$F(1, 11) = 1.597$ $p = 0.232$	$F(1, 11) = 8.371$ $p = \mathbf{0.014}$
Interaction (T,ID)	$F(5, 55) = 0.367$ $p = 0.868$	$F(3.3, 31.4)^* = 1.763$ $p^* = 0.167$	$F(2.9, 32.9)^* = 5.881$ $p^* = \mathbf{0.002}$	$F(2.4, 26.5)^* = 6.811$ $p^* = \mathbf{0.002}$
Interaction (D,ID)	$F(5, 55) = 1.277$ $p = 0.287$	$F(2.9, 31.5)^* = 0.308$ $p^* = 0.810$	$F(2.6, 28.5)^* = 0.857$ $p^* = 0.460$	$F(2.9, 32.3)^* = 1.653$ $p^* = 0.197$
Interaction (T,D,ID)	$F(5, 55) = 0.656$ $p = 0.658$	$F(2.8, 31.3)^* = 0.737$ $p^* = 0.531$	$F(1.9, 21.6)^* = 0.760$ $p^* = 0.477$	$F(3.5, 38.6)^* = 0.966$ $p^* = 0.428$

* These factors did not pass the [Mauchly sphericity test](#), thus [Greenhouse Geisser sphericity correction](#) was performed.

higher performance than the standard device ($IP = 2.25$ and intercept $a = 0.95$).

As shown in Fig. 8.21, the IP are not significantly different. However, as it can be appreciated in Fig. 8.22 the execution time for the task with orientation was found to be marginally-significantly lower for the ergonomic handle (the t-test resulted in $p = 0.055$). This effect might be the reason of the significant interaction between the task type and the device type previously found in the ANOVA.

8.5.3 Discussion and Conclusions

The task without orientations was performed in less time than the task involving orientations. As it will be discussed later, in the questionnaire most of the subjects affirmed that the task involving orientations was more difficult.

The maximum velocity was higher for the task without orientations and it was also affected by the ID ; for the three higher ID the maximum velocity increased because the distance between peg and hole was larger.

The accuracy was only affected by the ID . For the difficulty levels in which the clearance between hole and peg was smaller, the accuracy increased because the hole walls guided the movement, reducing the position error.

The maximum interaction force was affected by ID because the difficulty levels in which the clearance between peg and hole was smaller there were more collisions than in the other case.

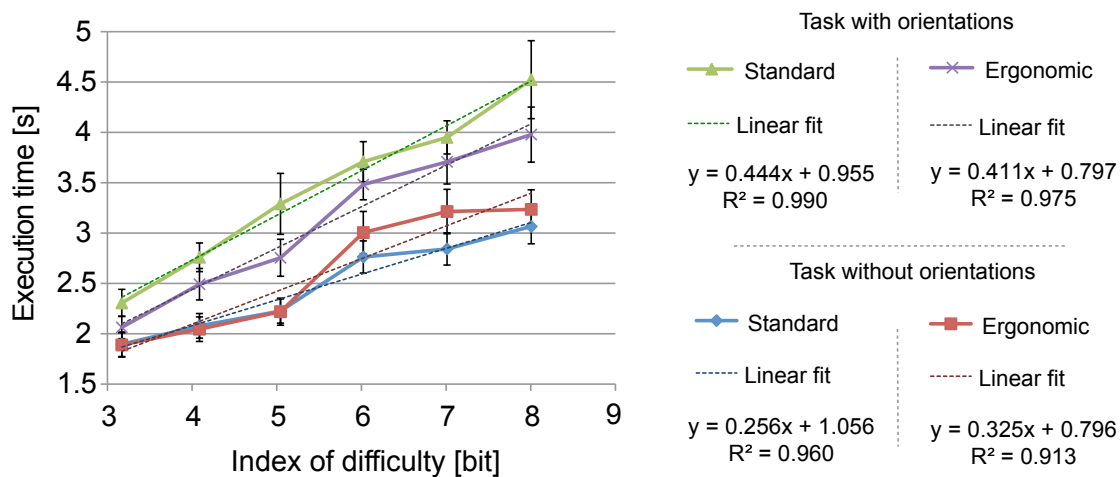


Figure 8.21: Task-completion time over index of difficulty for each task and device. The inverse of the slope of each regression line represents the index of performance of each device. In the task without orientations the ergonomic handle (red) performed worse than the standard handle (blue) for the higher difficulty levels. In the task with orientations ergonomic handle (purple) reduced the completion time along all difficulty levels and got a slightly better IP.

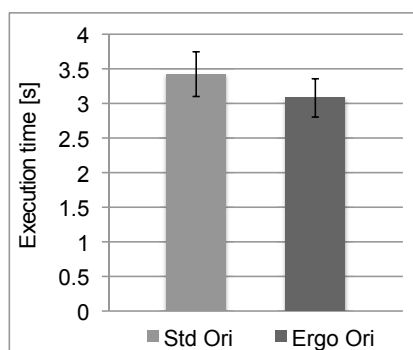


Figure 8.22: Average time for the peg-in-hole task with orientations. The t-test found a marginally significant difference with a $p = 0.055$ for the task-completion time with each device and across all difficulty levels.

The maximum interaction force was also significantly higher for the task involving orientations since an error orienting the peg could result in a collision between the edge of the cube and the hole walls.

The resulting *IP* and the intercept for the standard omega.7 device in the task without orientations ($IP = 3.90$ and intercept $a = 1.05$) is consistent with the one found by Samur (2010) for the omega.3 in the same task ($IP = 4.37$ and intercept $a = 1.36$). Note that the end-effector of these two devices are different.

In general, the performance of both devices was very similar since no significant differences were found between their *IP*. This means that the integration of a more complex handle in the omega.7 did not degrade the performance of the kinesthetic base. Therefore, the performance could be guaranteed while adding an ergonomic workspace and safety features.

For the task with orientations, the task-completion time was significantly reduced when using the ergonomic handle. This supports the hypothesis that combining both power and precision grip can help the user to control sudden changes on the interaction forces. In this case specific case it helped to control the incongruent forces introduced by the sensor/actuator asymmetry during the task involving orientations.

8.6 Ergonomic Evaluation

In order to assess the ergonomics of both the standard omega.7 device and the omega device with the ergonomic handle, the muscular activity during the peg-in-hole task was measured for a set of representative muscles. *electromyography (EMG)* measurement present high variability from person to person. However, the *EMG* values normalized with respect to the *Maximum Voluntary Contraction (MVC)* of each subject are a good estimation of the work carried out by each muscle along the task.

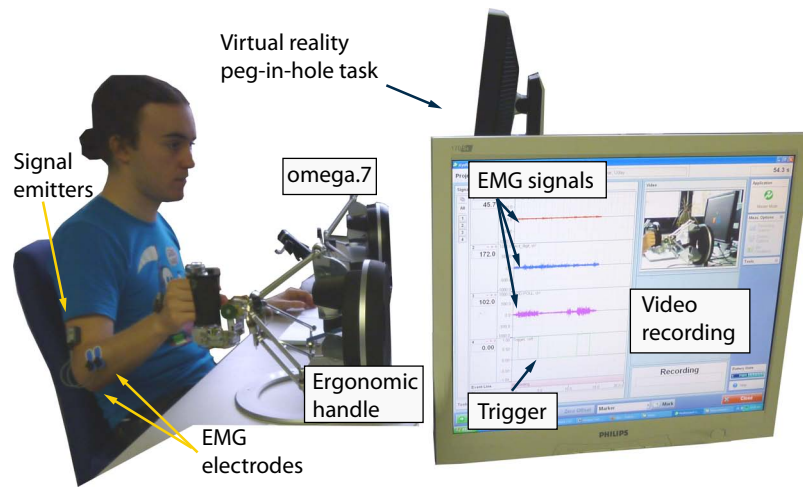


Figure 8.23: Setup for the EMG measurement. A video of the hand movements and EMG recordings were taken during the peg-in-hole task explained in Section 8.5. To synchronize the actions in the VR environment and the EMG records, a trigger signal was generated each time the subject grasped the peg.

8.6.1 Methods

A TeleMyo™ 2400T Direct Transmission System was used to measure the muscular activity (Noraxon U.S.A. Inc, Arizona). Two disposable, pre-gelled electrodes (Ambu Blue Sensor ECG Electrodes) were located along the contracting fibers of each muscle. The two electrodes were referenced to a common ground electrode integrated in the transmission wireless probe attached on the nearby skin, as illustrated in Fig. 8.23. The electrodes were then wired to the transmission wireless probes that amplified and sent the signal to the re-transmitter connected to the computer by USB.

A data acquisition card (Phidget interface kit 8/8/8) was used to generate a trigger signal to synchronize the EMG measurement with the peg-in-hole task. The trigger was switched on when the subject grasped the peg and switched off one the peg was released. A video of the hand movements was recorded at the same time with a webcam (Fig. 8.23).

Several muscle locations were measured during preliminary experiments to identify the muscles that were more involved in the grasping task. The set of muscles and the electrodes locations are shown in Fig. 8.24. After these preliminary experiments several locations had to be discarded:

1. the adductor pollicis longus was generally too contaminated with the activity of its neighbor muscle, the extensor pollicis longus;
2. the trapezius did not provide any useful information because its activity was the same for the two haptic devices and for the two task types; and

3. the extensor indicis provided the same information that the extensor digitorum but the amplitude of the signal was lower.

Protocol

To determine the exact location of the electrodes for each subject the surface was palpated while the subjects were asked to contract repeatedly that specific muscle. The skin was previously prepared by shaving the area in order to remove the hair and then lightly abrading and cleaning with a special gel. For some locations the effective stabilization of the electrodes needed additional adhesive tape. The electrodes were located prior to the training period for the psychophysical experiment. This way the measures were stable and the correct placement of the electrodes could be controlled directly during the training task. Before starting the actual experiment the maximum forces developed during 3 brief (1 second) **MVC** were recorded for each muscle. The subject had to contract each muscle by exerting force against a rigid object.

At the end of the experiment the subject was asked to make one **MVC** with each muscle

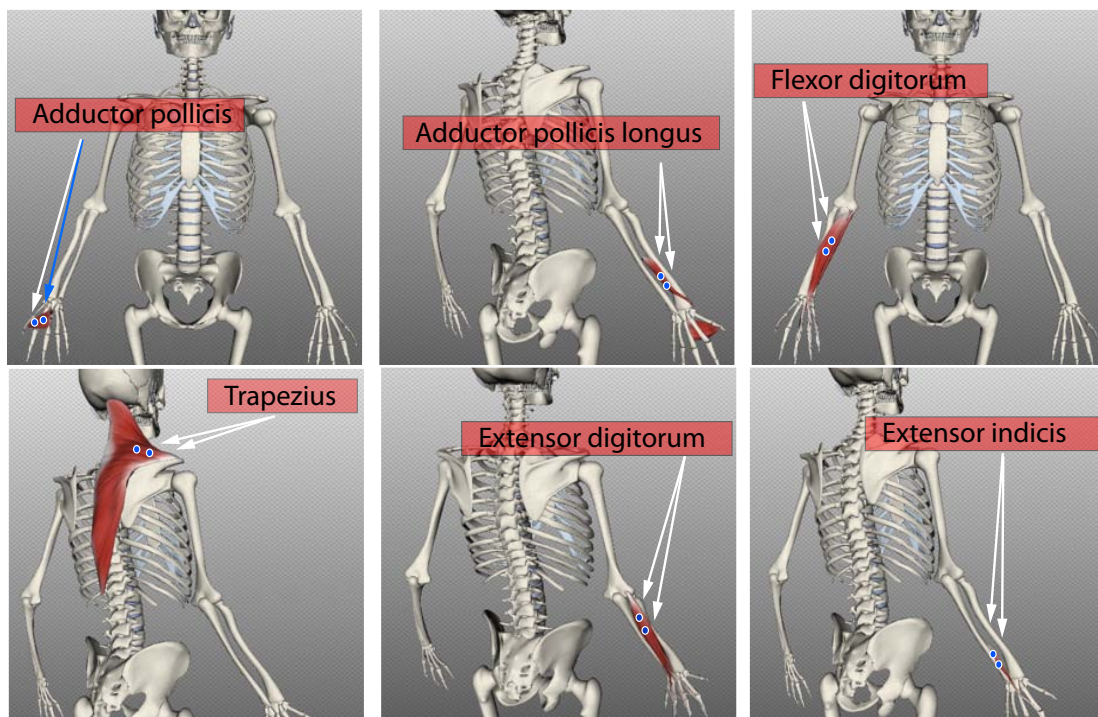


Figure 8.24: EMG electrodes placement for the adductor pollicis, adductor pollicis longus, flexor digitorum, trapezius, extensor digitorum and extensor indicis (images from www.biodigitalhuman.com). The blue points indicate the location of the EMG electrodes. After preliminary experiments, the measurement of the adductor pollicis longus, the trapezius and the extensor indicis were discarded.

to check that the electrodes were still properly located.

Analysis

The “Myo Research XP” software provided by Noraxon was used to analyze and treat the measurements. The **EMG** data was first visually inspected for artifacts that were indicative of sudden, unusual movements. Contaminated signals were marked for exclusion from further analysis. The signal was then rectified and the **Root Mean Square (RMS)** values were calculated for a window of 50 ms. The mean **RMS** values of the **MVC** for each muscle were used as a reference for each individual subject. Therefore, the muscular activity during the experiment was normalized with respect of the individual **MVC**. To analyze only the activity involved during the grasping action, the trigger was used to automatically select the periods of time in which the subject was grasping the peg. The average and the peak values of the each muscle activity were then calculated.

To compare the muscle activity for each haptic device and each task the average for all subjects was compared. Repeated measures **ANOVA** with the software STATISTICA (Stat Soft Inc.) was performed with the following factors: task type (with or without orientations) and handle type (standard or ergonomic).

8.6.2 Results

A total of 13 subjects performed the experiment, which was carried at the same time as the previous experiment. The subjects were therefore the same as in the peg-in-hole experiment. As mentioned in the previous section one subject did many errors during the psychophysical experiment and thus, his **EMG** data was also discarded. For the extensor digitorum and flexor digitorum muscles, the **EMG** data of 12 subjects could be used. However, the electrodes located in the adductor pollicis gave many problems because they were compressed during the grasping movement and often detached during the experiment. For most of the subjects the quality of the measurement was degraded along the experiment and could not be considered for further analysis. As a result only five measurements could be analyzed. In the repeated measures **ANOVA**, neither the device nor the task appeared to be a significant factor in the muscular activity, Table 8.5.

The muscular activity average values for each device during the two different tasks are shown in Fig. 8.25. For the extensor digitorum the muscular activity tends to be lower for the standard device. On the other hand, when the users used the ergonomic device, the muscular activity of the flexor digitorum and the adductor pollicis tended to be lower than with the standard device. However, none of the differences are statistically significant.

Table 8.5: Repeated measures ANOVA for the average EMG measurements

Measurement	Task type	Device	Interaction
Extensor digitorum (12 subjects)	$F(1, 11) = 0.319$ $p = 0.583$	$F(1, 11) = 2.896$ $p = 0.116$	$F(1, 11) = 1.128$ $p = 0.311$
Flexor digitorum (12 subjects)	$F(1, 11) = 1.217$ $p = 0.293$	$F(1, 11) = 0.925$ $p = 0.356$	$F(1, 11) = 0.290$ $p = 0.600$
Adductor Pollicis (5 subjects)	$F(1, 4) = 0.019$ $p = 0.894$	$F(1, 4) = 0.913$ $p = 0.393$	$F(1, 4) = 0.021$ $p = 0.890$

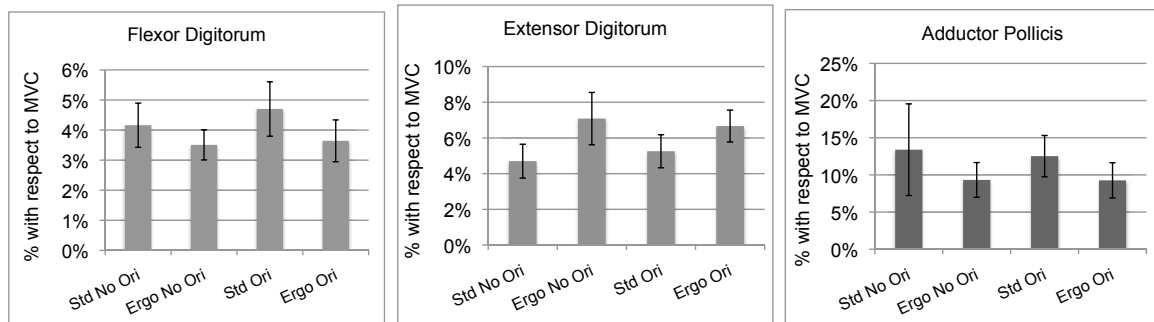


Figure 8.25: Average task EMG values for each muscle. The muscle activity for each subject has been normalized to his/her MVC values. The muscular activity tends to be lower for the extensor digitorum with the standard device, and for the flexor digitorum and the adductor pollicis with the ergonomic device. Since the peg-in-hole task demands low muscular activity none of the differences appear to be significant. The error bars represent the standard deviation of the mean.

8.6.3 Discussion and Conclusions

The **EMG** measurements show a trend for a decrease in the muscular activity in the flexor digitorum and the adductor pollicis with this design. However, the task did not involve high-enough forces (note that the muscular activation was generally lower than the 15% of **MVC**). To see a significant difference with this level of activation the experiment should be performed during a longer period of time, in this case the experiment lasted only one hour. The muscular activity of the extensor digitorum with the ergonomic handle was present not only during the grasping task for some of the subjects. Generally, these subjects had long fingers and they bent the fingertips at the end of the handle. This posture consequently produces a constant tension in the extensor digitorum. A modification of the plastic part of the handle should be performed to accommodate larger hands and avoid this effect.

8.7 Post-experiment Questionnaire

At the end of the experiment each subject filled in the following questionnaire.

8.7.1 Questionnaire

During the experiment the user could refer to the devices with a number in order not to bias the results: [1] referred to the standard and [2] referred to the ergonomic handle.

1. Age and gender.
2. During the task without orientations was it more difficult to control one device than the other? Yes [1], Yes [2] or No.
3. During the task with orientations was it more difficult to control one device than the other? Yes [1], Yes [2] or No.
4. Which task was more demanding? Without orientations, With orientations or Same.
5. In general, how difficult did you consider the peg-in-hole task? Very difficult, Difficult, Medium, Easy or Very easy.
6. Was it more difficult when the distance was higher? Yes or No.
7. Was it more difficult when the hole size was smaller? Yes or No.
8. What increased more the difficulty the distance or the hole size? Distance, Hole size or Same.
9. Did you feel fatigue in any of these areas? Thumb, Index finger, Forearm, Shoulder and No pain.
10. Did you feel a difference in the fatigue with any of the devices? Yes or No.

8.7.2 Results

As shown in Fig. 8.26, most of the subjects found the difficulty of the peg-in-hole task medium or easy but they found that the task with orientations was more demanding. In the task without orientations the 60% of subjects affirmed that the difficulty was the same with both devices, and 20% of them thought the standard handle was more difficult to control. In the task with orientations most of the subjects affirmed that the difficulty was the same with both devices, followed by that the ergonomic handle was more difficult to control. The majority of the subjects did not feel any difference in terms of fatigue with the two devices and most of them did not complain about fatigue.

In general, the subjects felt that both the hole size and the distance peg-hole had an influence in the difficulty. The hole size was felt to have more influence in the difficulty, which is coherent with the Fitts law formulation proposed to choose the ID levels (Eqn. 3.4).

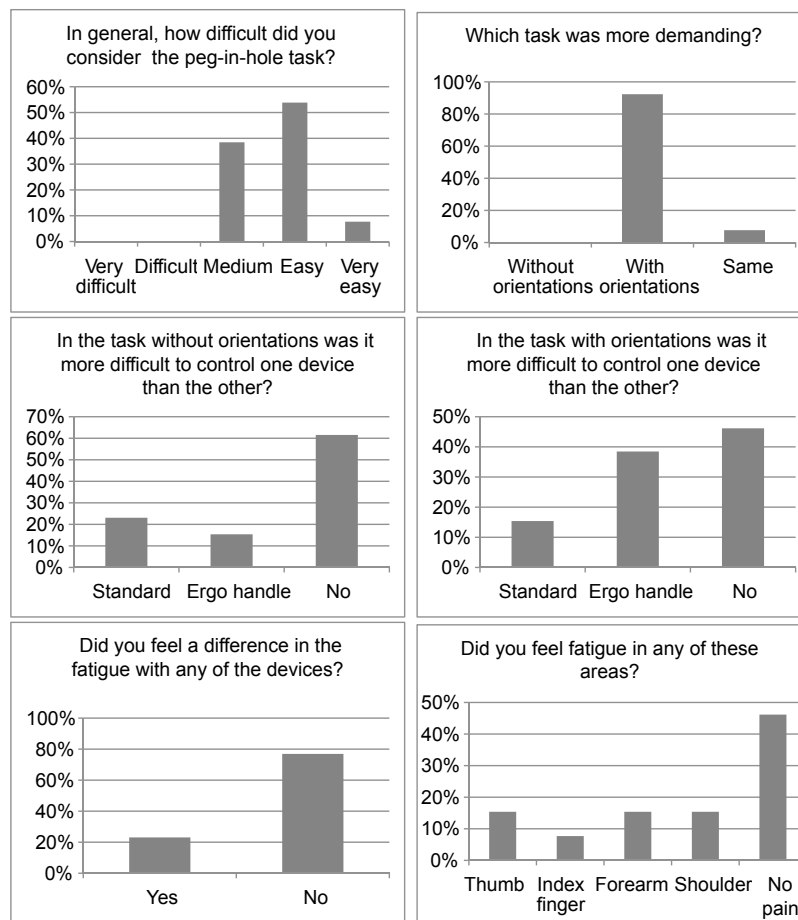


Figure 8.26: Bar chart with the questionnaire answers for the peg-in-hole task. The experiment was generally perceived as medium or easy but more difficult when the peg had to be oriented. In general the subjects did not complain about fatigue and this was similar for both devices. The influence of the distance and the hole size in the difficulty of the task were consistent with the Fitts law.

8.8 Chapter Summary and Conclusions

In this chapter, the development and the evaluation of a novel ergonomic haptic handle with active grasping feedback and safety features were presented. The spherical mechanism based on a double parallelogram allows enough dexterity to perform surgical gestures while excluding certain postures that could fatigue the surgeon's wrists. The prototype provides grasping feedback up to 8.5 N, a maximum stiffness of 11 N/mm and an impedance range of about 20 dB. Further improvement can be performed to reduce the static friction produced by a misalignment of the motor axis. Additional safety features integrated in the handle allow to automatically fix the handle orientations if the surgeon suddenly releases the device.

The psychophysical experiment proved the usability of the device. No significant difference

was found between the index of performance of the omega.7 device with the standard handle and the omega.7 device with the ergonomic handle. This means that the integration of the new handle in the omega.7 base did not degrade the performance of the haptic device.

The execution time for the peg-in-hole task involving orientations was significantly lower when using the ergonomic handle. The lower intercept value (a) obtained with the ergonomic handle means that the subjects spent less time in the target, in this case the hole. This shows that the handle helped the users to orient faster the peg. This outcome additionally supports the hypothesis that the combined power-precision grip can help the user to control sudden force changes. This is important especially in devices with sensor/actuator asymmetry in which incongruent forces may appear due to the absence of torque feedback.

The muscular activity of the extensor digitorum raised an issue in the handle shape that should be modified. The **EMG** measurements showed a potential decrease of the muscular activity in the flexor digitorum and the adductor pollicis with this design, which could result in lower fatigue in those muscles. However, longer experiments or experiments involving higher forces should be performed to verify this trend.

Chapter 9

Conclusions

MIS surgical procedures greatly benefit patients by decreasing post-operative pain, scarring and recovery times. Hence, such surgical techniques will obviously continue to be applied and will further develop. The reduced incisions these techniques involve, have withdrawn the surgeon's hands from the patient. Surgeons must now rely on their vision and many diagnostic procedures performed during open surgery - which are highly dependent on surgeons' sense of touch - are no longer possible.

At this point in time, surgeons experienced in robotic surgery have learned to compensate the lack of [haptic feedback](#) and are able to work relying only on vision and proprioceptive cues. This, along with the cost that adding [haptic feedback](#) incurs, explains why the introduction of this technology in surgical robotics is a controversial subject. Only recently has research begun to find evidence of how [haptic feedback](#) - and especially force feedback - can benefit robotic surgery. But exactly what is its added value? What types of tactile information are necessary and how much does it improve surgeons' performance? These are among some of the questions that were addressed during this thesis following a task-specific approach.

A lot of research is underway to improve [haptic feedback](#) fidelity. Technically, the term fidelity refers to the quality of conforming exactly to the truth. However, providing the user with a small, highly precise fraction of what real sense of touch is cannot be considered an accurate reflection of reality. This work proposes an alternative strategy, combining different haptic information in a simplified manner, depending on the nature of the task to give a more global picture of the actual tactile experience.

The practice of MIS procedures comprises a further major issue - it has caused what could be called an "ergonomic crisis" in the OR. The literature review and survey performed in this thesis showed obvious ergonomic issues brought by the MIS trend. The da Vinci surgical robotic system corrected the awkward postures affecting back and shoulders as well as the unnatural visuomotor manipulation adopted during laparoscopic procedures. Nevertheless, we have seen that there is still room for improvement in areas concerning the surgeon's neck posture and the design of the handles used in the master console.

This thesis therefore focuses on the two main issues of haptic feedback and ergonomics of robotic surgery. We believe that addressing these points will greatly benefit patient safety and at the same time also improve working conditions for surgeons.

The proposed **research methodology** to investigate the benefits of **haptic feedback** proceeds along the three following steps: First, an analysis of a surgical task was performed to identify the main haptic information involved during the tactile experience in question. Second, hardware setups providing that particular feedback and a **VR**-based testbed simulating the task were developed. Finally, experiments were performed to investigate how that feedback influences surgeons' performance.

Experiments targeting two specific surgical tasks were carried out: 1) a suturing gesture with a curved needle and 2) a tactile exploration task. The results of the experiment on a suturing task showed how force feedback significantly improved surgeons' precision while targeting the indicated suture points, reduced the maximum depth of the puncture and decreased the task-completion time. On the other hand, torque feedback did not additionally benefit the users during this specific task. In other surgical tasks such as the introduction of surgical screws, torque feedback may be essential to apply the correct forces.

The tactile exploration experiment to assess the vascularization of tissue revealed that tactile feedback significantly decreased the task-completion time when identifying the orientation of a hidden artery. Visual sensory substitution and tactile feedback obtained a similar performance across difficulty levels. However, their combination helped subjects to find the artery faster when the difficulty of the task was higher. Eighty percent of our subjects preferred the combined feedback. Several subjects also commented that receiving information simultaneously through several sensory channels allowed them to be more certain of their gestures. These comments support the hypothesis that giving redundant feedback to the surgeon might increase safety and reduce cognitive load.

The outcome of both studies answers the aforementioned open questions for two specific surgical tasks and thus represents an element of proof of how different types of **haptic feedbacks** could improve surgeons' performance. It thereby encourages the introduction of this technology in the growing field of robotic surgery.

Chapter 7 proposes guidelines to facilitate the design process of a surgeon's workstation while guaranteeing its ergonomics. Following these recommendations in terms of display disposition could, for instance, alleviate the discomfort suffered by surgeons on their neck due to the static non-neutral posture. Further suggestions are given concerning wrist-hand mobility, clearances as well as console layout to increase surgeon performance and safety while keeping teleoperation as intuitive as possible.

The survey carried out within this thesis found that 28% of surgeons complained about tension in their fingers when using the current da Vinci handle. This issue can be aggravated with the addition of **haptic feedback** because surgeons' fingers must sustain higher forces. A novel ergonomic handle was developed following the proposed guidelines to resolve this issue. The design aimed at lessening tension in the fingers and avoiding wrist postures that could lead to serious musculoskeletal disorders over time. A preliminary evaluation of this device in terms

of technical performance, usability and ergonomics was presented. The prototype provides a singularity-free workspace, rendering a maximum grasping force of 8.5 N and furnishing up to 0.3 Nm of braking torque in all three rotational directions. The ergonomic handle was integrated into the base of an omega.7 haptic device and a performance comparison with the standard handle of the omega.7 was carried out. Besides the slightly larger mass of the ergonomic handle, the index of performance of the device could be maintained. Furthermore, for a precise manipulation task involving orientations, the task-completion time obtained with the ergonomic handle was significantly lower than with the standard handle. This suggests that the ergonomic handle helped the subjects to achieve faster hand orientation in a simplified assembly task.

No significant difference was observed between the two handles in the [EMG](#) measurements assessing the muscular activity during the manipulation task. However, the ergonomic handle tended to decrease the muscular activity of the flexor digitorum and the adductor pollicis. These results suggest that the device can potentially mitigate the fatigue in those muscles. Nevertheless, longer experiments or a manipulation task involving higher forces should be performed to confirm this hypothesis.

9.1 Contributions and Originality

The main contributions of this thesis can be grouped into three categories: hardware and software developments, a multidisciplinary approach and ergonomic guidelines.

9.1.1 Task-specific and Physiologically Motivated Developments

A major contribution of this thesis is the implementation and evaluation of multimodal [haptic feedback](#) and its application to telemanipulated robotic surgery. The aim was to integrate the advantages of open surgery, where direct contact with the patient gives constant [haptic feedback](#), with the advantages of robotic surgery. Therefore, throughout this thesis physiologically motivated tactile feedback modalities were investigated and thereafter integrated with a state of the art force feedback technology. In particular three experimental setups were developed:

- A handle able to render torque feedback for a suturing task and a [VR](#)-based testbed of a soft tissue with a haptic model simulating the interaction forces that occur during a needle puncture.
- A tactile pulse display integrated into a haptic device and a [VR](#)-based testbed simulating a tactile exploration.
- An ergonomic handle for telesurgery with an original design that can provide grasping feedback and safety features (i.e. hand detection and orientation brakes).

9.1.2 Approach Combining Technology, Psychophysics and Ergonomics

All along this thesis a systematic methodology was followed to analyze the influence of different types of feedback on the surgeon's performance during common surgical tasks and also to evaluate the usability of various prototypes. The approach is multidisciplinary in both the design (survey, ergonomic guidelines, technical specs, etc.) and the evaluation (technical performance metrics, psychophysical studies, ergonomic measurements and questionnaires).

This work can be used as a tutorial to perform application-specific tests to evaluate the benefits that haptic devices can provide. The same procedure can be conducted in a generic context and thus, be applied to any other teleoperation environment.

9.1.3 Survey and Ergonomic Guidelines

To the author's best knowledge, there is no previous work addressing working conditions and subjective preferences of surgeons from different background in the same study. One of the contributions of this thesis is an across-surgical techniques study that attempts to identify the principal factors (background, ergonomics, working conditions, etc.) influencing surgical instrument acceptance. To understand the main criteria in which surgeons' acceptance is based can help engineers on to design the devices that better meet their needs which represents, basically, the foundation of a product success. Moreover, at the time being there are no specific ergonomic standards regarding the surgeon's console. This thesis collects recommendations to guide the design process of a workstation for this particular field.

9.2 Outlook and Further Research Directions

9.2.1 Haptics Research

Within this thesis only two specific surgical tasks could be studied in detail. However, there are numerous tactile explorations that can be no longer performed during MIS procedures. Consequently, this is still an open research topic that can be developed much further by evaluating other types of feedback involved in those tactile explorations. For instance, roughness to assess the fibrosis of internal surgical adhesions or the benefits of thermal information to evaluate the necrosis of tissues. For this last surgical task a high-density tactile thermal display based on four miniaturized Peltier cells was developed within this thesis. Unfortunately, there was not enough time to advance more in this study but it will be further investigated in the framework of another research project (Gallo et al., 2012).

One of the main challenges in haptics research is to understand the human sensory mechanisms that integrate and combine different tactile information with other sensory modalities (i.e. additional visual and auditory cues) for each type of tactile exploration. This knowledge is a must for multimodal haptic systems design and cannot be obtained by only performing questionnaires and psychophysical experiments. Instead, a strategy also taking into account

neurophysiology and physiological measures should be adopted.

An additional research trend is the development of standardized performance metrics in the frame of teleoperated surgical tasks. For instance, the widely used Fitts law is not applicable to every context and specifically in this work it could not be applied for a palpation task. The variability of metrics used by each research study makes it difficult to compare the performance under different feedbacks. These metrics could also represent the basis for the development of a standard curriculum for robotic surgery training.

A major technological bottleneck that delays the clinical application of multimodal [haptic feedback](#) in the field of robotic surgery is the lack of accurate and biocompatible tactile sensors. Current technology is not capable of measuring different tactile information in a compact manner allowing its integration in the slave robot. Considerable work on the development of high-density arrays of biocompatible tactile sensors is necessary in order to achieve this goal.

9.2.2 Ergonomics in Robotic Surgery

Surgeons are increasingly aware of and concerned about ergonomic issues. Regulatory authorities are beginning to address such issues as new [MIS](#) instrumentation evolves. In a surgical field that undergoes constant changes in surgical instruments, types of interventions and demographics (i.e. the increasing number of women working in the [OR](#)), the ergonomic guidelines proposed by this thesis should be regularly updated and thus represent a continuous field of research. This can only be performed through cooperative work between surgeons and engineers.

Another dimension of ergonomics that was not fully covered by the present work is the influence of different feedbacks on the surgeon's attention and mental workload. This was partially assessed through questionnaires. However, objective measurements could be used to quantify the psychological stress and optimize the information transfer of the overall surgical robotic system.

Technological innovation has already made great strides in matters affecting both patients and surgeons, albeit at the expense of some of the human hand's unique capabilities in terms of dexterity and sensitivity. This thesis aspires to contribute to advancing the sense of human touch in teleoperated surgery and raising awareness about the importance of ergonomics in the field.

References

- Abolhassani, N., Patel, R., and Moallem, M. (2007). Needle insertion into soft tissue: A survey. *Medical Engineering and Physics*, 29(4):413–431. [42](#)
- Akiyama, S., Sato, K., Makino, Y., and Maeno, T. (2012). Presentation of thermal sensation through preliminary presentation of thermal sensation through preliminary adjustment of adapting skin temperature. In *Proceedings of IEEE Haptics Symposium*, pages 355–358, Vancouver, BC, Canada. [22](#)
- Aspell, J., Lenggenhager, B., and Blanke, O. (2009). Keeping in touch with one’s self: multi-sensory mechanisms of self-consciousness. *PLoS One*, 4(8):e6488. [32](#)
- Astley, O. and Hayward, V. (2000). Design constraints for haptic surgery simulation. In *IEEE International Conference on Robotics and Automation, ICRA*, volume 3, pages 2446–2451. [36](#)
- Barbagli, F. and Salisbury, K. (2003). The effect of sensor/actuator asymmetries in haptic interfaces. In *11th Symposium on Haptic Interfaces for Virtual Environment and Teleoperator System (HAPTICS’03)*, page 140, Washington, DC, USA. [30](#)
- Barbé, L., Bayle, B., De Mathelin, M., and Gangi, A. (2007a). In vivo model estimation and haptic characterization of needle insertions. *International Journal of Robotics Research*, 26(11-12):1283–1301. [35](#), [42](#), [43](#), [45](#)
- Barbé, L., Bayle, B., de Mathelin, M., and Gangi, A. (2007b). Needle insertions modeling: Identifiability and limitations. *Biomedical Signal Processing and Control*, 2(3):191–198. [42](#), [43](#)
- Baumman, R. (1997). *Haptic Interfaces for Virtual Reality Based Laparoscopic Surgery Training Environment*. PhD thesis, EPFL, Switzerland. [29](#)
- Berguer, R. (1999). Surgery and ergonomics. *Archives of surgery*, 134(9):1011. [3](#), [4](#), [87](#)
- Berguer, R., Gerber, S., Kilpatrick, G., and Beckley, D. (1998). An ergonomic comparison of in-line vs pistol-grip handle configuration in a laparoscopic grasper. *Surgical endoscopy*, 12(6):805–808. [4](#), [87](#)
- Berguer, R., Smith, W., and Chung, Y. (2001). Performing laparoscopic surgery is significantly more stressful for the surgeon than open surgery. *Surgical endoscopy*, 15(10):1204–1207. [4](#), [87](#)

- Brebner, J. and Welford, A. (1980). Reaction time in personality theory. *Reaction times*, pages 309–320. [82](#)
- Brooks, T. (1990). Telerobotic response requirements. In *IEEE International Conference on Systems, Man and Cybernetics, Conference Proceedings.*, pages 113–120. IEEE. [26](#), [27](#)
- Burgner, J., Swaney, P., Rucker, D., Gilbert, H., Nill, S., Russell, P., Weaver, K., and Webster, R. (2011). A bimanual teleoperated system for endonasal skull base surgery. In *IEEE/RSJ International Conference on Intelligent Robots and Systems, IROS*, pages 2517–2523. [11](#), [14](#), [16](#), [165](#)
- Butterfly Haptics, LLC (2010). website: <http://butterflyhaptics.com>. [18](#), [19](#), [165](#)
- Campion, G. and Hayward, V. (2005). Fundamental limits in the rendering of virtual haptic textures. In *Eurohaptics Conference, 2005 and Symposium on Haptic Interfaces for Virtual Environment and Teleoperator Systems, 2005. World Haptics 2005. First Joint*, pages 263–270. IEEE. [28](#)
- Carswell, C., Clarke, D., and Seales, W. (2005). Assessing mental workload during laparoscopic surgery. *Surgical Innovation*, 12(1):80. [4](#), [87](#)
- Chamberlain, R. and Sakpal, S. (2009). A comprehensive review of single-incision laparoscopic surgery (sils) and natural orifice transluminal endoscopic surgery (notes) techniques for cholecystectomy. *Journal of Gastrointestinal Surgery*, 13(9):1733–1740. [1](#)
- Chen, C., Nevo, E., Fetics, B., Pak, P., Yin, F., Maughan, W., and Kass, D. (1997). Estimation of central aortic pressure waveform by mathematical transformation of radial tonometry pressure: validation of generalized transfer function. *Circulation*, 95(7):1827–1836. [62](#), [63](#)
- Chun, K., Verplank, B., Barbagli, F., and Salisbury, K. (2005). Evaluating haptics and 3d stereo displays using fitts’ law. In *Haptic, Audio and Visual Environments and Their Applications, 2004. HAVE 2004. Proceedings. The 3rd IEEE International Workshop on*, pages 53–58. [32](#), [34](#), [35](#)
- Colgate, J. and Brown, J. (1994). Factors affecting the z-width of a haptic display. In *IEEE International Conference on Robotics and Automation, ICRA*, pages 3205–3210. [30](#), [121](#)
- Conti, F., Morris, D., Barbagli, F., and Sewell, C. (2007). Chai 3d. Online: <http://www.chai3d.org>. [69](#)
- Cowan, N. (2001). The magical number 4 in short-term memory: A reconsideration of mental storage capacity. *Behavioral and brain sciences*, 24(01):87–114. [76](#)
- Eddings, M., Johnson, M., and Gale, B. (2008). Determining the optimal pdms–pdms bonding technique for microfluidic devices. *J Micromech Microeng*, 18(6). [59](#)
- Ernst, M. and Banks, M. (2002). Humans integrate visual and haptic information in a statistically optimal fashion. *Nature*, 415(6870):429–433. [31](#), [75](#)
- Fei, W., Su, E., Burdet, E., and Bleuler, H. (2008). Development of a microsurgery training system. In Dumont, G., editor, *30th Annual International Conference of the IEEE En-*

- gineering in Medicine and Biology Society (EMBS)*, pages 1935–1938, Vancouver, VC, Canada. [41](#)
- Feller, R., Lau, C., Wagner, C., Perrin, D., and Howe, R. (2004). The effect of force feedback on remote palpation. In *IEEE International Conference on Robotics and Automation, ICRA*, volume 1, pages 782–788, New Orleans. [35](#), [70](#), [82](#)
- Fitts, P. (1954). The information capacity of the human motor system in controlling the amplitude of movement. *Journal of Experimental Psychology: General*, 47(3):381–391. [33](#)
- Force Dimension (2011). website: <http://www.forcedimension.com>. [10](#), [11](#), [15](#), [16](#), [17](#), [19](#), [39](#), [112](#), [121](#), [165](#)
- Gallo, S., Santos-Carreras, L., Rognini, G., Hara, M., Yamamoto, A., Higuchi, T., and Bleuler, H. (2012). Towards multimodal haptics for teleoperation: Design of a tactile thermal display. In *The 12th International Workshop on Advanced Motion Control (AMC)*, Sarajevo. [144](#)
- Gassert, R., Dovat, L., Lamberg, O., Ruffieux, Y., Chapuis, D., Ganesh, G., Burdet, E., and Bleuler, H. (2006). A 2-dof fmri compatible haptic interface to investigate the neural control of arm movements. In *Robotics and Automation, 2006. ICRA 2006. Proceedings 2006 IEEE International Conference on*, pages 3825–3831. IEEE. [27](#)
- Gerovichev, O., Marayong, P., and Okamura, A. M. (2002). The effect of visual and haptic feedback on manual and teleoperated needle insertion. In Dohi, T. and Kikinis, R., editors, *MICCAI '02: Proceedings of the 5th International Conference on Medical Image Computing and Computer-Assisted Intervention-Part I (Tokyo Japan)*., volume 2488, pages 147–154, Berlin Germany. Springer Verlag. [45](#)
- Gescheider, G. (1997). *Psychophysics: the fundamentals*. Lawrence Erlbaum Associates. [63](#)
- Gescheider, G. A., Thorpe, J., Goodarz, J., and Bolanowski, S. J. (1997). The effects of skin temperature on the detection and discrimination of tactile stimulation. *Somatosensory & motor research*, 14(3):181–188. [22](#)
- Glickson (2012). Surgeons experience more ergonomic stress in the or. *Bulletin of the American College of Surgeons*, 97(4):20–26. [3](#), [87](#), [111](#)
- Gofrit, O., Mikahail, A., Zorn, K., Zagaja, G., Steinberg, G., and Shalhav, A. (2008). Surgeons’ perceptions and injuries during and after urologic laparoscopic surgery. *Urology*, 71(3):404–407. [4](#), [87](#), [96](#)
- Guiatni, M., Benallegue, A., and Kheddar, A. (2008). Learning-based thermal rendering in telepresence. *Haptics: Perception, Devices and Scenarios*, pages 820–825. [22](#)
- Guthart, G. and Salisbury, J. (2000). The intuitive tm telesurgery system: Overview and application. In *IEEE International Conference on Robotics and Automation, ICRA*, volume 1, pages 618–621. San Francisco, CA. USA. [55](#)
- Gwilliam, J., Pezzementi, Z., Jantho, E., Okamura, A., and Hsiao, S. (2010). Human vs.

- robotic tactile sensing: Detecting lumps in soft tissue. In *Haptics Symposium*, pages 21–28, Massachusetts. 70, 82
- Gwilliam, J. C., Degirmenci, A., Bianchi, M., and Okamura, A. M. (2012). Design and control of an air-jet lump display. In *Proceedings of IEEE Haptics Symposium*. 21, 57
- Hagn, U., Konietschke, R., Tobergte, A., Nickl, M., Jörg, S., Kübler, B., Passig, G., Gröger, M., Fröhlich, F., Seibold, U., et al. (2010). DLR mirosurge: a versatile system for research in endoscopic telesurgery. *International journal of computer assisted radiology and surgery*, 5(2):183–193. 11, 13, 16, 165
- Hannaford, B., Wood, L., McAfee, A., and Zak, H. (1991). Performance evaluation of a six-axis generalized force-reflecting teleoperator. *IEEE Transactions on systems, man and cybernetics Haptics*, 21(3):620–633. 32, 34, 125
- Hansen Medical Inc. (2011). website: <http://www.hansenmedical.com>. 10, 11, 15, 103, 113, 165
- Haption SA (2011). website: <http://www.haption.com>. 18, 19, 165
- Harders, M., Barlit, A., Akahane, K., Sato, M., and Szekely, G. (2006). Comparing 6dof haptic interfaces for application in 3d assembly tasks. In *Proceedings of Eurohaptics*. 125
- Hasser, C. (1995). Force-reflecting anthropomorphic hand masters. Technical report, DTIC Document. 27
- Hayward, V. and Astley, O. (1996). Performance measures for haptic interfaces. In *ROBOTICS RESEARCH-INTERNATIONAL SYMPOSIUM-*, volume 7, pages 195–206. MIT PRESS. 25, 28
- Hayward, V., Choksi, J., Lanvin, G., and Ramstein, C. (1994). Design and multi-objective optimization of a linkage for a haptic interface. *Advances in Robot Kinematics*, pages 352–359. 28
- Hayward, V., Gregorio, P., Astley, O., Greenish, S., Doyon, M., Lessard, L., McDougall, J., Sinclair, I., Boelen, S., Chen, X., et al. (1998). Freedom-7: A high fidelity seven axis haptic device with application to surgical training. *Experimental Robotics V*, pages 443–456. 19, 112
- Hayward, V. and MacLean, K. E. (2007). Do it yourself haptics: Part i. *IEEE Robotics & Automation Magazine*, 14(4):88–104. 41
- Hendrix, R. (2011). *Robotically assisted eye surgery: A haptic master console*. PhD thesis, Technische Universiteit Eindhoven, Eindhoven. 11, 14, 16, 165
- Imrhan, S. (1991). The influence of wrist position on different types of pinch strength. *Applied Ergonomics*, 22(6):379–384. 107
- Ino, S., Shimizu, S., Odagawa, T., Sato, M., Takahashi, M., Izumi, T., and Ifukube, T. (1993). A tactile display for presenting quality of materials by changing the temperature of skin surface. In *2nd IEEE International Workshop on Robot and Human Communication*,

- pages 220–224. [22](#)
- Intuitive Surgical Inc. (2010). website: <http://www.intuitivesurgical.com/>. [4](#), [9](#), [10](#), [15](#), [89](#), [93](#), [98](#), [165](#)
- Iwamoto, H., Osaki, H., and Sheki, S. (1993). The technical skill in suturing: An analysis of the actual suture tracks. *Surgery Today*, (23):800–806. [37](#), [39](#), [45](#), [46](#), [166](#)
- Jandura, L. and Srinivasan, M. (1994). Experiments on human performance in torque discrimination and control. *Dynamic Systems and Control, ASME, DSC-55*, 1:369–375. [26](#)
- Jansen, S., Vicki Kocian, C., and Pinkerton, J. (2003). Measurement of maximum voluntary pinch strength:: Effects of forearm position and outcome score. *Journal of Hand Therapy*, 16(4):326–336. [107](#)
- Jet Propulsion Laboratory (JPL), NASA (2011). Rams robot system description: <http://www-robotics.jpl.nasa.gov>. [15](#)
- Jones, D. (2002). The 7±2 urban legend. In University, T. P. S., editor, *MISRA C 2002 conference www.knosof.co.uk/cbook/misart.pdf*, pages 1–7, Pennsylvania. The College of Information Sciences and Technology. Citeseerx. [76](#)
- Jones, L. (2000). Kinesthetic sensing. In *in Human and Machine Haptics*. Citeseer. [27](#)
- Jones, L. and Hunter, I. (1990). Influence of the mechanical properties of a manipulandum on human operator dynamics. *Biological cybernetics*, 62(4):299–307. [27](#)
- Jourdan, I., Dutson, E., Garcia, A., Vleugels, T., Leroy, J., Mutter, D., and Marescaux, J. (2004). Stereoscopic vision provides a significant advantage for precision robotic laparoscopy. *British journal of surgery*, 91(7):879–885. [103](#)
- Kataoka, H., Washio, T., Chinzei, K., Mizuhara, K., Simone, C., and Okamura, A. (2002). Measurement of the tip and friction force acting on a needle during penetration. In Dohi, T. and R Kikinis, E., editors, *In MICCAI, 2002*, volume 2488, pages 216–223, London UK. Springer Verlag. [43](#)
- Kim, Y., Oakley, I., and Ryu, J. (2006). Design and psychophysical evaluation of pneumatic tactile display. In *SICE-ICASE, 2006. International Joint Conference*, pages 1933–1938. [59](#)
- King, C., Culjat, M., Franco, M., Bisley, J., Dutson, E., and Grundfest, W. (2008a). Optimization of a pneumatic balloon tactile display for robotic surgery based on human perception. *IEEE Transactions of Biomedical Engineering*. [58](#), [61](#), [64](#)
- King, C., Culjat, M., Franco, M., Lewis, C., Dutson, E., Grundfest, W., and Bisley, J. (2009). Tactile feedback induces reduced grasping force in robot-assisted surgery. *IEEE Transactions on Haptics*, 2(2):103–110. [21](#), [57](#), [58](#), [165](#)
- King, C., Franco, M., Culjat, M., Bisley, J., Dutson, E., and Grundfest, W. (2008b). Fabrication and characterization of a balloon actuator array for haptic feedback in robotic surgery. *ASME Journal of Medical Devices*. [59](#)

- Kitagawa, M., Dokko, D., Okamura, A., and Yuh, D. (2005a). Effect of sensory substitution on suture-manipulation forces for robotic surgical systems. *Journal of Thoracic and Cardiovascular Surgery*, 129(1):151–158. [5](#), [37](#)
- Kitagawa, M., Dokko, D., Okamura, A., and Yuh, D. (2005b). Effect of sensory substitution on suture-manipulation forces for robotic surgical systems. *Journal of Thoracic and Cardiovascular Surgery*, 129(1):151–158. [20](#), [69](#)
- Klaiber, C., Metzger, A., Petelin, J., and König, W. (1993). *Manual of laparoscopic surgery*. Hogrefe & Huber. [2](#), [165](#)
- Klein, D., Freimuth, H., Monkman, G., Egersdörfer, S., Meier, A., Böse, H., Baumann, M., Ermert, H., and Bruhns, O. (2005). Electrorheological tactel elements. *Mechatronics*, 15(7):883–897. [58](#)
- Konyo, M., Yamada, H., Okamoto, S., and Tadokoro, S. (2008). Alternative display of friction represented by tactile stimulation without tangential force. *Haptics: Perception, Devices and Scenarios*, pages 619–629. [20](#)
- Kunesch, E., Binkofski, F., and Freund, H. (1989). Invariant temporal characteristics of manipulative hand movements. *Experimental Brain Research*, 78(3):539–546. [27](#)
- Kwoh, Y., Hou, J., Jonckheere, E., and Hayati, S. (1988). A robot with improved absolute positioning accuracy for ct guided stereotactic brain surgery. *Biomedical Engineering, IEEE Transactions on*, 35(2):153–160. [9](#)
- Lawrence, D., Pao, L., Salada, M., and Dougherty, A. (1996). Quantitative experimental analysis of transparency and stability in haptic interfaces. 58:441–449. [28](#)
- Lawson, E., Curet, M., Sanchez, B., Schuster, R., and Berguer, R. (2007). Postural ergonomics during robotic and laparoscopic gastric bypass surgery: a pilot project. *Journal of Robotic Surgery*, 1(1):61–67. [3](#), [4](#), [87](#), [96](#), [97](#)
- Lawther, R., Kirk, G., and Regan, M. (2002). Laparoscopic procedures are associated with a significant risk of digital nerve injury for general surgeons. *Annals of The Royal College of Surgeons of England*, 84(6):443. [4](#), [87](#)
- Lécuyer, A. (2009). Simulating haptic feedback using vision: A survey of research and applications of pseudo-haptic feedback. *Presence: Teleoperators and Virtual Environments*, 18(1):39–53. [20](#)
- Lee, E., Rafiq, A., Merrell, R., Ackerman, R., and Dennerlein, J. (2005). Ergonomics and human factors in endoscopic surgery: a comparison of manual vs telerobotic simulation systems. *Surgical endoscopy*, 19(8):1064–1070. [3](#)
- Lee, J., Hwang, I., Kim, K., Choi, S., Chung, W. K., and Kim, Y. S. (2009). Cooperative robotic assistant with drill-by-wire end-effector for spinal fusion surgery. *Industrial Robot-An International Journal*, 36(1):60–72. [31](#)
- Lehman, A., Dumpert, J., Wood, N., Redden, L., Visty, A., Farritor, S., Varnell, B., and Oleynikov, D. (2009). Natural orifice cholecystectomy using a miniature robot. *Surgical*

- endoscopy*, 23(2):260–266. [13](#), [16](#)
- Leist, A., Freund, H., and Cohen, B. (1987). Comparative characteristics of predictive eye-hand tracking. *Human neurobiology*. [26](#)
- Leung, R., MacLean, K., Bertelsen, M., and Saubhasik, M. (2007). Evaluation of haptically augmented touchscreen gui elements under cognitive load. In *Proceedings of the 9th international conference on Multimodal interfaces*, pages 374–381. ACM. [5](#)
- Loomis, J. (1993). Understanding synthetic experience must begin with the analysis of ordinary perceptual experience. In *Virtual Reality, 1993. Proceedings., IEEE 1993 Symposium on Research Frontiers in*, pages 54–57. [5](#)
- Lum, M., Friedman, D., Sankaranarayanan, G., King, H., Fodero, K., Leuschke, R., Hanaford, B., Rosen, J., and Sinanan, M. (2009). The raven: Design and validation of a telesurgery system. *The International Journal of Robotics Research*, 28(9):1183–1197. [12](#), [14](#), [16](#), [165](#)
- Lux, M., Marshall, M., Erturk, E., and Joseph, J. (2010). Ergonomic evaluation and guidelines for use of the davinci robot system. *Journal of Endourology*, 24(3):371–375. [97](#)
- MacKenzie, I. and Buxton, W. (1992). Extending fitts’ law to two-dimensional tasks. In *Proceedings of the SIGCHI conference on Human factors in computing systems*, page 226. ACM. [34](#)
- Madhani, A., Niemeyer, G., and Salisbury Jr, J. (1998). The black falcon: a teleoperated surgical instrument for minimally invasive surgery. In *IEEE/RSJ International Conference on Intelligent Robots and Systems, IROS*, volume 2, pages 936–944. [112](#)
- Maeder, T., Fahrny, V., Stauss, S., Corradini, G., and Ryser, P. (2005). Design and characterisation of low-cost thick-film piezoresistive force sensors for the 100 mn to 100 n range. In *Proc. XXIX IMAPS Poland Chapter Conf., Koszalin, Poland*, pages 429–34. [120](#)
- Mahvash, M. and Hayward, V. (2001). Haptic rendering of cutting: A fracture mechanics approach. *The Electronic Journal of Haptics Research, Haptics-e*, 2(3):1–12. [35](#)
- Mahvash, M. and Hayward, V. (2005). High-fidelity passive force-reflecting virtual environments. *IEEE Transactions on Robotics*, 21(1):38–46. [36](#)
- Massie, T. H. and Salisbury, J. K. (1994). The phantom haptic interface: A device for probing virtual objects. In Cole, K. D., editor, *Proceedings of the ASME winter annual meeting.*, volume 55-1 of *Proceedings of the 1994 International Mechanical Engineering Congress and Exposition*, pages 259–299, New York, NY, USA. ASME. [112](#)
- Matern, U. and Waller, P. (1999). Instruments for minimally invasive surgery. *Surgical endoscopy*, 13(2):174–182. [4](#), [87](#)
- Mathiowetz, V., Kashman, N., Volland, G., Weber, K., Dowe, M., and Rogers, S. (1985). Grip and pinch strength: normative data for adults. *Archives of Physical Medicine and Rehabilitation*, 66(2):69. [27](#), [109](#)

- Mattern, U. and Weller, P. (1996). Medizinische handhabungsg erat,international patent specification. pct/de1995/001176. [89](#), [93](#), [100](#)
- Mauger, D. and Kauffman Jr, G. (2001). Statistical analysis. *Surgical research*, page 71. [89](#)
- McMahan, W., Gewirtz, J., Dorsey Standish, P., Kunkel, J., Lilavois, M., Wedmid, A., Lee, D., and Kuchenbecker, K. (2011a). Tool contact acceleration feedback for telerobotic surgery. *IEEE Transactions on Haptics*. [22](#), [165](#)
- McMahan, W., Gewirtz, J., Standish, D., Martin, P., Kunkel, J., Lilavois, M., Wedmid, A., Lee, D., and Kuchenbecker, K. (2011b). Verrotouch: Vibrotactile feedback for robotic minimally invasive surgery. *The Journal of Urology*, 185(4):373–373. [22](#)
- Meenink, H. M. (2011). *Vitreo-retinal eye surgery robot: sustainable precision*. PhD thesis., PhD thesis, Technische Universiteit Eindhoven, Eindhoven. [11](#), [13](#), [14](#), [16](#), [165](#)
- Mimic Technologies (2011). website: www.mimic.ws. [17](#), [18](#), [165](#)
- Moy, G., Wagner, C., and Fearing, R. (2000). A compliant tactile display for teletaction. In *IEEE International Conference on Robotics and Automation, ICRA*, volume 4, pages 3409–3415. Citeseer. [58](#)
- Munz, Y., Moorthy, K., Dosis, A., Hernandez, J., Bann, S., Bello, F., Martin, S., Darzi, A., and Rockall, T. (2004). The benefits of stereoscopic vision in robotic-assisted performance on bench models. *Surgical endoscopy*, 18(4):611–616. [103](#)
- Napier, J. (1956). The prehensile movements of the human hand. *Journal of Bone and Joint Surgery*, 38(4):902–913. [89](#), [113](#)
- NASA (1995). *Man-Systems Integration Standards, (NASA-STD-3000 Rev. B)*. NASA. [101](#), [104](#)
- Neilson, P. (1972). Speed of response or bandwidth of voluntary system controlling elbow position in intact man. *Medical and Biological Engineering and Computing*, 10(4):450–459. [27](#)
- Neuroarm Project (2008). website: <http://www.neuroarm.org/project/>. [10](#)
- Ng, J., Man, J., Fels, S., Dumont, G., and Ansermino, J. (2005). An evaluation of a vibro-tactile display prototype for physiological monitoring. *Anesthesia & Analgesia*, 101(6):1719. [103](#)
- Nguyen, N., Ho, H., Smith, W., Philipps, C., Lewis, C., De Vera, R., Berguer, R., and JONES, D. (2001). An ergonomic evaluation of surgeons’ axial skeletal and upper extremity movements during laparoscopic and open surgery. *The American journal of surgery*, 182(6):720–724. [4](#), [87](#), [96](#)
- Nio, D., Bemelman, W., Boer, K., Dunker, M., Gouma, D., and Gulik, T. (2002). Efficiency of manual versus robotical (zeus) assisted laparoscopic surgery in the performance of standardized tasks. *Surgical endoscopy*, 16(3):412–415. [37](#)
- Nio, D., Bemelman, W., Busch, O., Vrouenraets, B., and Gouma, D. (2004). Robot-assisted

- laparoscopic cholecystectomy versus conventional laparoscopic cholecystectomy: a comparative study. *Surgical endoscopy*, 18(3):379–382. 97
- Novare (2010). website: <http://www.novaresurgical.com>. 89, 93, 100
- O’Hara, J., Brown, W., Lewis, P., and Persensky, J. (2002). *Human-System Interface Design Review Guidelines (NUREG-0700 rev.2)*. Energy Sciences and Technology Department. Brookhaven National Laboratory, Office of Nuclear Regulatory Research, U.S. Nuclear Regulatory Commission, Washington, DC. 101, 102, 103, 105, 167
- Okamura, A. M., Simone, C., and O’Leary, M. (2004). Force modeling for needle insertion into soft tissue. *IEEE transactions on biomedical engineering*, 51(10):1707–1716. 35, 38, 39, 42, 43, 45
- Ottermo, M., Stavdahl, O., and Johansen, T. (2004). Palpation instrument for augmented minimally invasive surgery. In *IEEE/RSJ International Conference on Intelligent Robots and Systems, IROS*, pages 3960–3964. 58
- Ottermo, M., Stavdahl, Ø., and Johansen, T. (2008). Design and performance of a prototype tactile shape display for minimally invasive surgery. *The Electronic Journal of Haptics Research, Haptics-e*, 4. 21, 57, 165
- Pang, X., Tan, H., and Durlach, N. (1991). Manual discrimination of force using active finger motion. *Attention, Perception, & Psychophysics*, 49(6):531–540. 26
- Pasquero, J., Lévesque, V., Hayward, V., and Legault, M. (2004). Display of virtual braille dots by lateral skin deformation: A pilot study. In *Proceedings of The 4th European Conference on Haptics*, pages 96–103. Citeseer. 58
- Pavani, F., Spence, C., and Driver, J. (2000). Visual capture of touch: Out-of-the-body experiences with rubber gloves. *Psychological Science*, 11(5):353–359. 32
- Pheasant, S. and Haslegrave, C. (2006). *Bodyspace: anthropometry, ergonomics, and the design of work*. CRC Press. 26, 38, 101, 104, 105, 108, 109, 167
- Quanser (2011). website: <http://www.quanser.com/>. 10, 15
- Rados, C. (2003). FDA works to reduce preventable medical device injuries. *FDA consumer*, 37(4):28–34. 4
- Riva, G., Davide, F., and IJsselsteijn, W. (2003). Measuring presence: Subjective, behavioral and physiological methods. *Being there: Concepts, effects and measurement of user presence in synthetic environments*, pages 110–118. 31
- Robles-De-La-Torre, G. and Hayward, V. (2001). Force can overcome object geometry in the perception of shape through active touch. *Nature*, 412(6845):445–448. 26
- Rock, I. and Victor, J. (1964). Vision and touch: An experimentally created conflict between the two senses. *Science*, 143(3606):594. 75
- Ruurda, J., Visser, P., and Broeders, I. (2003). Analysis of procedure time in robot-assisted surgery: comparative study in laparoscopic cholecystectomy. *Computer aided surgery*,

- 8(1):24–29. 97
- RWOLF (2010). website: <http://www.richardwolfusa.com>. 89, 93, 100
- Safwat, B., Su, E., Gassert, R., Teo, C., and Burdet, E. (2009). The role of posture, magnification, and grip force on microscopic accuracy. *Annals of biomedical engineering*, 37(5):997–1006. 27, 102
- Samur, E. (2010). *Systematic Evaluation Methodology and Performance Metrics for Haptic Interfaces*. PhD thesis, EPFL, Switzerland. 30, 32, 132
- Samur, E., Sedef, M., Basdogan, C., Avtan, L., and Duzgun, O. (2007a). A robotic indenter for minimally invasive measurement and characterization of soft tissue response. *Medical Image Analysis*, 11(4):361–373. 38
- Samur, E., Wang, F., Spaelter, U., and Bleuler, H. (2007b). Generic and systematic evaluation of haptic interfaces based on testbeds. In *IEEE/RSJ International Conference on Intelligent Robots and Systems, IROS.*, pages 2113–2119. 32, 34, 35, 126
- Sanders, A. (1998). *Elements of Human Performance: Reaction Processes and Attention in Human Skill*. Lawrence Erlbaum, New Jersey. 75
- Sanders, M., McCormick, E., and McCormick, E. (1993). *Human factors in engineering and design*. McGraw-Hill. 108
- Santos-Carreras, L., Beira, R., Sengül, A., Gassert, R., and Bleuler, H. (2010a). Influence of force and torque feedback on operator performance in a VR-based suturing task. *Applied Bionics and Biomechanics*, 7(3):217–230. 38
- Santos-Carreras, L., Hagen, M., Gassert, R., and Bleuler, H. (2011). Survey on surgical instrument handle design: Ergonomics and acceptance. *Surgical Innovation*. 88
- Santos-Carreras, L., Leuenberger, K., Re tornaz, P., Gassert, R., and Bleuler, H. (2010b). Design and psychophysical evaluation of a tactile pulse display for teleoperated artery palpation. In *IEEE/RSJ International Conference on Intelligent Robots and Systems, IROS.*, pages 5060–5066. IEEE. 58
- Satyanarayana, S., Karnik, R., and Majumdar, A. (2005). Stamp-and-stick room-temperature bonding technique for microdevices. *Journal of Microelectromechanical Systems*, 14(2):392–399. 59
- Schostek, S., Ho, C., Kalanovic, D., and Schurr, M. (2006). Artificial tactile sensing in minimally invasive surgery—a new technical approach. *Minimally Invasive Therapy & Allied Technologies*, 15(5):296–304. 20, 21, 69, 70, 82, 165
- Seibold, U., Kuebler, B., and Hirzinger, G. (2008). Prototypic force feedback instrument for minimally invasive robotic surgery. *Medical robotics. I-Tech Education and Publishing, Vienna*, pages 377–400. 30
- Seki, S. (1987). Accuracy of suture techniques of surgeons with different surgical experience. *Japanese journal of surgery*, 17(6):465/469. 45, 46

- Seki, S. (1988). Techniques for better suturing. *Br J Surg*, 75(12):1181–1184. 37
- Semere, W., Kitagawa, M., and Okamura, A. M. (2004). Teleoperation with sensor/actuator asymmetry: Task performance with partial force feedback. In *HAPTICS*, pages 121–127. 31, 69
- Sengupta, A. K. and Das, B. (2004). Determination of worker physiological cost in workspace reach envelopes. *Ergonomics*, 47(3):330–342. 104
- Sensible Technologies (2011). website: <http://www.sensible.com>. 12, 16, 17, 19, 112, 165
- Shadmehr, R. and Mussa-Ivaldi, F. (1994). Adaptive representation of dynamics during learning of a motor task. *Journal of Neuroscience*, 14(5):3208. 51
- Sheridan, T. (1992). Musings on telepresence and virtual presence. *Presence: Teleoperators and virtual environments*, 1(1):120–126. 5
- Shivers, C., Mirka, G., and Kaber, D. (2002). Effect of grip span on lateral pinch grip strength. *Human Factors: The Journal of the Human Factors and Ergonomics Society*, 44(4):569. 107
- Simone, C. and Okamura, A. (2002). Modeling of needle insertion forces for robot-assisted percutaneous therapy. In *IEEE International Conference on Robotics and Automation, ICRA*, volume 2, pages 2085–2091, Washington, DC, USA. 42
- Solis, J., Oshima, N., Ishii, H., Matsuoka, N., Hatake, K., and Takanishi, A. (2008). Towards understanding the suture/ligature skills during the training process using wks-2rii. *International Journal of Computer Assisted Radiology and Surgery*, 3(3):231–239. 45, 46
- Spence, C., Pavani, F., and Driver, J. (2004). Spatial constraints on visual-tactile cross-modal distractor congruency effects. *Cognitive, Affective, & Behavioral Neuroscience*, 4(2):148–169. 32
- Srinivasan, M. and Chen, J. (1993). Human performance in controlling normal forces of contact with rigid objects. *ASME DYN SYST CONTROL DIV PUBL DSC, ASME, NEW YORK, NY,(USA), 1993,*, 49:119–125. 27
- Stevens, J. and Patterson, M. (1995). Dimensions of spatial acuity in the touch sense: changes over the life span. *Somatosensory and Motor Research*, 12(1):29–47. 66
- Sutherland, G., McBeth, P., and Louw, D. (2003). Neuroarm: an MR compatible robot for microsurgery. In *International Congress Series*, volume 1256, pages 504–508. Elsevier. 11, 12, 15, 165
- Swanson, A., Matev, I., and De Groot, G. (1970). The strength of the hand. *Bulletin of Prosthetics Research*, 10(14):145–153. 27, 109
- Tadano, K. and Kawashima, K. (2007). Development of a master slave system with force sensing using pneumatic servo system for laparoscopic surgery. In *IEEE International Conference on Robotics and Automation, ICRA*, pages 947–952. 112
- Takahashi, H., Yonemura, T., Sugita, N., Mitsuishi, M., Sora, S., Morita, A., and Mochizuki,

- R. (2008). Master manipulator with higher operability designed for micro neuro surgical system. In *IEEE International Conference on Robotics and Automation, ICRA*, pages 3902–3907. 105, 112
- Talasaz, A., Patel, R., and Naish, M. (2010). Haptics-enabled teleoperation for robot-assisted tumor localization. In *IEEE International Conference on Robotics and Automation, ICRA*, pages 5340–5345, Alaska. 35, 70, 82
- Tan, H. (1997). Identification of sphere size using the phantom: Towards a set of building blocks for rendering haptic environment. In *Proceedings of the 6th International Symposium on Haptic Interfaces for Virtual Environment and Teleoperator Systems*, volume 61, pages 197–203, Dallas. 32, 33, 77
- Tan, H., Durlach, N., Reed, C., and Rabinowitz, W. (1999). Information transmission with a multifinger tactual display. *Attention, Perception, & Psychophysics*, 61(6):993–1008. 26, 27
- Tan, H., Reed, C., Durlach, N., Haptics, K., and Lafayette, W. (2010). Optimum information-transfer rates for communication through haptic and other sensory modalities (pdf). *IEEE Transactions on Haptics*, 3(2):98–108. 32
- Tan, H., Srinivasan, M., Eberman, B., and Cheng, B. (1994). Human factors for the design of force-reflecting haptic interfaces. *Dynamic Systems and Control*, 55(1):353–359. 26, 27
- Tan, H., Srinivasan, M., Reed, C., and Durlach, N. (2007). Discrimination and identification of finger joint-angle position using active motion. *ACM Transactions on Applied Perception (TAP)*, 4(2):10. 76
- Titan Medical Inc. (2011). website: <http://www.titanmedicalinc.com>. 10, 12, 15, 165
- Tobergte, A., Helmer, P., Hagn, U., Rouiller, P., Thielmann, S., Grange, S., Albu-Schaffer, A., Conti, F., and Hirzinger, G. (2011). The sigma. 7 haptic interface for mirosurge: A new bi-manual surgical console. In *IEEE/RSJ International Conference on Intelligent Robots and Systems, IROS*, pages 3023–3030. 112
- Toffin, D., Reymond, G., Kemeny, A., and Droulez, J. (2007). Role of steering wheel feedback on driver performance: driving simulator and modeling analysis. *Vehicle System Dynamics*, 45(4):375–388. 31
- Trejos, A., Jayender, J., Perri, M., Naish, M., Patel, R., and Malthaner, R. (2009). Robot-assisted tactile sensing for minimally invasive tumor localization. *The International Journal of Robotics Research*, 28(9):1118. 20, 35, 70, 82, 165
- Unger, B., Nicolaidis, A., Berkelman, P., Thompson, A., Klatzky, R., and Hollis, R. (2001). Comparison of 3-d haptic peg-in-hole tasks in real and virtual environments. In *IEEE/RSJ International Conference on Intelligent Robots and Systems, IROS*, volume 3, pages 1751–1756. 126
- US Department of Defense (2000). *Human Engineering Design Criteria for Military Systems, Equipment and Facilities (MIL-STD 1472F)*. Washington, D.C. 102

- Van Beers, R., Sittig, A., and Denier van der Gon, J. (1998). The precision of proprioceptive position sense. *Experimental Brain Research*, 122(4):367–377. [26](#)
- van den Bedem, L. (2010). *Realization of a demonstrator slave for robotic minimally invasive surgery. PhD thesis.*. PhD thesis, Technische Universiteit Eindhoven,, Eindhoven. [11](#), [13](#), [165](#)
- Van Veelen, M., Nederlof, E., Goossens, R., Schot, C., and Jakimowicz, J. (2003). Ergonomic problems encountered by the medical team related to products used for minimally invasive surgery. *Surgical endoscopy*, 17(7):1077–1081. [3](#)
- Verner, L. N. and Okamura, A. M. (2007). Effects of translational and gripping force feedback are decoupled in a 4-degree-of-freedom telemanipulator. In Iwata, H., editor, *WHC'07: World Haptics Conference.*, number 0-7695-2738-8, pages 286–291, Tsukuba, Japan. [31](#)
- Verner, L. N. and Okamura, A. M. (2009). Force and torque feedback vs force only feedback. In O'Malley, M. and Ernst, M., editors, *WHC '09: Proceedings of the World Haptics.*, number 978-1-4244-3858-7, pages 406–410, Salt Lake city, UT, USA. [31](#)
- Wagner, C., Stylopoulos, N., Jackson, P., and Howe, R. (2007). The benefit of force feedback in surgery: Examination of blunt dissection. *Presence: teleoperators and virtual environments*, 16(3):252–262. [69](#)
- Wall, S. and Harwin, W. (2000). Quantification of the effects of haptic feedback during a motor skills task in a simulated environment. In *Proc. Second PHANTOM users research symposium*. Citeseer. [32](#), [34](#)
- Wang, F. (2009). *VR simulation of interventional radiology and microsurgery*. PhD thesis, EPFL, Switzerland. [36](#)
- Wang, Q. and Hayward, V. (2010). Biomechanically optimized distributed tactile transducer based on lateral skin deformation. *The International Journal of Robotics Research*, 29(4):323–335. [58](#)
- Wauben, L., Van Veelen, M., Gossot, D., and Goossens, R. (2006). Application of ergonomic guidelines during minimally invasive surgery: a questionnaire survey of 284 surgeons. *Surgical endoscopy*, 20(8):1268–1274. [3](#)
- Wiker, S., Hershkowitz, E., and Zik, J. (1989). Teleoperator comfort and psychometric stability: Criteria for limiting master-controller forces of operation and feedback during telemanipulation. In *JPL, California Inst. of Tech, Proceedings of the NASA Conference on Space Telerobotics.*, volume 1. [109](#)
- Winfield, L., Glassmire, J., Colgate, J., and Peshkin, M. (2007). T-pad: Tactile pattern display through variable friction reduction. *World Haptics*, pages 421–426. [58](#)
- Xu, P., Jingjun, Y., and Guanghua, B. (2007). Enumeration and type synthesis of one-dof remote-center-of-motion mechanisms. In *The 12th world congress in mechanism an machine science, June*, pages 18–21. [114](#)
- Yamamoto, A., Cros, B., Hashimoto, H., and Higuchi, T. (2004). Control of thermal tactile

- display based on prediction of contact temperature. In *IEEE International Conference on Robotics and Automation, ICRA*, volume 2, pages 1536–1541. [22](#)
- Yamamoto, T., Vagvolgyi, B., Balaji, K., Whitcomb, L., and Okamura, A. (2009). Tissue property estimation and graphical display for teleoperated robot-assisted surgery. In *IEEE International Conference on Robotics and Automation, ICRA*, pages 4239–4245, Kobe, Japan. IEEE. [20](#), [69](#), [70](#), [82](#), [165](#)
- Yoshikawa, T. (1985). Manipulability of robotic mechanisms. *The international journal of Robotics Research*, 4(2):3–9. [29](#)
- Yuh-Chuan Shih, Y.-C. O. (2005). Influences of span and wrist posture on peak chuck pinch strength and time needed to reach peak strength. *International Journal of Industrial Ergonomics*, (35):527–536. [107](#)
- Zhai, S., Kong, J., and Ren, X. (2004). Speed-accuracy tradeoff in fitts' law tasks—on the equivalency of actual and nominal pointing precision. *International Journal of Human-Computer Studies*, 61(6):823–856. [34](#)
- Zheng, B., Cassera, M., Martinec, D., Spaun, G., and Swanstr
"om, L. (2010). Measuring mental workload during the performance of advanced laparoscopic tasks. *Surgical endoscopy*, 24(1):45–50. [4](#), [87](#)
- Zimmerli, L., Krewer, C., Gassert, R., Müller, F., Riener, R., and Lünenburger, L. (2012). Validation of a mechanism to balance exercise difficulty in robot-assisted upper-extremity rehabilitation after stroke. *Journal of NeuroEngineering and Rehabilitation*, 9(1):6. [34](#)
- Zopf, R., Savage, G., and Williams, M. (2010). Crossmodal congruency measures of lateral distance effects on the rubber hand illusion. *Neuropsychologia*, 48(3):713–725. [32](#)

Glossary

capstan or cable drive this transmission system is composed by a rotating cylinder (also called capstan) and a rope or cable. The cylinder winds the cable around it to transmit the movement. This type of mechanical transmission offers several advantages such as high stiffness to weight ratio, high strength, low friction, and absence of backlash, which makes them suitable for challenging mechanical applications. Furthermore, they can properly operate even with modest manufacturing and assembly tolerances.

dexterity is the ability of a manipulator to move and apply forces and torques in arbitrary directions. Definition from “Performance evaluation and design criteria. In Springer Handbook of Robotics”, pages 229-244. B. J. Angeles and F. C. Park. Springer, 2008.

direct drive type of transmission in which the actuator is connected directly to the load without a torque amplifying mechanism. Advantages are simplicity and the absence of the backlash or friction present in most transmissions.

friction drive this type of transmission by contact friction offers smooth operations with almost none ripple nor backlash. The components of the transmission have to be maintained in contact by a preloading mechanism, which generally consist in a spring. This type of transmission has to be carefully design with very small tolerances to guarantee the desired force range with no slip.

Greenhouse Geisser sphericity correction An approach to deal with violations of sphericity is to apply an adjustment to the standard ANOVA. The most well known adjustment methods are the Greenhouse-Geisser correction and the Huynh-Feldt correction. Both work roughly in the same way. They adjust the degrees of freedom in the ANOVA in order to produce a more accurate significance (p) value. If sphericity is violated the p values need to be adjusted upwards (and this can be accomplished by adjusting the degrees of freedom downwards). In practice both adjustment methods produce similar corrections but the Greenhouse Geisser sphericity correction is more conservative.

haptic feedback The term “haptics” comes from the greek haptikos, from haptesthai, to grasp, to touch. This adjective means: Of or relating to the sense of touch. Haptic

feedback is generally used to define human-interface devices that can render tactile information to the user. Whereas haptic feedback refers to both force (or kinesthetic) and tactile feedback, it is conventionally used to define devices that provide force feedback alone.

Mauchley sphericity test Sphericity is a mathematical assumption in repeated measures ANOVA designs. The sphericity assumption means that the all the variances of the differences are equal (in the population sampled). Thus, the results from ANOVAs violating this assumption can not be trusted. The Mauchley sphericity test checks if this violation is significant or can be neglected.

telepresence is the experience of being there at the remote site or in the location of the slave robot.

transparency is a term used in teleoperation to quantify the fidelity with which the physical properties of the distal or virtual objects are rendered to the user.

Acronyms

AIP Absolute Identification Paradigm.

ANOVA Analysis of Variance.

BPM Beats Per Minute.

CCE Cross-modal Congruency Effect.

CPT Counts Per Turn.

CRE Convenient Reach Envelope.

DLR German Aerospace Research Establishment.

DOF Degree(s) Of Freedom.

EEG Electroencephalography.

EMG electromyography.

EPFL École Polytechnique Fédérale de Lausanne.

FDA Food and Drug Administration.

FFT Fast Fourier Transform.

HMI Human Machine Interface.

ID Index of Difficulty.

IOM Institute Of Medicine.

IP Index of Performance.

IT Information Transfer.

JND Just Noticeable Difference.

MIS Minimally Invasive Surgery.

MRI Magnetic Resonance Imaging.

MT Movement Time.

MVC Maximum Voluntary Contraction.

NASA US National Aeronautics and Space Administration.

NOTES Natural Orifice Translumenal Endoscopic Surgery.

NUREG US Nuclear Regulatory Commission.

NWA Normal Working Area.

OR Operating Room.

PCB Printed Circuit Board.

PDMS Polydimethylsiloxane.

PID Proportional Integral Derivative.

PWM Pulse Width Modulation.

RCM Remote Center of Motion.

RMS Root Mean Square.

SCARA Selective Compliance Assembly Robot Arm.

SILS Single Incision Laparoscopic Surgery.

TU/e Technische Universiteit Eindhoven.

UART Universal Asynchronous Receiver Transmitter.

UDP User Datagram Protocol.

USB Universal Serial Bus.

VR Virtual Reality.

List of Figures

1.1	Open surgery (image from MD Web)	2
1.2	Fulcrum effect as described in Klaiber et al. (1993) and laparoscopic surgery (Image from Ever Green Surgical)	2
1.3	SILS instruments (image from UFirstHealth Web) and NOTES device (Transport Multi-lumen Operating Platform image from USGI Medical Inc.)	3
1.4	Da Vinci Surgical system (Intuitive Surgical Inc., 2010)	4
2.1	Components of the da Vinci Surgical System: from left to right, the master console; handles and instruments; and the slave robot. (Intuitive Surgical Inc., 2010)	10
2.2	Sensei Robotic Catheter (Hansen Medical Inc., 2011)	11
2.3	Amadeus Composer Robotic System (Titan Medical Inc., 2011)	12
2.4	NeuroArm project (Sutherland et al., 2003)	12
2.5	Miro Surge system from DLR (Hagn et al., 2010)	13
2.6	Sophie-robot from TU/e (van den Bedem, 2010 ; Meenink, 2011)	13
2.7	Eye-robot from TU/e (Hendrix, 2011)	14
2.8	Robot for endonasal surgery from Vanderbilt University (Burgner et al., 2011)	14
2.9	RAVEN: open source surgical robot (Lum et al., 2009)	14
2.10	Phantom Premium 1.5/6 DOF from Sensable Technologies (2011) , omega.3 and omega.7 haptic devices from Force Dimension (2011)	17
2.11	dV-Trainer (Mimic Technologies, 2011) and Maglev 200 haptic device (Butterfly Haptics, LLC, 2010)	18
2.12	The Virtuouse 6D40-40 and the Inca 6D haptic devices (Haption SA, 2011)	18
2.13	Examples of visual sensory substitution (Yamamoto et al., 2009 ; Trejos et al., 2009 ; Schostek et al., 2006)	20
2.14	Tactile displays for MIS surgery (Ottermo et al., 2008 ; King et al., 2009)	21
2.15	The VerroTouch system (McMahan et al., 2011a)	22
3.1	Motor task associated to Fitts law	34
4.1	Wrist rotation around the axis of the forearm during needle insertion (pronosupination)	38
4.2	Hardware experimental setup for the suturing experiment	39

4.3	Virtual suturing testbed	41
4.4	Simulation of the needle insertion	41
4.5	Control scheme of the overall experimental setup.	42
4.6	One-DOF needle insertion phases	43
4.7	Customized omega.7 device used in the experiment and VR testbed.	43
4.8	Force interaction model	44
4.9	Interaction forces and needle tip position along each axis for a suturing trial . .	46
4.10	Optimal insertion of an arc-shaped-needle and real suture tracks recorded on X-ray film by Iwamoto et al. (1993)	46
4.11	Needle position	47
4.12	Mean values (1 st configuration)	49
4.13	Results per subject and for each feedback type (1 st configuration)	50
4.14	Mean values (2 nd configuration)	51
4.15	Results per subject and for each feedback type (2 nd configuration)	51
4.16	Normalized distributions of <i>exit point error</i> and <i>task-completion time</i>	52
4.17	Questionnaire statistics	54
5.1	Balloon arrangement and tactile pulse display	59
5.2	Pulse display electronic board	60
5.3	Pressure output with respect to the PWM signal sent to the valve	61
5.4	Balloon deformation deformation plotted against input pneumatic pressure . .	61
5.5	Pressure output bandwidth for different filters	62
5.6	Radial artery pressure profile and proposed simplification	63
5.7	Magnitude estimation as a function of balloon pressure on the tactile display.	64
5.8	Experimental protocol for pattern identification experiment.	65
5.9	Mean values of answer correctness of pattern identification and number of pulses per answer	66
5.10	Omega.3 device customized with a thimble integrating the tactile pulse display.	68
5.11	Components of the VR-based testbed and pulse rendering	69
5.12	Experimental setup	71
5.13	Difficulty levels of the exploration task experiment	72
5.14	Experimental protocol for the exploration task	73
5.15	Average task-completion times for the exploration task	74
5.16	Global average values per feedback type	75
5.17	Virtual testbed to assess the effect of the feedback type on users' performance identifying the orientation of the hidden artery	77
5.18	Experimental protocol for the identification task	78
5.19	Average task-completion times for the identification task	79
5.20	Questionnaire statistics	81
6.1	Handles evaluated in the survey	89
6.2	Surgeons' country of practice	91
6.3	Body parts where the surgeons felt discomfort during or after surgery	91
6.4	Score for each handle in terms of: intuitiveness, comfort, precision and stability	93

6.5	Number of votes per handle	95
6.6	Regression model: handle preference as a function of comfort and precision	96
6.7	Percentage of surgeons who voted each handle separated by background	97
7.1	Vertical arrangement of the displays in a workstation (O'Hara et al., 2002)	103
7.2	Convenient Reach Envelope (CRE) and Normal Working Area (NWA)	104
7.3	NWA construction for different body dimensions	106
7.4	Surgeon's console developed at the Imperial College London	107
7.5	Wrist mobility ranges for the 50 th % ^{ile} of population (Pheasant and Haslegrave, 2006)	108
8.1	Double-parallelogram concept	115
8.2	CAD model of the ergonomic haptic handle	115
8.3	Mobility of the spherical mechanism with respect to the user's wrist	116
8.4	Location of the mechanism center of mass	116
8.5	Detailed view of the grasping force-feedback module	117
8.6	Exploded view and assembly of the brake system.	118
8.7	Hand-presence detection	119
8.8	Workspace of the spherical mechanism	120
8.9	Ergonomic handle assembled in a haptic device	121
8.10	Force measurement setup	121
8.11	Maximum continuous force of the grasping module	122
8.12	Setup for the Z-width measurement	122
8.13	Z-width	123
8.14	Virtual wall	123
8.15	Setup for the brake assessment	124
8.16	Brake torque in function of input pressure	124
8.17	Standard and ergonomic handle	126
8.18	Index of difficulty (ID) of the peg-in-hole task	127
8.19	Setup for the peg-in-hole experiment	128
8.20	Experimental protocol for the peg-in-hole task	129
8.21	IP results of the peg-in-hole task	131
8.22	Average time for the peg-in-hole task with orientations	132
8.23	Setup for the EMG measurements	133
8.24	Placement of the EMG electrodes for each muscle	134
8.25	Average task EMG values for each muscle	136
8.26	Questionnaire statistics for the peg-in-hole task	138

List of Tables

2.1	Summary of current Teleoperated Surgical Robotic Systems	15
2.2	Summary of the presented haptic devices and their technical characteristics . .	19
4.1	Characteristics of the torque feedback module components	40
4.2	ANOVA for the 1 st experimental configuration	48
4.3	ANOVA for the 2 nd experimental configuration	50
4.4	ANOVA comparing the influence of the experimental configuration	52
5.1	Results of the repeated measures ANOVA for the pattern identification test . .	66
5.2	Index of difficulty (ID) depending on artery dimensions.	72
5.3	Exploration task: repeated measures ANOVA for task-completion time	74
5.4	Identifying the orientation of the hidden artery: repeated measures ANOVA for correctness and task-completion time.	79
6.1	Surgeons' demographic and background characteristics	90
6.2	Duration of the surgical procedure (percentage of surgeons)	92
6.3	Repeated measures ANOVA 4×7 for handle-type and evaluation criteria . . .	92
6.4	p-values resulting from the Bonferroni post hoc test for the intuitiveness scores.	93
6.5	p-values resulting from the Bonferroni post hoc test for the comfort scores. . .	94
6.6	p-values resulting from the Bonferroni post hoc test for the precision scores. . .	94
6.7	p-values resulting from the Bonferroni post hoc test for the stability scores. . .	95
6.8	Correlation matrix between the four evaluation criteria and the preference score	95
8.1	Motor and encoder characteristics before and after the reduction	118
8.2	Mobility ranges of the mechanism	119
8.3	Index of difficulty of the peg-in-hole task	127
8.4	Results of the repeated measures ANOVA for the peg-in-hole test	130
8.5	Repeated measures ANOVA for the average EMG measurements	136

Curriculum Vitae

Personal Data

Name: Laura Santos-Carreras
Date of Birth: 6th of May, 1984
Place of Birth: Madrid, Spain
Nationality: Spanish
Languages: Spanish (mother tongue), English (fluent), French (fluent) and German (basic A1)

Education

2008-2012 Ph.D. student at the Laboratory of Robotic systems (LSRO),
École Polytechnique Fédérale de Lausanne (EPFL), Switzerland
2005-2007 Master of Science in Automatic and Electronic Engineering,
Technical University of Madrid (UPM), Spain (ranked first among the graduates)
2002-2005 Bachelor of Science Technical Industrial Engineering. Intensification in Industrial
Electronics and Advanced Control, Technical University of Madrid (UPM), Spain
2002 High School of Science, Madrid, Spain
Graduated with A+ levels (ranked first among the graduates)

Professional Experience

2008-2012 **Laboratory of Robotic systems (EPFL)**, Switzerland.
Research, teaching activities and supervision of Master and Semester projects.
Management of budget and derivables for the EU-FP7 project ARAKNES.
Secretary of IEEE- EPFL Student Branch and chair of the local IEEE-EPFL
Student Paper Contest 2012.
2006-2007 **Technical University of Madrid (UPM)**, Spain.
Development of multifunctional microrobots for the inspection of pipelines,

- student assistant contract.
- 2007 **InduForum'07.**
Organization of the Professional Forum for engineering students,
computing department.
- Jul.-Sep. 2007 **European Organization for Nuclear Research (CERN)**, Switzerland.
Tests and studies about the interchangeability of the HLS sensor components,
CERN Summer Student program - technical support group.
- 2004-2005 **Technical University of Madrid (UPM)**, Spain.
Development of a Diagnostic Medical Imaging Software:
Quantification of the Hepatitis-C-infection-level on digitalized liver samples,
student assistant contract.
- Jul.-Dec. 2004 **Technical University of Madrid (UPM)**, Spain.
Development of a Diagnostic Medical Imaging Software:
Analysis of digitalized samples obtained by Sperm Chromatin Dispersion
technique to determine the sperms' DNA quality,
student assistant contract.

Grants and Awards

- 2005-2006 *Outstanding Academic Performance,*
Ministry of Education. Madrid Regional Authority.
- 2005-2006 *Best technological Design* at the Cybertech Robotic Contest,
Technical University of Madrid (UPM).
- 2005 *Best Bachelor project Award,*
Official Industrial Engineers Association of Madrid (COITIM).
- 2004-2005 *Outstanding Academic Performance,*
Ministry of Education. Madrid Regional Authority.
- 2002-2003 *Outstanding Academic Performance,*
Ministry of Education. Madrid Regional Authority.

Training Courses

- Oct. 2011 *Project management*
EPFL Staff training, Switzerland.
- Sep. 2011 *Speak with Impact*
EPFL Staff training, Switzerland.
- Apr. 2011 *The key to success, knowing about my competences*
CUSO, Switzerland

- Jun. 2010 *iPhone application development*
Cross Systems SA., Switzerland.
- Nov. 2008 *Hands-On Endoluminal, Single Site and NOTES Surgery Symposium*
UC San Diego, California.
- Summer 2007 *CERN Summer School of Physics*
European Organization for Nuclear Research (CERN), Switzerland.
- May 2006 *Biomedical Engineering Course*
Engineering University of Łódź, Poland.

List of Publications

Patents

1. Santos-Carreras L, Beira R, Bleuler H. *Ergonomic Handle for Haptic Devices*. Patent Cooperation Treaty PCT/IB2012/051303, filed March 19, 2012.
2. Santos-Carreras L, Rinderknecht M. D. , Gassert R, Kim Y. *Device and Virtual Reality Setup for Hand and Wrist Rehabilitation Based on Tendon Vibration*. Provisional European patent application EP 12001925.2, filed March 19, 2012.

Journal Papers

1. Santos-Carreras L, Leuenberger K, Samur E, Gassert R and Bleuler H. *Tactile Feedback Improves Performance in a Palpation Task: Results in a VR Based Testbed*. MIT Journal: Presence: Teleoperators and Virtual Environments, 2012, awaiting-publication.
2. Santos-Carreras L, Hagen M, Gassert R, Bleuler H. *Survey on Surgical Instrument Handle Design: Ergonomics and Acceptance*. Surgical Innovation, 2011.
3. Beira R, Santos-Carreras L, Sengül A, Samur E, Bleuler H and Clavel R. *An External Positioning Mechanism for Robotic Surgery*. JSME Technical Journal ,2011.
4. Santos-Carreras L, Beira R , Sengül A , Gassert R and Bleuler H. *Influence of Force and Torque Feedback on Operator Performance in a VR-Based Suturing Task*. Applied Bionics and Biomechanics, 2010.
5. Beira R, Santos-Carreras L, Rognini G, Bleuler H and Clavel R. *Dionis: A Novel Remote-Center-of-Motion Parallel Manipulator for Minimally Invasive Surgery*. Applied Bionics and Biomechanics, 2010.

Peer-reviewed Conference Proceedings

1. Gallo S, Santos-Carreras L, Rognini G, Hara M, Yamamoto A, Higuichi T and Bleuler H. *Towards multimodal Haptics for teleoperation: Design of a Tactile Thermal Display*.

International Workshop on Advanced Motion Control (AMC) 2012, Sarajevo.

2. Santos-Carreras L, Leuenberger K, Beira R and Bleuler H. *ARAKNES Haptic Interface: User-Centered Design Approach*. pHealth, 2010, Berlin.
3. Santos-Carreras L, Leuenberger K, Retornaz P, Gassert R and Bleuler H. *Design and Psychophysical Evaluation of a Tactile Pulse Display for Teleoperated Artery Palpation*. IEEE/RSJ International Conference on Intelligent Robots and Systems (IROS) 2010. Taiwan.
4. Santos-Carreras L, Sengül A, Vollenweider M, Bleuler H. *Multimodal Haptic Interface for Surgical Robotics*. International Conference on Human System Interaction (HSI) 2011, Japan.
5. S. Gallo, D. Chapuis, L. Santos-Carreras, P. Retornaz, Y. Kim H. Bleuler and R. Gassert. *Augmented White Cane with Multimodal Haptic Feedback*. BioRob, 2010, Japan.
6. Stephan M, Rognini G, Sengul A, Beira R, Santos-Carreras L and Bleuler H. *Modeling and Design of a Gripper for a Robotic Surgical System Integrating Force Sensing Capabilities in 4 DOF*. International Conference on Control Automation and Systems (ICASS) 2010, Korea.
7. A. Sengül, M. Stephan, G. Rognini, R. Beira, L. Santos-Carreras, and H. Bleuler. *Ein Greifer für Minimal-invasive Robotisierte Chirurgie mit integriertem Kraftsensor*. In *Automatisierungstechnische Verfahren für die Medizin (Automed)* 2010, Zürich.